ROLE OF PROSTAGLANDINS IN ENDOMETRIAL RECEPTIVITY AND PREGNANCY SUCCESS IN THE MURINE MODEL

By

Noura Massri

A DISSERTATION

Submitted to
Michigan State University
in partial fulfillment of the requirements
for the degree of

Cell and Molecular Biology – Doctor of Philosophy

2025

ABSTRACT

Non-steroidal anti-inflammatory drugs (NSAIDs) that inhibit prostaglandin synthase (PTGS) enzymes have been associated with increased miscarriage risk. While studies show diminished PTGS2-derived prostaglandins in the endometrium of patients with implantation failure, the role of PTGS2 during peri-implantation remains controversial in mouse models. Conflicting research suggests that PTGS2 knockout (*Ptgs2*$^{-/-}$) mice show either comprehensive reproductive impairments or effects limited to ovulation. Furthermore, the specific uterine cell types involved in PTGS2 activity and its role in implantation chamber formation remain unclear. This thesis investigates prostaglandin's reproductive role through two complementary approaches in mouse models. First, we employed genetic deletion of PTGS2 in specific uterine cell types using multiple mouse models: *Ptgs2*$^{-/-}$ (global deletion), *Ltf*$^{cre/+}$*; Ptgs2*$^{f/f}$ (uterine epithelial deletion), *Pax2*$^{cre/+}$*; Ptgs2*$^{f/f}$ (uterine epithelial and endothelial deletion), and *Pgr*$^{cre/+}$*; Ptgs2*$^{f/f}$ (deletion in ovary, oviduct, uterine epithelium, stroma, and circular smooth muscle). Second, we used pharmacological inhibition through NSAIDs: Aspirin (PTGS1-specific), Dup-697 (PTGS2-specific), and indomethacin (PTGS1 and PTGS2 inhibitor). Both approaches were enhanced by three-dimensional (3D) imaging techniques to evaluate uterine tissue remodeling during peri-implantation. Using tissue-specific knockout models, we demonstrate in Chapter 3 that deletion of PTGS2 in uterine stroma using *Pgr*$^{cre/+}$*; Ptgs2*$^{f/f}$ impairs multiple reproductive processes: timely embryo implantation, post-implantation embryonic development, implantation chamber formation, vascular remodeling, decidualization, and overall pregnancy success. In contrast, epithelial and endothelial PTGS2 deletion shows no significant impact on these processes. Our analysis of NSAID effects in Chapter 4 reveals critical timing windows for PTGS activity during pregnancy establishment. Specifically, indomethacin treatment results in delayed implantation, disrupted embryo spacing, restricted embryonic growth, impaired implantation chamber formation, and vascular remodeling. These findings advance our understanding of prostaglandin signaling regulation during early pregnancy with important clinical implications. Understanding the cell type-

specific and temporal requirements for prostaglandin signaling could help resolve controversies surrounding NSAID use during pregnancy and guide the development of safer anti-inflammatory therapy protocols. Additionally, variations in prostaglandin signaling across populations may explain differential susceptibility to implantation failure, highlighting the importance of personalized care approaches for optimal pregnancy outcomes.

Copyright by
NOURA MASSRI
2025

A book is the ultimate companion at all times.

ACKNOWLEDGMENTS

I sincerely thank my PhD mentor, Dr. Ripla Arora, for her invaluable support, guidance, and mentorship. Her patience, insightful feedback, and encouragement have profoundly impacted my research and scientific growth. I truly appreciate her time and effort in helping me navigate challenges, refine my ideas, and develop as a graduate student. Her dedication and expertise have inspired me, and I feel incredibly fortunate to have had the opportunity to learn from her.

I want to express my sincere gratitude to the esteemed members of my thesis committee: Dr. David Arnosti, Dr. Asgi T. Fazleabas, Dr. Stephanie Watts, and Dr. Kathleen Gallo. Each member contributed unique expertise that has significantly enhanced my research. Dr. Arnosti provided valuable insights into molecular biology, Dr. Fazleabas shared his knowledge of reproductive biology, Dr. Watts offered physiological and pharmacological perspectives, and Dr. Gallo contributed her expertise in signaling pathways and physiological perspectives. Each member's distinct perspectives and expertise have greatly improved my work and deepened my scientific understanding.

The Cell and Molecular Biology (CMB) Program has fostered an outstanding environment that strongly supports my academic growth. The program's success is built on exceptional leadership: Dr. Margaret Petroff, whose mentorship guided me through graduate education; Alaina M. Burghardt, whose administrative expertise ensured smooth operations; Geoffrey Grzesiak, whose support for CMB ensured efficient procedures; and past and present associate directors, Drs. Amy Ralston and Ron Chandler, whose strategic vision enhanced our training environment. I am also truly grateful to my fellow CMB graduate students and the Graduate Student Organization (GSO) for creating a supportive and collaborative peer community.

I am also grateful to the co-directors of the Reproductive and Developmental Sciences Program (RDSP), Drs. Asgi T. Fazleabas and Keith Latham, for granting me the opportunity to join the pre-doctoral Eunice Kennedy Shriver National Institute of Child Health and Human Development T32 training program. This fellowship provided essential financial support while

offering invaluable training opportunities that greatly enhanced my research skills and professional growth. Additionally, the administrative support from Ms. Laurie Felton and Amanda Sterling was instrumental in helping me navigate the program's requirements.

Regular joint laboratory meetings with our Rutgers University collaborators, Drs. Nataki Douglas and Shuo Xiao provided invaluable insights that shaped our experimental strategies—the expertise of Dr. Fazleabas's lab members, particularly Drs. Gregory Burns and Yong Song were instrumental in refining my methodologies and interpretations.

To my past and present laboratory colleagues, you have been more than just coworkers and partners in this scientific journey. I am incredibly grateful to Dr. Manoj Madhavan, Dr. Diana Flores, Sarah Fitch, Hannah Lufkin, Madeline Dawson, May Shen, Katrina Granger, Kaylie Chiles, Harini Raghu Kumar, Lisa Zou, Aishwarya Bhurke, Savannah Wright, Sameed Khan, Michelle Lupa, Curtis Chen, and Anish Deshpande for your unwavering support, insightful discussions, and collaborative spirit. Your encouragement and camaraderie have made our lab feel like a second home, and your friendship and intellectual contributions have been invaluable to my research progress.

I am also deeply grateful to the Campus Animal Resources (CAR) team at Michigan State University for their dedicated care of the mouse population, which ensures their well-being and health. Their meticulous attention to animal welfare is essential for maintaining the reliability and reproducibility of our research. I appreciate Autumn Miner, Jessica Topolski, and Katherine Alexander's invaluable support and commitment.

I am deeply grateful to my friends in Syria and my second home, Michigan, for their unwavering support throughout this journey. Your presence has brought balance to my life, celebrating my achievements and offering comfort during tough times. Your friendship has been a lasting source of strength, joy, and inspiration.

Finally, I sincerely thank my family, my parents, Dr. Zouheir Massri and Hanna Dakhel, and my siblings, Louai, Lama, and Lubna. Your unwavering love, patience, and support have been the

foundation of my journey. Even during moments of doubt, you believed in me, and your encouragement has fueled my persistence and resilience. This achievement is not just mine; it's yours, too.

This research was made possible through generous funding from the March of Dimes (grant #5-FY20-209 to Dr. Ripla Arora), the Eunice Kennedy Shriver National Institute of Child Health & Human Development of the National Institutes of Health (award #T32HD087166 to Noura Massri), and the University of Virginia Center for Research in Reproduction Ligand Assay and Analysis Core (award #R24 HD102061).

My work wouldn't have been possible without the collective support of all the fantastic people who have played a crucial role in my development as a scientist and an individual. Thank you all for being a part of my PhD journey.

TABLE OF CONTENTS

Chapter 1: Introduction to the female reproductive system and prostaglandin signaling pathway

1.1: The female reproductive system development and anatomy

1.1.1: Background

The continuation of species through successful reproduction represents one of nature's most intricate and vital biological processes (Flaws and Spencer, 2018). In mammals, this process relies on the precise orchestration of molecular signals within the female reproductive system, with a particularly critical emphasis on the role of prostaglandin signaling in regulating fertility, pregnancy, and fetal development (Clark and Myatt, 2008; Wang and Dey, 2006).

A comprehensive understanding of these complex molecular mechanisms that contribute to pregnancy success carries profound implications for reproductive medicine. Disruptions in these pathways contribute to reproductive disorders affecting approximately 15% of couples globally, adversely impacting fertility and pregnancy outcomes (Cox et al., 2022; Vander Borght and Wyns, 2018; Wang and Dey, 2006).

Moreover, epidemiological data from the American College of Obstetricians and Gynecologists indicates that spontaneous pregnancy loss occurs in approximately one-quarter (26%) of all gestations, though clinical detection is limited to about 10% of these incidents (Bulletins—Gynecology, 2018). This limitation arises primarily because many losses occur prior to clinical confirmation of pregnancy through ultrasound or laboratory testing (Bulletins—Gynecology, 2018). Additionally, 1-2% of women experience idiopathic recurrent pregnancy loss, defined by three or more consecutive pregnancy losses prior to 20 weeks of gestation, where standard diagnostic evaluations have not identified an underlying cause (Turesheva et al., 2023). Understanding the causes of recurrent miscarriages is essential for creating targeted treatments, enhancing reproductive technologies, addressing complications, and improving maternal-fetal health outcomes (Cha et al., 2012; Wang and Dey, 2006).

1.1.2: Embryonic development of the female reproductive system

The female reproductive system develops during embryonic stages from the intermediate mesoderm. Within this framework, Müllerian ducts, also known as paramesonephric ducts, give rise to the fallopian tubes (or oviducts in mice), uterus, cervix, and upper vagina (Flaws and Spencer, 2018; Machado et al., 2022). Concurrently, in the absence of SRY expression, which is a key factor in male sex determination, the ovaries develop from gonadal ridges, with their development regulated through specific factors, including WNT4 and FOXL2, RSPO1, and β-catenin (Biason-Lauber and Chaboissier, 2015; Monsivais et al., 2017). During the early stages of ovarian development, primordial germ cells (PGCs) migrate from the yolk sac to the indifferent gonadal ridges, typically colonizing around embryonic day 9.5 and day 11.5 in mice (Biason-Lauber and Chaboissier, 2015; Machado et al., 2022). These cells undergo proliferation and mitotic divisions and eventually form germ cell nests surrounded by pregranulosa cells (Richards and Pangas, 2010). This developmental cascade, beginning around week 6 in humans and embryonic day 13.5 in rodents (Machado et al., 2022), results in the formation of interconnected reproductive organs, including the ovaries, fallopian tubes in humans and oviducts in mice, uterus, and vagina, which ultimately coordinate with the placenta and fetus during pregnancy (Machado et al., 2022).

1.1.3: Female reproductive system morphology among species

While the early stages of Müllerian duct development are conserved across various species, the later stages exhibit notable differences among mammals, leading to diverse uterine morphologies (Machado et al., 2022). For instance, rabbits possess a duplex uterus with two uterine horns and two cervices, whereas rodents, such as rats and mice, have a bipartite uterus with two uterine horns and one cervix. In cows, the uterus appears bicornuate, characterized by a uterine body, uterine horns, and a single cervix (Machado et al., 2022). For humans, the Müllerian ducts fuse to create a single chamber, resulting in one uterus and one cervix. Generally, these varied uterine morphologies are categorized based on the number of cervixes and the

presence or absence of uterine horns and uterine body (Fig. 1.1 A and B) (Machado et al., 2022).

1.1.4: The role of the hypothalamus, pituitary, and ovarian axis (HPO Axis) in regulating the reproductive cycle

The mature female reproductive system functions through a precisely coordinated network of endocrine signaling between the hypothalamus (a region of the brain), the pituitary glands, and the ovaries, collectively referred to as the HPO axis (Padmanabhan et al., 2018). The hypothalamus produces gonadotropin-releasing hormones (GnRH), which stimulate the anterior pituitary gland to secrete follicle-stimulating hormones (FSH) and luteinizing hormones (LH) (Padmanabhan et al., 2018). These gonadotropins are critical for regulating ovarian functions by binding to their specific receptors and controlling follicular growth and steroidogenesis (Padmanabhan et al., 2018). In response to stimulation from these hormones, the ovaries generate steroid hormones, estrogen and progesterone (Padmanabhan et al., 2018). These ovarian hormones play a crucial role in modulating the functions of the reproductive tract and establish a negative feedback loop to the hypothalamus and the pituitary glands (Padmanabhan et al., 2018). These hormones are vital for orchestrating the menstrual cycle in humans and primates and the estrus cycle in other mammals and rodents, as well as preparing the uterus for pregnancy (Chen et al., 2013; Richards and Pangas, 2010). Despite being regulated by the same HPO axis and sharing approximately similar uterine anatomy, humans' and rodents' reproductive cycles differ (Nowak, 2018).

1.1.5: Human uterus anatomy and the menstrual cycle

The human uterus consists of several essential components: the myometrium, which is a smooth muscle layer; the endometrium, which is the inner mucosal lining surrounding mesenchymal stroma and includes uterine glands, immune cells, and extensive networks of blood vessels (Ferenczy, 1994). The endometrium is further divided into two layers: the deep stratum basalis, which lies adjacent to the myometrium, and the superficial stratum functionalis (Fig. 1.1 A, A') (Ferenczy, 1994; Massri et al., 2023). The typical human menstrual cycle lasts 21 to 35

days and can be divided into two main phases. The first is the estrogen-dominated proliferative phase, characterized by significant endometrial layer thickening (Ferenczy, 1994). This phase is followed by the progesterone-dominated secretory phase, which begins with ovulation, an oocyte's release, and the corpus luteum's formation (Fig. 1.2 A) (Ferenczy, 1994; Hickey and Fraser, 2003). During the secretory phase, progesterone facilitates the differentiation of the endometrium in preparation for potential embryo implantation (Fig. 1.2 A) (Massri et al., 2023). In the absence of pregnancy, the endometrium and its associated vasculature undergo shedding, triggered by the demise of the ovarian corpus luteum and the subsequent withdrawal of ovarian hormones (Ferenczy, 1994; Massri et al., 2023; Nowak, 2018).

1.1.6: Rodent uterus anatomy and the estrous cycle

The rodent uterus, similar to the human uterus, consists of two layers of smooth muscle: an outer longitudinal smooth muscle and an inner circular smooth muscle encircling the endometrium (Pang et al., 2013a) (Fig. 1.1 B, B'). The endometrium compromises stroma, uterine glands, immune cells, and an intricate network of blood vessels (Pang et al., 2013a) (Fig. 1.1 B, B'). These various tissue types undergo remodeling during the estrus cycle and pregnancy to support fetal development (Bertolin and D. Murphy, 2014; Edwards et al., 2013; Massri et al., 2023; Rogers et al., 1982). Resembling the human menstrual cycle, the rodent estrous cycle is orchestrated by ovarian-derived hormones, which prepare the uterus for embryo implantation and pregnancy (Padmanabhan et al., 2018). The cyclic remodeling of the uterus in rodents occurs throughout 4 to 5 days (Padmanabhan et al., 2018) (Fig. 1.2 B). This remodeling process entails morphologic changes in the uterine and glandular epithelium, alterations of stromal cells, modifications in uterine gland secretions, and variations in the size and shape of the uterine lumen, depending on the volume of uterine luminal fluid (Bertolin and D. Murphy, 2014). While existing literature provides some insight into alteration in uterine vasculature during pregnancy, information regarding vascular remodeling during the estrus cycle remains limited, likely due to the absence of menstruation in mice (Massri et al., 2023). Although mice do not experience

menstruation, experimental models exist in which endometrial shedding can be induced following decidualization through the withdrawal of progesterone treatment (Cousins et al., 2014). Due to ethical considerations surrounding human pregnancy studies, rodents, especially mice, are an excellent experimental model. Mice share key reproductive mechanisms with humans and allow for genetic manipulation to better understand pregnancy events.

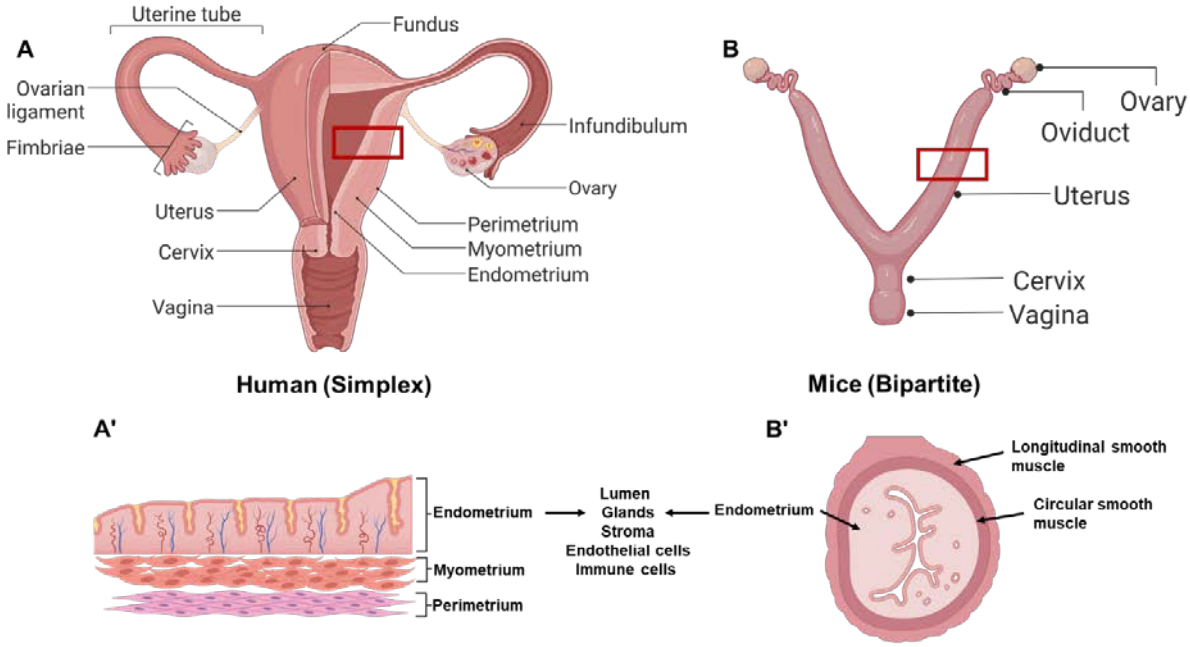

Figure 1.1. The anatomy of the female reproductive system encompasses several essential components. Part (**A**) illustrates the simplex female reproductive structure in humans, comprising the ovaries, fallopian tubes, a single-chambered uterus, cervix, and vagina. Part (**A'**) presents a cross-section of the human uterus, which consists of three layers: the perimetrium and myometrium (both formed of smooth muscle), and the endometrium. The endometrium contains the uterine cavity, which includes the lumen, glands, stroma, endothelial cells, and immune cells. Part (**B**) depicts the bipartite or duplex form of the female reproductive structure in mice, which features the ovaries, oviducts, two uterine horns, one cervix, and one vagina. Part (**B'**) shows a transverse cross-section of the mouse uterus, composed of two smooth muscle layers: a longitudinal smooth muscle layer on the outer side and a circular smooth muscle layer on the inner side. Additionally, the endometrium is made up of the lumen, uterine glands, stroma, endothelial cells, and immune cells.

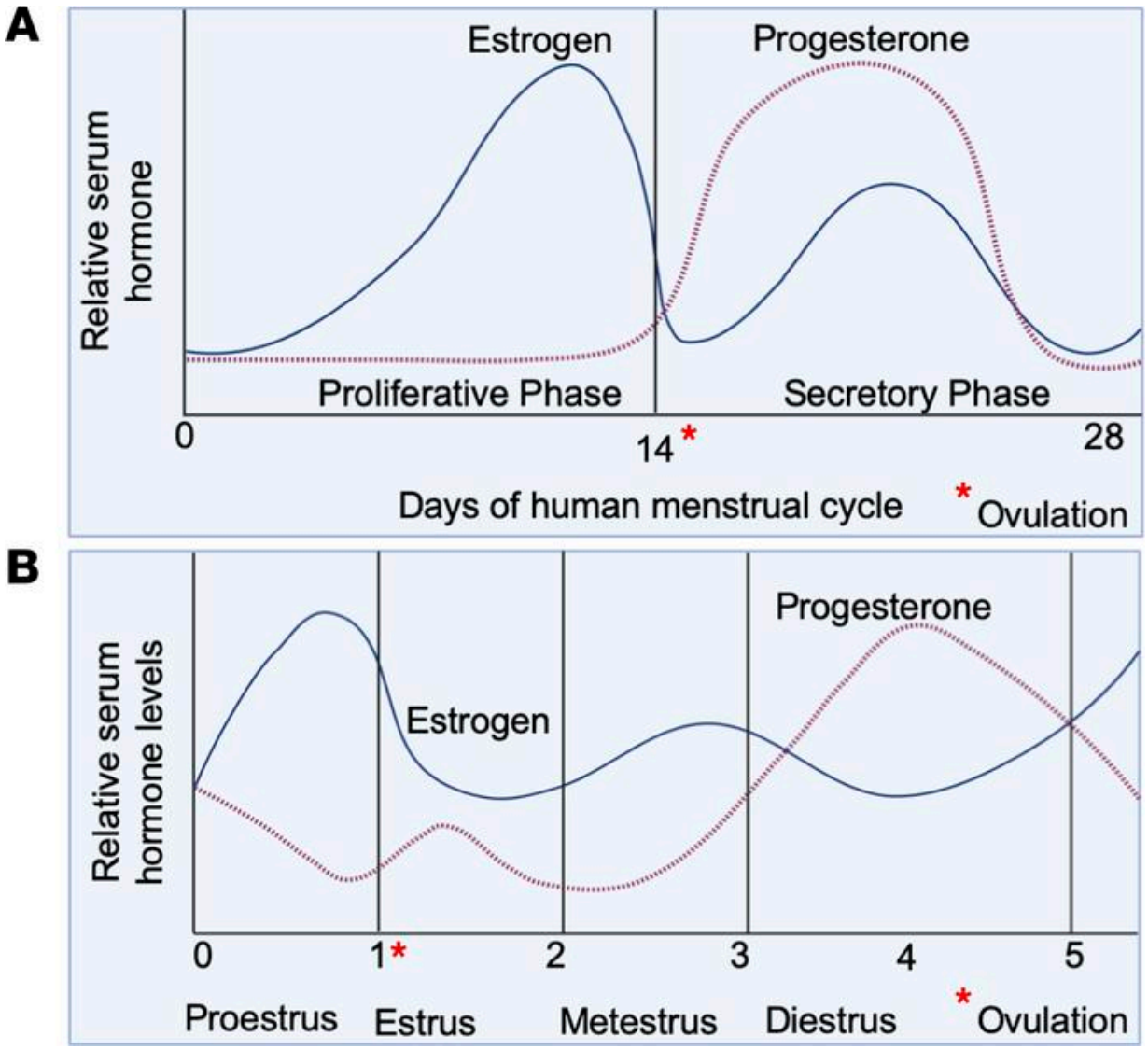

Figure 1.2. Comparison of the human menstrual cycle and rodent estrous cycle. (**A**) The human menstrual cycle is divided into the proliferative (follicular) phase and the secretory (luteal) phase. Under the influence of ovarian estrogen (blue line) in the follicular phase, the endometrium regenerates, endothelial cells proliferate, and vascular permeability increases. Mid-cycle, a surge in luteinizing hormone results in follicle rupture, ovulation of the oocyte, and formation of the corpus luteum. In the secretory phase, progesterone (red dashed line) regulates stromal cell decidualization and increases endometrial edema in preparation for embryo implantation. In the absence of embryo implantation, the corpus luteum demises, and estrogen and progesterone levels fall. This is followed by menstruation and the start of another menstrual cycle. (**B**) The rodent estrous cycle is composed of four different phases: proestrus, estrus, metestrus, and diestrus. In the proestrus phase, which lasts between 21 and 32 hours, estrogen increases. The estrus phase and ovulation follow the proestrus phase. The estrus phase lasts 12–48 hours. The formation of the corpus luteum following ovulation marks the shift from an estrogen- to a progesterone-dominated stage. The metestrus and diestrus phases represent the secretory phases of the cycle. The metestrus phase lasts 8–24 hours, while the diestrus phase lasts 48–72 hours.

1.2: Events in early rodent pregnancy

In early rodent pregnancy, the mating event can be documented by detecting a copulation plug formed from male seminal proteins, marking gestational day (GD) 0.5, which enables precise staging of subsequent pregnancy events (Edwards et al., 2013; Pang et al., 2013b). Following mating, sperm transport through the female reproductive tract leads to fertilization in the ampulla region of the oviducts (the rodent equivalent of fallopian tubes) (Miller, 2018). The fertilized egg undergoes precisely timed cleavage divisions from the 2-cell to 8-cell stage, followed by compaction to form a morula, and finally, cavitation to form a blastocyst with distinct inner cell mass and trophectoderm lineages (Miller, 2018; Wang and Dey, 2006). Concurrent with these embryonic events, the post-ovulatory rise in progesterone initiates the preparation of the uterine vasculature for implantation. The uterine vasculature begins preparing for blastocyst implantation through increased endothelial cell proliferation throughout the endometrium and dilation of subepithelial capillaries (Rogers et al., 1982; Takemori et al., 1984).

In mice, multiple blastocysts enter the uterus early on GD3.0, undergoing unidirectional and bidirectional movement to achieve precise spacing before aligning along the anti-mesometrial-mesometrial axis for attachment on GD4.0 (Flores et al., 2020; Madhavan et al., 2022). Following attachment, the uterine epithelium undergoes morphological transformation to create a specialized V-shaped implantation chamber that facilitates embryo invasion (Madhavan et al., 2022; Massri and Arora, 2025). Rapid vascular remodeling occurs in the subepithelial capillaries at the anti-mesometrial pole, where embryos first attach. The endothelial adherens junctions undergo dynamic reorganization through phosphorylation-dependent internalization of vascular endothelial cadherin (VE-cadherin), triggered by vascular endothelial growth factor (VEGF) induced Src kinase activation (Claesson-Welsh et al., 2021). This molecular cascade leads to controlled vascular permeability, which can be precisely visualized using Chicago Blue dye. When injected intravenously, this albumin-binding dye extravasates specifically at implantation sites where endothelial barrier function is modified, creating visible blue bands within

5 minutes at GD4.5 (Pang et al., 2013b). The observation of this localized vascular permeability at implantation sites across several mammalian species underscores its fundamental role in establishing maternal-embryo communication (Boshier, 1970; Deanesly, 1967; Keys et al., 1986). This vascular response is orchestrated by multiple signaling pathways, including steroid hormones, vascular endothelial growth factor (VEGF), and lipid mediators such as prostaglandin (Massri et al., 2023).

As the implantation chamber elongates, it invades the underlying stroma as the luminal epithelium around the embryo undergoes programmed cell death (Edwards et al., 2013; Massri and Arora, 2025; Pang et al., 2013a). The surrounding stromal cells undergo a remarkable transformation termed decidualization, a mesenchymal-to-epithelial differentiation process characterized by cytoskeletal reorganization, altered glucose metabolism, and polyploidization (Edwards et al., 2013). This stromal transformation is accompanied by an extensive vascular remodeling program from GD4.5-7.5 that establishes a hierarchical vascular network critical for embryo support (Figure 1.4 C) (Kim et al., 2013). Analysis of the decidual transcriptome at GD5.5 shows upregulation of endothelial cell-associated genes, including VEGF, Notch signaling components, and angiogenic matrix proteins (Lustgarten Guahmich et al., 2020), with peak endothelial cell proliferation at GD6.5 (Douglas et al., 2009). By GD7.5, the decidual vasculature shows distinct regional specialization: the mesometrial region contains spiral arterioles covered with vascular smooth muscle cells and pericytes, the central region has capillaries with minimal pericyte coverage, and the anti-mesometrial region contains capillaries closely associated with pericytes. Both sprouting and intussusceptive angiogenesis contribute to the forming and remodeling of these decidual vessels (Figure 1.4 D) (Kim et al., 2013; Marchetto et al., 2020). When comparing the vasculature in different decidual regions to the estrous stage non-pregnant vasculature, there was a 14.9-fold increase in the vascular sprouts in the central region and a 7.4-fold increase in the vascular sprouts in the AMR. During early pregnancy, the intussusceptive

blood vessels also increase by 2.8-fold and 2.4-fold in the CTR and AMR, respectively (Figure 1.4 D) (Massri et al., 2023).

The embryo continues developing within this vascularized decidua, and by GD8.5, embryonic umbilical vessels connect with the maternal circulation to form the placenta by GD9.5 (Edwards et al., 2013; Pang et al., 2013a). Multiple factors regulate this coordinated vascular remodeling, including steroid hormones establishing the basic tissue architecture through nuclear receptor signaling. VEGF family members (VEGF-A, PlGF) and their receptors (VEGFR1/2) drive vessel growth and specialization. Angiopoietins (Ang1/2) work through Tie2 receptors to regulate vessel stability and remodeling, while Delta-like/Jagged ligands signaling through Notch receptors control vessel branching patterns. Natural killer cells and macrophages contribute by secreting cytokines and matrix-remodeling enzymes that facilitate spiral artery modification. Prostaglandin, particularly PGE2 and PGI2, modulate vascular tone and permeability through specific G-protein-coupled receptors (Massri et al., 2023; Sugimoto et al., 2015). The pregnancy then progresses to term at approximately GD19 in mice (Fig. 1.3 and Fig. 1.4 A and B) (Edwards et al., 2013), with rat gestation being about two days longer (Kennedy et al., 2007). Due to ethical and technical limitations in studying early human pregnancy, these rodent models have been instrumental in elucidating the complex endometrial required for successful implantation and pregnancy progression.

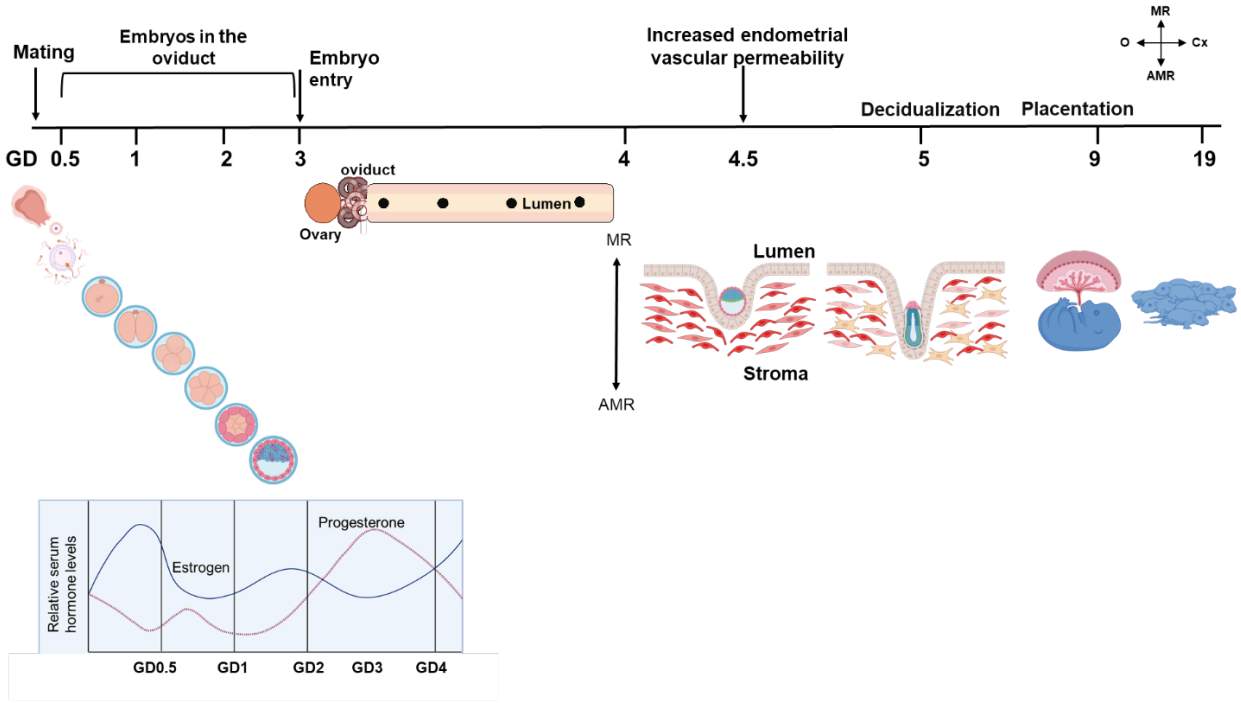

Figure 1.3. Timeline of mouse pregnancy. During the estrus stage, female mice are primed to mate with fertile males, and successful mating is indicated by the presence of a vaginal plug in the females, marking gestational day 0.5 (GD0.5) and the beginning of pregnancy. Post-mating, the oocyte released from the ovary becomes fertilized in the oviduct, and the embryos undergo division from the one-cell stage to the morula stage between GD0.5 and GD3. The onset of GD3 is characterized by the embryos entering the uterine horns through the uterine-oviductal junction, where they navigate the uterus to locate a site for attachment around GD4. At GD4.5, the blood vessels surrounding the implantation sites of the embryos become permeable. Following an intravenous injection of blue dye and subsequent dissection, blue dye can be observed at these attachment sites. By this stage, the embryos reach the blastocyst stage and are positioned in the uterus with the inner cell mass facing the mesometrial pole. Additionally, an implantation chamber is formed at GD4.5, which subsequently elongates, leading to decidualization at GD5.5, where stromal cells transform into decidualized cells. The blastocyst also elongates to adopt an epiblast shape. As development progresses, there are significant maternal adaptations and vascular remodeling that contribute to the establishment of the placenta by GD9 and the formation of the fetus. Mid-gestation is marked at GD12.5, with pregnancy reaching term around GD19, at which point female mice typically give birth to approximately 5-12 pups. GD: gestational day, O: ovary, CX: cervix, MR: mesometrial region, AMR: anti-mesometrial region.

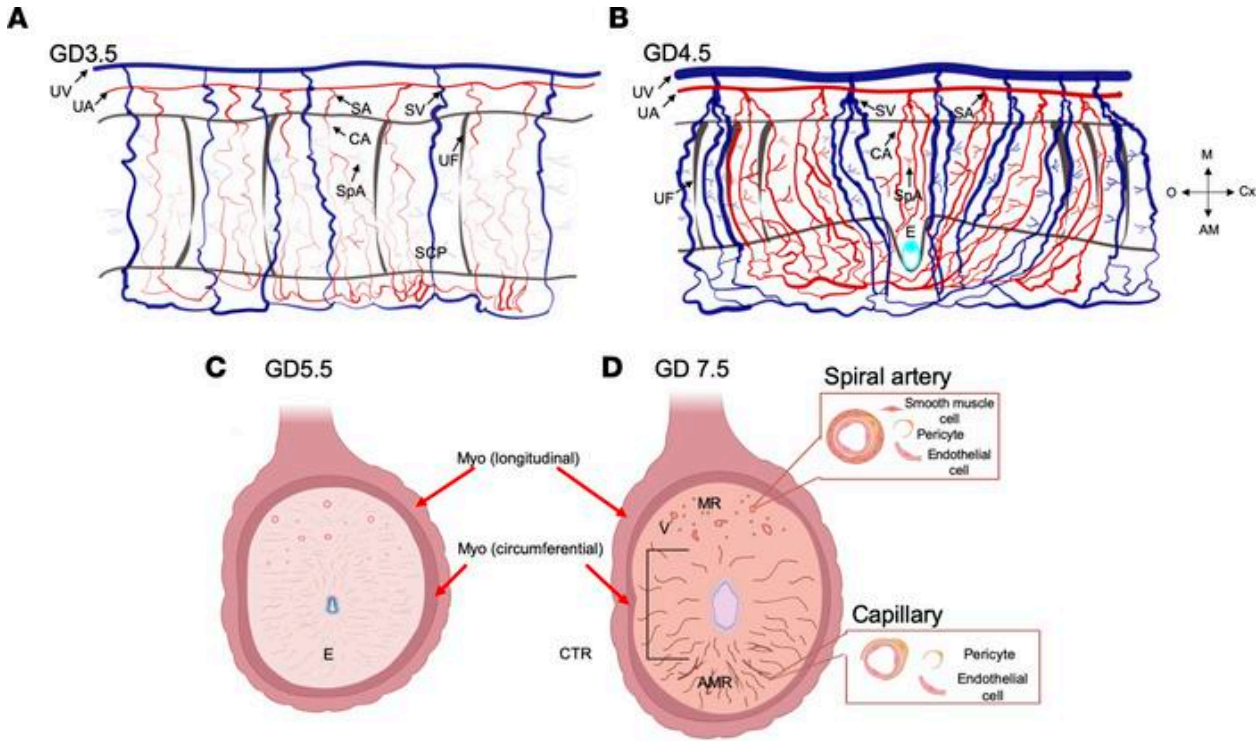

Figure 1.4. Vascular remodeling and implantation chamber formation from pre-implantation through decidualization. (**A and B**) Longitudinal cross sections of the GD3.5 (**A**) and the GD4.5 (**B**) mouse uterus illustrating arteries (red), veins (blue), and the uterine lumen (outlined in gray). The utero-ovarian artery (UA) and vein (UV) give rise to the segmental arteries and veins, respectively (SA and SV). The segmental arteries divide into circumferential arterioles (CA) that then branch to form the spiral arterioles (SpA). Subepithelial capillary plexus (SCP) arise from the spiral arterioles and supply blood to the endometrium. Following embryo attachment at GD4.5 (**B**), the vessels remodel and dilate in proximity to the implantation region. (**C and D**) Transverse cross sections at GD5.5 (**C**) and GD7.5 (D). At GD5.5 (**C**) the newly formed decidual capillaries are readily apparent. By GD7.5 (**D**), the vasculature surrounding the implantation chamber can be divided into different regions — the central region surrounding the embryo (CTR), the mesometrial region (MR), and the anti–mesometrial region (AMR) — each with a unique composition of vessels. The MR is composed of spiral arterioles and capillaries. The spiral arterioles contain endothelial cells and mural cells (pericytes and VSMCs). The decidual capillaries in the AMR are smaller vessels composed of endothelial cells associated with pericytes, while the decidual capillaries in the CTR contain very few pericytes. AM, anti-mesometrial pole; Cx, cervix; E, embryo; M, mesometrial pole; Myo, myometrium; O, ovary; UF, uterine fold.

1.3: Molecular mediators of early pregnancy success

Pregnancy success depends on a complex network of signals or molecular mediators that operate in precisely timed sequences during gestation. These mediators form interconnected signaling cascades that coordinate essential reproductive events, ranging from ovulation to uterine preparation for implantation and sustaining pregnancy. Understanding how these signaling pathways interact and regulate each other is crucial for comprehending normal reproductive function and pathological conditions. The major signaling systems include steroid hormones, growth factors, cytokines, and lipid mediators, each playing distinct yet interconnected roles in reproductive success (Chen et al., 2013; Wang and Dey, 2006). These signaling molecules can be broadly classified into several major signaling systems.

1.3.1: Steroid hormones signaling

In rodents, the interplay between estrogen and progesterone (P4) orchestrates crucial early pregnancy events through their nuclear receptors (ERα, ERβ, PR-A, and PR-B) (Cha et al., 2012; Chen et al., 2013). The initial ovulatory estrogen initiates a critical phase of epithelial proliferation during gestation days 1 to 2 (GD1–GD2) by activating stromal estrogen receptor alpha (Erα), which stimulates insulin growth factor (IGF1) production, epidermal growth factor (EGF) and its receptor in the stroma and transforming growth factor alpha (TGF-α). These growth factors are critical for coordinating cellular growth and tissue remodeling in the uterine environment (Ma et al., 2003; Zhu and Pollard, 2007). Furthermore, this early estrogen surge induces progesterone receptor (PR) expression, sensitizing the uterus for subsequent progesterone signaling (Kim et al., 2018b; Patel et al., 2015). Simultaneously, this initial spike in estrogen levels triggers rapid VEGF transcription and induces VEGF and VEGFR2 expression in the stroma within 6 hours (Ma et al., 2001), which sets the stage for subsequent processes, including uterine epithelial proliferation and vascular development, fundamental for creating a receptive environment for the developing embryo (Das et al., 2009).

By gestation day 3 (GD3.0), a modest increase in estrogen levels and elevated P4 levels play a pivotal role in supporting embryo implantation (Winuthayanon et al., 2017). The second, smaller estrogen surge on GD3 induces LIF expression in the glandular epithelium (Song et al., 2000; Stewart et al., 1992), which is essential for embryo implantation (Chen et al., 2000). During this period, estrogen also induces cell cycle regulators, which include C/EBPβ, which is rapidly induced in the pregnant uterus at the time of blastocyst attachment and increases further during the decidualization phase (Mantena et al., 2006). Also, estrogen is crucial in regulating mitotic checkpoint proteins, such as Mad2l1, centromere protein E (Cenpe), and checkpoint kinases Chek1 and Chek2. Notably, these proteins are significantly upregulated in wild-type uteri, while this upregulation is absent in conditional ERα knockout uteri (Mantena et al., 2006; Winuthayanon et al., 2014). This distinction highlights the importance of estrogen signaling in maintaining proper mitotic regulation within uterine cells. On the other hand, the PR-expressing stromal cells respond to P4 and induce stromal VEGFR2 expression within 12 hours and regulate blood vessel density and vascular sinus fold formation (Hyder and Stancel, 1999; Kim et al., 2013).

As pregnancy progresses beyond GD3, P4 signaling, enabled by the earlier estrogen-induced PR expression, becomes dominant. Then, progesterone signaling triggers developmental transcription factors such as HOXA10 and HOXA11, which are critical for stromal cell decidualization (Cha et al., 2012; Lim et al., 1999b). P4 also induces Indian hedgehog (Ihh) expression in the uterine epithelium, which binds to its receptors Patched (PTCH1) and signal transducer Smoothened (SMO) in the stroma to mediate stromal cell proliferation through activation of downstream targets including COUP-TFII (NR2F2) in the subepithelial stroma (Cha et al., 2012; Simon et al., 2009). The loss of Indian hedgehog (Ihh) expression in the uterine epithelium has been shown to lead to implantation failure, highlighting the essential role of the epithelial-stromal signaling pathway in establishing uterine receptivity (Cha et al., 2012; Wei et al., 2010). P4 signaling also induces HAND2, a transcription factor in uterine stromal cells crucial for implantation (Winuthayanon et al., 2014) During this period, local estrogen production from

decidualizing stromal cells promotes angiogenesis through EPAS1, ANGPT2, and ANGPT4 (Das et al., 2009). Notably, P4's effects on post-implantation vascular remodeling are primarily mediated through VEGF and ANGPT2 signaling (Kim et al., 2013; Park et al., 2020b).

Steroid hormones receptors

The distribution of hormone receptors follows distinct patterns across uterine cells, influencing their response to steroid hormones. Estrogen receptor alpha (Erα) is expressed in all uterine cell layers, including luminal and glandular epithelium, stroma, and myometrium, while estrogen receptor beta (Erβ) shows minimal expression in the uterus (Cha et al., 2012; Winuthayanon et al., 2014). Knock-out studies indicate that ERα-deficient mice are infertile (Lubahn et al., 1993), while studies using tissue-specific ERα knockout models have revealed that stromal ERα is crucial for mediating the initial proliferative effects of estrogen through paracrine signaling (Winuthayanon et al., 2017), while epithelial ERα is essential for subsequent uterine responses and overall fertility (Winuthayanon et al., 2010). In contrast, Progesterone receptor (PR) expression displays a dynamic pattern of expression during early pregnancy, as it is initially expressed in the uterine epithelium, but during the window of implantation, PR expression decreases in the uterine epithelium and increases in the stromal cells (Winuthayanon et al., 2014). Furthermore, mice lacking PR-A and PR-B are entirely infertile due to defects in both ovarian and uterine function (Lydon et al., 1995). Among the two isoforms, PR-A is the essential isoform for reproductive success, as PR-B-deficient mice exhibit normal fertility (Mulac-Jericevic et al., 2000).

The intricate hormonal interplay underscores the importance of estrogen and progesterone in reproductive biology, highlighting their essential roles in establishing a conducive environment for embryo development (Chen et al., 2013). Moreover, the significance of these hormones extends beyond mere implantation; they are also involved in modulating immune responses within the uterus, ensuring that the maternal body does not reject the semi-allogeneic embryo (Kong et al., 2021). This multifaceted role of estrogen and progesterone illustrates the

complexity of reproductive physiology and emphasizes the need for a finely tuned hormonal environment to support successful gestation (Cha et al., 2012; Chen et al., 2013; Wang and Dey, 2006).

1.3.2: Growth factors signaling

Vascular endothelial growth factor (VEGF) signaling

The VEGF signaling plays a critical role in embryonic development and pregnancy progression in peri-implantation stages in mice. VEGF164, the predominant VEGF isoform in the mouse uterus, is expressed in epithelial cells from GD0 to GD3 and in subepithelial stroma on GD2 and GD3 (Chakraborty et al., 1995). Following embryo implantation, VEGF164 becomes localized to the luminal epithelium and stromal cells surrounding the blastocyst(Chakraborty et al., 1995). The presence of an embryo is necessary to induce VEGF expression between GD4.5 and GD6.5, as this elevation is not observed during pseudopregnancy (Tan et al., 2014). VEGF signals through multiple receptors in the peri-implantation mouse uterus, including VEGFR1, VEGFR2, VEGFR3, and neuropilin 1 (NRP1) (Halder et al., 2000). VEGF/VEGFR2 signaling is particularly crucial, as it promotes increased vascular permeability and endothelial cell proliferation around the implantation site (Kim et al., 2013). Studies using VEGF-blocking antibodies have demonstrated that VEGF signaling is essential for successful implantation, as its inhibition reduces vascular permeability at implantation sites (Massri et al., 2023; Rabbani and Rogers, 2001).

The angiopoietin (ANGPT)

The Angiopoietin family also plays a significant role in vascular remodeling during the early stages of pregnancy. Following implantation, Angpt2 and Angpt3, along with their receptor Tie2, are expressed in the endometrium, reaching peak expression levels after decidualization at GD8.5 (Matsumoto et al., 2002; Park et al., 2020b). Moreover, ANGPT4 is expressed in endometrial fibroblasts and endothelial cell populations during decidualization (Scott et al., 2012).

This coordinated expression of angiogenic factors ensures proper vascular development, which is necessary for successful pregnancy progression (Massri et al., 2023).

Epidermal growth factor (EGF)

The epidermal Growth Factor (EGF) family consists of essential signaling molecules that are pivotal during the process of embryonic attachment to the maternal environment in both mice and humans (Governini et al., 2021; Lim and Dey, 2009). The EGF family includes EGF, transforming growth factor-α (TGF-α), heparin-binding EGF-like growth factor (HB-EGF), amphiregulin, epiregulin, betacellulin, and neuregulin (Bhurke et al., 2018; Governini et al., 2021). These critical growth factors signal through four receptor tyrosine kinases: EGFR (ErbB1), ErbB2, ErbB3, and ErbB4, which are present in uterine stromal cells and regulated by steroid hormones. (Franco et al., 2010). In early gestation in mice, progesterone plays a crucial role in modulating the uterine environment and enhances the secretion of Indian hedgehog (IHH) from the uterine epithelial cells (Simon et al., 2009). IHH subsequently binds to its receptor, PATCH, located in the uterine stromal cells (Simon et al., 2009). This receptor-ligand interaction upregulates the expression of epidermal growth factor receptor (EGFR) in the stromal cells (Franco et al., 2010). The activation of EGFR is essential for the proliferation and differentiation of these stromal cells, thereby contributing to the establishment and maintenance of a supportive uterine microenvironment for embryonic development (Bhurke et al., 2018; Franco et al., 2010). Genetic studies have revealed that mice lacking *Egfr* are sub-fertile, with pregnancy failure occurring shortly after implantation due to defects in decidualization and stromal cell proliferation, and differentiation (Large et al., 2014).

Among the EGF family members, HB-EGF serves as one of the earliest molecular markers of implantation, with both transmembrane and soluble forms being exclusively expressed at implantation sites prior to embryo attachment (Lim and Dey, 2009; Paria et al., 2001). This expression begins around 1600 hours on GD3, coinciding with a pivotal moment of uterine receptivity (Chen et al., 2013; Paria et al., 2001). The soluble form of HB-EGF promotes human

blastocyst development and hatching in vitro, while the transmembrane form functions as a juxtacrine growth factor for the blastocyst expressing ErbB4 (Das et al., 1994; Franco et al., 2010). Although other EGF growth factors such as amphiregulin, betacellulin, epiregulin, and neuregulin are expressed during embryo implantation, targeted disruptions of these factors do not result in implantation defects (Bhurke et al., 2018; Lim and Dey, 2009), suggesting a compensatory mechanism due to their overlapping expression (Bhurke et al., 2018).

Fibroblast growth factor (FGF) family

The Fibroblast Growth Factor (FGF) family represents a critical group of growth factors (Beenken and Mohammadi, 2009) within the context of uterine biology, particularly during the peri-implantation phase (Bhurke et al., 2018; Filant et al., 2014). Specific isoforms, including FGF-1, -10, -18, and -21, exhibit predominant expression in stromal cells, with their respective receptors, fibroblast growth factor receptors (FGFRs), notably localized in the epithelial cells of rodent uteri (Li et al., 2011). This expression pattern facilitates critical communication between epithelial and stromal cells, essential for successful implantation. Activating FGFR1 and FGFR2 initiates downstream signaling pathways, notably the Extracellular Signal-Regulated Kinases 1 and 2 (ERK1/2) and Phosphatidylinositol 3-kinase (PI3K) pathways (Ornitz and Itoh, 2015). This signaling cascade enhances the expression of cyclin D1, an essential element for the proliferation of uterine epithelial cells (Filant et al., 2014; Li et al., 2011; Ornitz and Itoh, 2015). Notably, progesterone can inhibit the FGFR-ERK1/2 signaling pathway, facilitating the exit of epithelial cells from the cell cycle and preparing them for embryo implantation (Li et al., 2011). Research demonstrates that the loss of FGFR2 in adult female mice leads to subfertility and eventual infertility, particularly with increased parity (Filant et al., 2014). This highlights the critical nature of FGF signaling in reproductive health (Bhurke et al., 2018). Furthermore, previous research has shown that FGF signaling interacts with other pathways, including the Bone Morphogenetic Protein (BMP) and Wnt pathways, which regulate uterine receptivity and implantation (Monsivais et al., 2017; Wang et al., 2018).

Transforming growth factor-β (TGF-β) superfamily

The Transforming Growth Factor-β (TGF-β) superfamily consists of TGF-β1-3, bone morphogenetic protein (BMP), activins and inhibins, and anti-Müllerian Hormone (AMH). These proteins are crucial for the production of extracellular matrix (ECM), cell growth, and differentiation during embryo implantation (Bhurke et al., 2018; Li, 2014). In human endometrium, the isoforms TGF-β1-3 exhibit unique expression patterns in epithelial and stromal cells throughout the reproductive cycle and early pregnancy, with TGF-β3 showing notable variation across the menstrual cycle, mostly rising in glandular epithelium during the late secretory phase (Bhurke et al., 2018; Dimitriadis et al., 2005; Monsivais et al., 2017). In mouse uteri, TGF-β1 is expressed in the uterine epithelium and TGF-β2/3 present in stromal cells during pre-implantation stages (Das et al., 1992). As embryo implantation approaches, the TGF-β expression intensifies in the uterine compartments, with increased expression of TGF-β2 in the decidualized stroma (Li, 2014).

The TGF-β pathway communicates through two main pathways: SMAD-dependent pathways and non-canonical routes, such as The MAPK and PI3K/AKT signaling pathways, which play significant roles in decidualization, influencing decidual marker expression and trophoblast invasion into the maternal environment (Bhurke et al., 2018; Li, 2014). Specifically, the TGF-β1 regulates decidualization through SMAD-dependent suppression of progesterone receptor (PR) expression and SMAD-independent modulation of Dickkopf (DKK), a Wnt signaling inhibitor, in human endometrial stromal cells (Kane et al., 2008; Monsivais et al., 2017). In contrast, BMP2, which is stimulated by progesterone, promotes decidualization through SMAD1/5/8 signaling (Lee et al., 2007). The dysregulation of TGF-β signaling has been linked to reproductive disorders, including recurrent pregnancy loss and preeclampsia, highlighting its clinical importance (Monsivais et al., 2017).

Other growth factors

Another significant factor is the bone-morphogenetic protein (BMP) family, which is locally activated in the stroma during the embryo attachment. BMP signaling is vital for maintaining the

appropriate spacing of embryos during implantation, underscoring its pivotal role in facilitating successful embryonic development (Paria et al., 2001). Furthermore, the insulin-like growth factor (IGF) system, which includes IGF1, IGF2, and their associated binding proteins, is crucial for multiple roles during pregnancy. This system involves various processes, including pre- and post-implantation embryo development and placentation. In early pregnancy, IGF proteins have been identified in mouse epithelium, stromal cells, and human endometrial decidualized cells, suggesting conserved regulation mechanisms across species. This regulation occurs through intricate autocrine and paracrine signaling mechanisms, highlighting the system's significance in early developmental processes (Bhurke et al., 2018).

1.3.3: Cytokines networks

Cytokines are critical regulators of the complex molecular dialogue during implantation, functioning through autocrine, paracrine, and juxtracrine signaling pathways to orchestrate the precise coordination between the fetal and maternal environment (Bhurke et al., 2018). Among these, the Leukemia Inhibitory Factor (LIF) is essential in establishing uterine receptivity. LIF is expressed in uterine glandular epithelium and is stimulated by the nidatory estrogen surge, which coincides with the period of uterine receptivity on GD3. Lif acts through its receptor complex (LIFR/gp130) to activate STAT3 signaling. Studies using *Lif*$^{-/-}$ mice have demonstrated its essential role in implantation, as these mice fail entirely to achieve implantation despite having normal ovulation and embryo development (Chen et al., 2000; Stewart, 1994). In human endometrium, LIF expression is detected throughout the menstrual cycle with an increase during the mid to late-secretory phase, coinciding with the window of embryo implantation in humans (Chen et al., 1995; Governini et al., 2021).

The interleukin family represents another crucial group of cytokines essential for successful embryo implantation. Interleukin-11 (IL-11) signaling through its receptor IL-11Rα, is particularly critical for decidualization in both mice and humans (Karpovich et al., 2005; Robb et al., 1998). IL-11 plays a crucial role in regulating the proliferation and differentiation of stromal

cells. Research indicates that mice lacking IL-11Rα demonstrate significant impairments in decidual responses, which ultimately leads to failures in implantation (Robb et al., 1998). This highlights the importance of IL-11 signaling in reproductive processes and its potential implications for fertility studies. The interleukin-1 (IL-1) system also plays a role in facilitating communication between the embryo and the uterus by regulating the adhesion molecules involved in implantation (Achache and Revel, 2006). Previous studies have found that IL-1β affects stromal differentiation through modulation of gap junction (connexin 43) and promotes the expression of implantation-related genes (Yu et al., 2017).

The complex cytokine network interacts with other inflammatory and lipid mediators, including prostaglandin and growth factors, to create the controlled inflammatory response essential for successful implantation (Achache and Revel, 2006; Bhurke et al., 2018; Chen et al., 2013; Song et al., 2000; Stewart, 1994). Dysregulation of this cytokine network has significant clinical implications and has been associated with various reproductive disorders, including recurrent implantation failure, early pregnancy loss, impaired decidualization, and abnormal placental development. For example, altered levels of IL-11 and its receptor, along with LIF, have been observed in women with recurrent miscarriages and endometriosis (Dimitriadis et al., 2006), highlighting the importance of proper cytokine regulation for successful pregnancy outcomes.

1.3.4: Lipids mediators signaling

Lipid mediators, often known as eicosanoids, include various bioactive molecules essential for reproductive success. Within the uterine environment, these signaling molecules are synthesized from membrane phospholipids through the action of specific enzymes, playing a significant role in various aspects of early pregnancy (Aikawa and Hirota, 2024). The process begins with the phospholipase A2 enzyme, which cleaves arachidonic acid from the phospholipid bilayer. This released arachidonic acid serves as a substrate for multiple enzymatic pathways, facilitating the production of lipid mediators and oxidized arachidonic acid metabolites essential for the proper functioning of reproductive processes. Eicosanoids are integral to numerous

physiological functions in mammals, including inflammation, cardiovascular functions (such as vasoregulation and platelet functions), temperature homeostasis, pain perception, kidney functions, central nervous system function, and reproduction (Dennis and Norris, 2015). Furthermore, lipid mediators regulate inflammation and immune responses while influencing cellular communication and tissue remodeling. Their role is particularly significant in establishing a successful pregnancy (Clark and Myatt, 2008; Shah and Catt, 2005; Ye et al., 2005). By deepening our understanding of these lipid mediators and their intricate functions, we can gain valuable insights into reproductive health and identify potential therapeutic targets for related disorders such as spontaneous miscarriage and increased infertility risk (Aikawa and Hirota, 2024). Among the various lipid mediators, lysophosphatidic acid, prostaglandin, and cytosolic phospholipase A2 (which plays a crucial role in the production of lipid mediators) (Song et al., 2002) have emerged as critical regulators of inflammation, embryo implantation, and overall reproductive success (Clark and Myatt, 2008; Dennis and Norris, 2015; Kennedy et al., 2007; Shah and Catt, 2005).

Lysophosphatidic (LPA) signaling in embryo implantation

Lysophosphatidic acid (LPA) is a bioactive phospholipid that acts as a potent signaling agonist through G-protein coupled receptors (GPCRs), mediating a variety of physiological and pathological processes, including cellular differentiation, survival, proliferation, migration, tumorigenesis, and cell-cell interactions (Yung et al., 2014). The LPA signaling operates through distinct GPCRs (LPAR1-6), which are differentially expressed across various tissues, including the central nervous system, cardiovascular system, reproductive organs, and immune cells (Kihara et al., 2014). Each type of LPA receptor is associated with distinct G protein subunits, which account for the diverse downstream physiological responses triggered by these receptors (Mutoh et al., 2012).

Among these receptors, LPAR3 has been identified as critical to the success of early pregnancy in murine models. While all LPA receptors are present in the uterine environment

during gestation, genetic studies have demonstrated that only LPAR3 deletion results in significant reproduction deficits (Diao et al., 2015; Ye et al., 2005). Knockout of other LPA receptors, such as LPAR1 and LPAR2, does not impact embryo implantation capacity (Ye et al., 2011). The expression of the Lpar3 receptor peaks in the uterine luminal epithelium on the day when the embryos enter the uterus in a manner dependent on hormonal signals (Hama et al., 2006).

LPAR3-deficient mice display two distinct phenotypes: delayed implantation and abnormal embryo spacing along the oviductal-cervical axis. These phenotypes reveal that LPAR3 normally regulates implantation timing and embryo spacing by ensuring proper uterine receptivity and embryo uterine interactions through multiple mechanisms. These mechanisms include promoting stromal cell proliferation, suppressing progesterone receptor expression in the uterine luminal epithelium, and upregulating prostaglandin synthase 2 (PTGS2) expression to ensure proper prostaglandin biosynthesis essential for implantation. Disruption of these processes in LPAR3-deficient mice manifests in shared placental abnormalities among littermates, ultimately resulting in embryonic resorption and a reduction in litter size (Ye et al., 2005). Notably, exogenous administration of PTGS2-derived prostaglandin (PGE2 and PGI2) to LPAR3-deficient mice partially rescued the implantation delay but failed to correct the embryo spacing defects (Ye et al., 2005). Similarly, pharmacological administration of low-dose (RU486), progesterone receptor antagonist, or estradiol treatment rescues the implantation timing but not the embryo spacing defects (Diao et al., 2015). This selective rescue suggests that LPAR3 regulates implantation timing and embryo spacing through distinct molecular mechanisms. The regulation of LPAR3 expression affects prostaglandin synthesis and hormone receptor signaling, establishing it as crucial for early pregnancy events that integrate paracrine and endocrine signals for successful implantation. These findings hold clinical significance for understanding implantation failure and progesterone resistance. Identifying LPAR3 as a regulator of the uterine hormonal environment

during early pregnancy, opens new therapeutic opportunities for reproductive disorders (Shah and Catt, 2005).

Cytosolic phospholipase A2 (cPLA2) in embryo implantation

While it is not a lipid mediator, cytosolic phospholipase A2 (cPLA2) serves as another critical regulator of the complex process of embryo implantation (Wang and Dey, 2006). The cytosolic phospholipase A2 family comprises six intracellular enzymes: cPLA2α, -β, -γ, -δ, -ε, and -ζ (Leslie, 2015). The $cPLA_2$ enzymes play a crucial role by catalyzing the release of arachidonic acid from the phospholipid membrane, thereby initiating the prostaglandin synthesis pathway, which is essential for pregnancy success; cPLA2α is a key regulator in pregnancy establishment (Song et al., 2002).

During the peri-implantation period in a murine model, cPLA2α expression and activity are tightly regulated by steroid hormones and embryonic signals. The enzyme activity peaks during the peri-implantation window, which coordinates with the expression of PTGS1 in the epithelial cells and PTGS2 in the stromal cells (Chakraborty et al., 1996; Massri and Arora, 2025; Song et al., 2002). The temporal and spatial regulation of cPLA2α expression in the uterine environment is critical, as demonstrated by cPLA2α-deficient mice, which exhibit significant fertility issues (Bonventre et al., 1997). Notably, these reproductive defects parallel those observed in LPAR3-deficient mice (Ye et al., 2005), including both delayed implantation and abnormal embryo spacing, suggesting the potential convergence of these signaling pathways in regulating implantation success (Song et al., 2002). Administration of prostaglandin E2 and carbaprostacyclin (stable analog of prostacyclin) to cPLA2α-deficient mice can restore the on-time implantation, but not the spacing defects, suggesting prostaglandin deficiency is the contributing factor in the observed phenotype (Song et al., 2002).

From a clinical standpoint, the role of cPLA2α in implantation has significant implications for reproductive medicine. Abnormal activity of cPLA2α may be linked to various fertility concerns, including implantation failure and recurrent pregnancy loss (Achache and Revel, 2006). Given the

enzyme's essential function in prostaglandin synthesis and the timing of implantation, it presents a potential therapeutic target for addressing certain types of infertility. Furthermore, assessing cPLA2α activity or expression could act as a biomarker for uterine receptivity, which may aid in optimizing the timing of embryo transfers during assisted reproductive procedures.

1.4: Prostaglandin signaling

Prostaglandins are synthesized by a diverse array of cells throughout the body and function as important autocrine and paracrine signaling mediators, meaning they exert their effects at or near their site of production. Unlike many other signaling molecules, prostaglandins are not stored within cells; rather, they are generated de novo from arachidonic acid released from cell membranes. Various stimuli, including mechanical trauma, specific cytokines, growth factors, and the attachment of blastocysts, can stimulate prostaglandin synthesis (Funk, 2001).

The synthesis pathway for prostaglandin begins with the action of phospholipase A2, which liberates arachidonic acid from membrane phospholipids. This acid serves as the primary substrate for the prostaglandin synthesis pathway (Funk, 2001; Smith et al., 2000). The rate-limiting step is catalyzed by two distinct prostaglandin synthase enzymes, PTGS1 and PTGS2, commonly referred to as COX1 and COX2. Although they are encoded by different genes, these enzymes exhibit similar structural and kinetics properties (Simmons et al., 2004; Smith and Song, 2002). These enzymes perform two critical two-step conversions; the first step is a cyclooxygenase reaction, which converts the arachidonic acid to prostaglandin G2 (PGG2), followed by a peroxidase reaction that reduces PGG2 to prostaglandin H2 (PGH2) (Rouzer and Marnett, 2009). PGH2 serves as the common substrate for terminal prostaglandin synthases that generate five primary bioactive prostaglandins, including PGD2, PGE2, PGF2α, PGI2 (prostacyclin), and thromboxane A2 (Fig. 1.5) (Smith et al., 2000). Once synthesized, prostaglandin is released from the cell through the action of the prostaglandin transporter (PGT). Due to the short half-life of certain compounds, such as prostacyclin and thromboxane, these molecules must act in close proximity to their site of action (Funk, 2001).

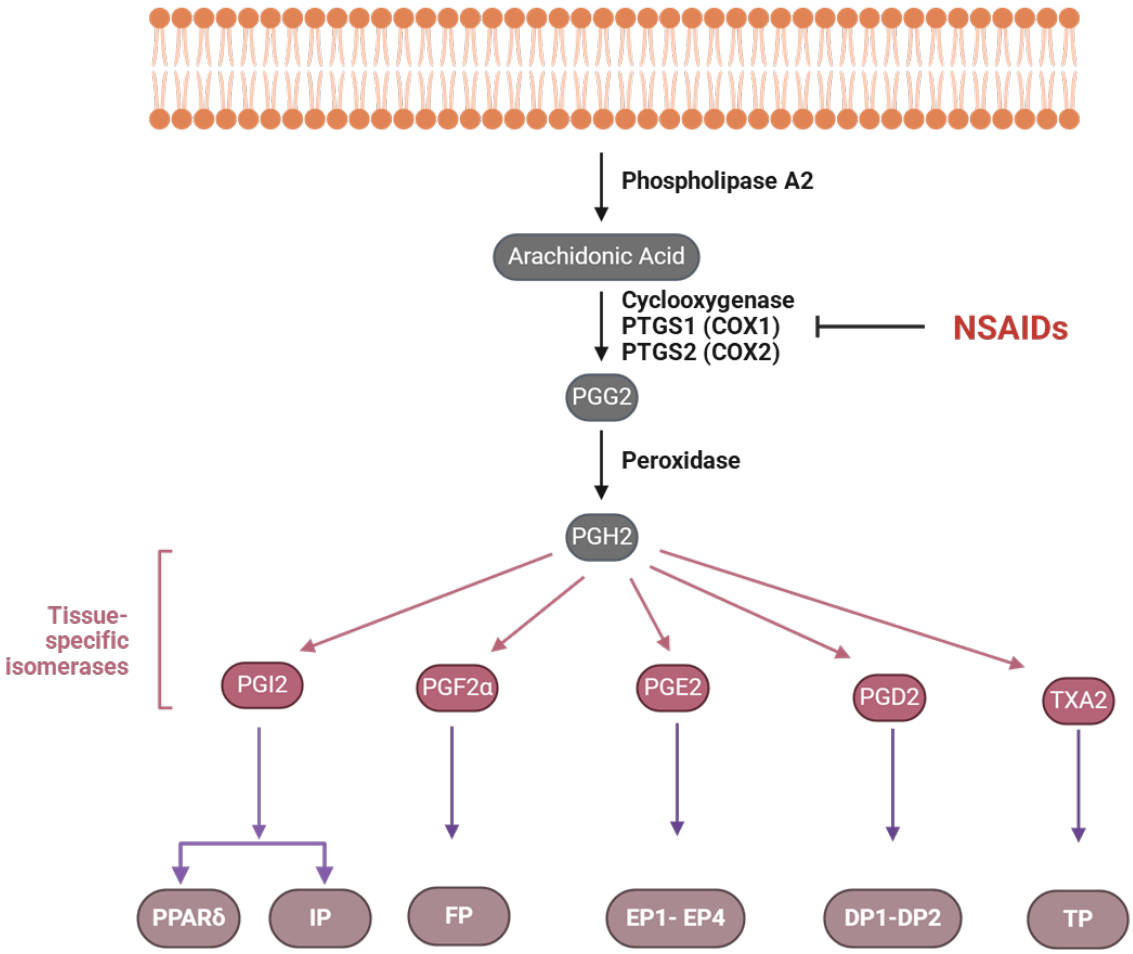

Figure 1.5. Prostaglandin synthesis pathway.

1.4.1: PTGS enzymes structure and function

General structure

Comprehension of the structural features of PTGS enzymes is essential for recognizing their specific roles in prostaglandin synthesis and their varied responses to therapeutic agents, particularly in reproductive processes (Smith et al., 2000). Although PTGS1 and PTGS2 enzymes exhibit approximately 60% amino acid sequence identity and share similar catalytic functions, they possess distinct structural differences that influence their biological and physiological roles (Smith et al., 2000). Both enzymes are homodimeric membrane proteins comprising three primary domains: an N-terminal epidermal growth factor (EGF)-like domain, a membrane-binding motif (MBD), and a large C-terminal catalytic domain (Funk, 2001; Rouzer and Marnett, 2009). Within the catalytic domain, both enzymes include active sites for cyclooxygenase and peroxidase activities (Funk, 2001; Rouzer and Marnett, 2009). The cyclooxygenase site is located in a hydrophobic channel within the protein core, while the peroxidase site is positioned adjacent to a heme prosthetic group near the protein surface (Funk, 2001; Rouzer and Marnett, 2009). These structural features enable PTGS1 and PTGS2 to fulfill several functions across numerous physiological contexts.

Catalytic mechanism

The catalytic mechanism of PTGS enzymes involves a two-step reaction process. In the cyclooxygenase reaction, Tyr-385 initiates the removal of the hydrogen atom from the C-13 position from arachidonic acid. This is followed by adding oxygen at the C-11 and C-15 positions, forming PGG2. Subsequently, the peroxidase reaction reduces the 15-hydroperoxyl group of PGG2 to produce PGH2 through a heme-dependent mechanism (Rouzer and Marnett, 2009; Rouzer and Marnett, 2020).

Key structural differences

A notable distinction between PTGS1 and PTGS2 lies in their substrate-binding channels. PTGS2 features an additional side pocket arising from an amino acid substitution, specifically,

isoleucine at position 523 in PTGS1, with valine at the corresponding position in PTGS2 (Jaén et al., 2018). The amino acid substitution leads to an enlarged side pocket in PTGS2, enhancing the enzyme's capacity to accommodate a broader range of substrates and altering its interactions with endogenous fatty acids and various inhibitors, thereby enhancing substrate binding potential. X-ray crystallographic studies have illustrated how these structural differences influence the binding modes of both substrates and inhibitors, which has aided in the development of selective therapeutic agents, such as celecoxib (Jaén et al., 2018; Rouzer and Marnett, 2009). Furthermore, the substrate-binding channels of PTGS1 and PTGS2 contain critical residues, namely Arg-120, Tyr-355, and Glu-524, that play essential roles in substrate positioning and catalysis (Rouzer and Marnett, 2009; Rouzer and Marnett, 2020).

1.4.2: Transcription and post-transcriptional regulation

The regulation of PTGS1 and PTGS2 differ significantly, highlighting their unique physiological and pathophysiological roles.

PTGS1 regulation

PTGS1, often referred to as the "housekeeping" isoform, is consistently expressed across a wide range of tissues (Dubois et al., 1998; Tanabe and Tohnai, 2002). It plays an essential role in maintaining a baseline level of prostaglandin, critical for various physiological processes such as protecting the gastrointestinal tract from renal perfusion and stomach acid, vascular homeostasis, and reproductive function (Bindu et al., 2020; Herington et al., 2018; Langenbach et al., 1995; Tanabe and Tohnai, 2002). This isoform is found in the stomach, kidneys, intestines, blood vessels, and uterine tissues. While its expression is primarily constitutive, PTGS1 expression can be modulated in certain conditions, particularly when compensatory mechanisms are required (Dubois et al., 1998; Wang et al., 2004a).

PTGS2 regulation

In contrast, PTGS2 is inducible and tightly regulated and can be activated in response to various stimuli, including cytokines, growth factors, inflammatory facilitators, mechanical stress,

and embryo attachment (Dubois et al., 1998; Tanabe and Tohnai, 2002). PTGS2 is expressed in vascular endothelium, macrophages, leukocytes, and fibroblasts (Tanabe and Tohnai, 2002). This differential regulation of PTGS enzymes emphasizes the importance of each isoform in the body's response to normal physiological conditions and pathological challenges (Dubois et al., 1998; Tanabe and Tohnai, 2002).

The PTGS2 promoter contains regulatory elements, including nuclear factor kappa B (NF-κB), cAMP response element (CRE), and nuclear receptor binding sites (Harper and Tyson-Capper, 2008; Jaén et al., 2018). Post-transcriptional regulation is vital for modulating mRNA stability, primarily through the action of AU-rich elements found in the 3'-untranslated region (3'-UTR) and the specific targeting by microRNAs (Harper and Tyson-Capper, 2008; Jaén et al., 2018). Among these, microRNAs such as miR-101 and miR-199a play a critical role in precisely regulating the expression levels of PTGS2 (Harper and Tyson-Capper, 2008; Jaén et al., 2018). This complex regulatory mechanism highlights the significance of both mRNA structural components and microRNA interactions in sustaining cellular homeostasis and effectively responding to physiological and pathophysiological challenges (Harper and Tyson-Capper, 2008; Jaén et al., 2018).

Post-translational control

It is also noteworthy that both enzymes undergo post-translational modifications, including N-glycosylation at multiple sites, which are vital for their proper folding and catalytic efficiency (Harper and Tyson-Capper, 2008; Jaén et al., 2018). These insights underscore the importance of structural differences in enzyme function and the potential for targeted therapeutic interventions (Rouzer and Marnett, 2020). In reproductive tissues, regulatory mechanisms are essential for ensuring the appropriate production of prostaglandin during key reproductive events (Chen et al., 2013).

This precise regulation of PTGS1 and PTGS2 enzymes ensures proper prostaglandin production in both physiological and pathological events. However, while the regulation of PTGS

enzymes determines where and when prostaglandins are synthesized, the specific effects of these prostaglandins are dictated by the distribution and types of prostaglandin receptors present in target tissues.

1.4.3: PTGS enzyme expression in early pregnancy in mammalian species

Having established the structure and regulation of PTGS enzymes, we now turn to their specific roles in early pregnancy, where their expression patterns are crucial for successful reproduction in multiple species (Chakraborty et al., 1996; Cong et al., 2006; Massri and Arora, 2025; Wang et al., 2004b). PTGS enzymes are fundamental regulators of reproductive function, with distinct spatiotemporal expression patterns that respond to both hormonal signals and embryonic cues (Chakraborty et al., 1996; Duffy et al., 2019). The inflammatory nature of key reproductive events shares similarities to classical inflammation, such as increased vascular permeability, immune cell infiltration, and cytokine signaling networks, but differs in being a controlled physiological process without causing tissue damage (Mayoral Andrade et al., 2020). This orchestrated inflammatory-like state requires carefully regulated prostaglandin synthesis across different reproductive tissues (Kennedy et al., 2007; Mayoral Andrade et al., 2020; Richards et al., 2002). These expression patterns show conserved and species-specific variations, as demonstrated by studies across multiple mammalian species (Chakraborty et al., 1996; Cong et al., 2006; Evans and Kennedy, 1978; Kennedy et al., 2007; Wang et al., 2004b).

PTGS1 and PTGS2 expression in mice:

Chakraborty and colleagues identified distinct expression patterns for PTGS1 and PTGS2 during early pregnancy in mice. PTGS1 is consistently expressed in various uterine cell types, with significant luminal and glandular epithelium localization by day 3. Although its expression temporarily decreases during embryo attachment, it resurges in the secondary decidual beds by days 6-7 and can be induced by progesterone and estradiol treatment. In contrast, PTGS2 shows a dynamic expression pattern influenced by embryo presence. It first appears in the luminal epithelium on day 1 and extends to surrounding stromal cells by days 3-4. As pregnancy

advances, PTGS2 expression shifts from the anti-mesometrial to the mesometrial pole between days 5-7 to pregnancy (Chakraborty et al., 1996; Massri and Arora, 2025).

PTGS1 and PTGS2 expression in hamster, skunk, and baboon

In the hamster, the PTGS1 expression decreases in the uterine luminal epithelium as blastocysts proceed to implant. However, PTGS2 expression shows distinct and spatial changes during pregnancy. From day 1-4 of pregnancy, PTGS2 is expressed in the uterine epithelium. During the implantation period, PTGS2 is expressed in the epithelial and the stromal cells and expands to the decidual cells surrounding the implanting embryo. In later stages of pregnancy, PTGS2 is primarily expressed in the trophoblast cells of the embryo (Wang et al., 2004b).

In the skunk uterus, PTGS1 was consistently expressed throughout all examined stages of pregnancy. In contrast, PTGS2 exhibits a tightly regulated expression pattern during this period. Specifically, during the activation of implantation, PTGS2 is first detected in the luminal epithelium when the blastocyst reaches a size of 1.5-1.6 mm. As pregnancy progresses, there is a notable increase in PTGS2 expression in both the luminal and glandular epithelium within the implantation chambers, a pattern that varies depending on the species (Das et al., 1999).

Also, the baboon uterus displays distinct expression patterns of PTGS enzymes during the menstrual cycle and pregnancy. PTGS1 is absent in the follicular phase but shows high expression in the luteal phase, particularly in the luminal and glandular epithelium. In contrast, PTGS2 is present throughout the cycle, mainly in the luminal epithelium. During pregnancy, PTGS1 expression decreases significantly in epithelial cells, while PTGS2 remains expressed in the surface epithelium and increases in stromal cells at implantation sites. By the end of pregnancy, neither PTGS1 nor PTGS2 is detectable in the decidua. Antiprogestin treatment inhibits PTGS1 in the epithelium and causes PTGS2 to disappear from the epithelium but increase in the stroma (Kim et al., 1999).

PTGS1 and PTGS2 expression in humans:

Previous research has also demonstrated the expression of PTGS1 and PTGS2 in various compartments of the human uterus during the implantation process (Marions and Danielsson, 1999). PTGS1 is expressed at a consistent level in the human endometrium. In contrast, PTGS2 is expressed explicitly in glandular epithelial cells, endothelial cells (Marions and Danielsson, 1999), and stromal cells (Stavreus-Evers et al., 2005). These diverse expression patterns of PTGS enzymes across species highlight the conserved nature of prostaglandin signaling in reproduction and the species-specific adaptations that have evolved to support different reproductive strategies.

1.4.4: Components of prostaglandin signaling pathway

Different types of prostaglandins (PGE2/PGI/PGF2a) are essential in pregnancy

Various classes of prostaglandins are pivotal in orchestrating critical functions during pregnancy across mammalian species, utilizing distinct mechanisms and regulated timing (Clark and Myatt, 2008). Among these, PGE2, PGI, and PGF2α play particularly crucial roles at different stages of pregnancy (Clark and Myatt, 2008).

PGE2 functions through four specific receptors (EP1-EP4) and is essential for multiple reproductive processes (Sugimoto et al., 2015). During early pregnancy, PGE2 facilitates ovulation, as demonstrated by studies of EP2-deficient mice that exhibit reduced fertility attributed to compromised ovulation and fertilization processes (Hizaki et al., 1999; Matsumoto et al., 2001). While PGE2 concentrations are elevated at embryo implantation sites (Lim et al., 1999a), and its receptors maintain normal distribution in *Ptgs2*$^{-/-}$ mice (Lim et al., 1997) and in control mice (Yang et al., 1997), exogenous PGE2 administration fails to restore decidualization in *Ptgs2*$^{-/-}$ mice (Lim et al., 1997). This implies that other prostaglandins contribute to successful implantation and decidualization. The absence of implantation or decidualization phenotypes in mice lacking PGE2 receptors further indicates functional redundancy among prostaglandin receptors or that PGE2 signaling is not critical for early pregnancy (Sugimoto et al., 2015; Sugimoto and Narumiya, 2007).

Species-specific studies reveal varied roles for PGE2. In rats, PGE2 increases at blastocyst implantation sites, where it enhances endometrial vascular permeability and decidualization more effectively than other prostaglandins (Kennedy, 1977; Kennedy, 1979; Kennedy, 1985). PGE2 mediates these effects through receptors located at the antimesometrial pole when the rat uterus is primed for decidualization (Papay and Kennedy, 2000), coordinating with other signaling pathways to regulate vascular remodeling and stromal cell differentiation (Kennedy, 1977; Kennedy, 1979; Kennedy, 1985). In humans, reduced endometrial PGE2 levels correlate with recurrent implantation failure, highlighting its clinical importance in endometrial receptivity and implantation success (Achache et al., 2010). Additionally, PGE2 analogs are clinically used to ripen the cervix before labor induction in humans (Clark and Myatt, 2008), and PGE2 signaling is critical for parturition in mice as well (Sugimoto et al., 2015; Thomas et al., 2014).

PGI2 can potentially signal through multiple pathways; research shows that the nuclear receptor PPARδ, rather than the membrane-bound prostacyclin receptor (IP receptor), is the primary mediator of its effects during implantation (Lim et al., 1999a). PPARδ forms heterodimers with RXRα in decidual cell nuclei to regulate genes that are essential for decidualization and angiogenesis (Lim et al., 1999a). The significance of PGI2 signaling is demonstrated by the significant improvement of implantation rates in PTGS2-deficient mice through carbaprostacyclin (cPGI) administration (Lim et al., 1999a). In humans, PGI2 deficiency in the endometrium is associated with unexplained recurrent pregnancy loss in human (Wang et al., 2010).

PGF2α plays critical and diverse roles in pregnancy across different species, though its function can vary between mammals. In mice, PGF2α is particularly essential for parturition, where it is produced through the cPLA2-PTGS1 pathway in uterine decidual cells, which peak around GD17 (Clark and Myatt, 2008; Li et al., 2021; Sugimoto et al., 2015). PGF2α acts primarily through its FP receptors, which induce luteolysis, eventually ceasing progesterone secretion and initiating labor (Sugimoto et al., 2015). Mice lacking FP receptors experience parturition failure

because of an inability to decrease progesterone levels and the upregulation of oxytocin receptors (Sugimoto et al., 1997). PGF2α can be clinically used as a labor-inducing drug, working alongside PGE2 to stimulate myometrial contractions during parturition (Li et al., 2021; Skinner and Challis, 1985; Sugimoto et al., 2015).

The diverse and essential roles of PGE2, PGI2, and PGF2α during pregnancy are mediated through their specific receptors, which show distinct expression patterns and signaling mechanisms throughout gestation (Hirata and Narumiya, 2011; Sugimoto et al., 2015; Yang et al., 1997).

Prostaglandin receptors

The regulated expression of prostaglandin receptors plays a vital role in overall pregnancy success (Sugimoto et al., 2015; Yang et al., 1997). The primary prostaglandin G-protein coupled receptors (GPCRs) compromise several distinct receptor types, including EP1, EP2, EP3, and EP4 (which respond to PGE2), IP (for PGI2), FP (for PGF2α), DP1-2 (for PGD2), and TP (for TXA2). Each receptor is coupled with different G protein subunits, enabling them to stimulate various downstream physiological responses (Sugimoto et al., 2015; Yang et al., 1997). In reproductive tissues, these receptors exhibit distinct functional profiles - EP1, EP3, FP, and TP induce contractile effects on the myometrium, while DP1-2, EP2, EP4, and IP promote relaxant effects (Chen et al., 2013; Sugimoto et al., 2015).

The EP receptor family demonstrates particularly diverse signaling mechanisms. Notably, the EP1 receptor couples with Gq protein, activating phospholipase C, to initiate calcium signaling cascades crucial for decidual function (Sugimoto et al., 2015; Yang et al., 1997). EP1 is expressed in major uterine cell types between GD0-4, and from GD5, EP1 is localized in the decidual cells of the mesometrial pole (Yang et al., 1997). In contrast, EP2 and EP4 receptors couple to Gs proteins, stimulating adenylyl cyclase to increase cAMP levels (Regan, 2003; Sugimoto et al., 2015). Studies of knockout mice have revealed critical roles for these receptors - EP2-deficient mice exhibit infertility and reduced litter size due to failures in both ovulation and

fertilization (Hizaki et al., 1999; Matsumoto et al., 2001). Conversely, EP4 is believed to play a critical role in decidualization, with expression in the stromal cells during the post-implantation stages (Sakamoto et al., 2024; Yang et al., 1997). However, EP4-deficient mice do not survive beyond the perinatal period due to patent ductus arteriosus (Segi et al., 1998), suggesting the need to employ uterine-specific deletion models to illustrate its function (Daikoku et al., 2014; Kim et al., 2018a; Ohyama and Groves, 2004; Soyal et al., 2005). In the peri-implantation uterus, EP4 is present in the uterine luminal epithelium from GD 0 to 1, in the uterine stromal cells and glands from GD 2 to 3 (Lim et al., 1997), and in the uterine epithelium and the stroma surrounding the blastocyst at gestational day 4. Following implantation, EP4 is expressed in both the primary and secondary decidual zones (Yang et al., 1997). The EP3 receptor, which is expressed in the circular smooth muscle between GD2-4 (Lim et al., 1997), is coupled with the Gi protein, inhibits adenylyl cyclase, and shows regulation by steroid hormones along with EP4 (Yang et al., 1997). This suggests their integration within steroid hormone pathways (Yang et al., 1997). Additionally, the FP receptor (PGF2α) links to phospholipase C stimulation and calcium mobilization, accumulating in the decidual cell at the mesometrial pole and undifferentiated stroma pole between GD6-7 (Yang et al., 1997).

Beyond the classical EP and FP receptors, prostacyclin (PGI2) employs dual signaling mechanisms vital for implantation (Lim et al., 1999a). The first mechanism involves the IP receptor, which is not detected during implantation, indicating a potentially limited role (Lim et al., 1999a). Additionally, PGI2 mediates its effects through the nuclear receptor PPARδ pathway, highlighting a unique aspect of prostaglandin signaling in reproduction. PPARδ expression is induced in the peri-implantation stroma, first appearing on the evening of GD3 and peaking around the time of implantation and appearing in the decidua during post-implantation (Lim et al., 1999a). The activation of PPARδ regulates genes integral to decidualization, angiogenesis, and the development of the maternal-fetal interface (Lim et al., 1999a). This dual signaling mechanism enables both immediate cellular responses and longer-term transcriptional regulation.

This intricate network of prostaglandin receptors and their temporally regulated expression patterns highlights the critical importance of precise prostaglandin signaling in reproductive success (Sugimoto et al., 2015). Understanding these pathways not only provides insights into normal pregnancy progression but also offers potential therapeutic targets for reproductive disorders (Sugimoto et al., 2015).

G-protein coupled receptors (GPCRs) and nuclear receptors

Prostaglandin mediates various biological and physiological effects through specific G protein-coupled receptors (GPCRs) or nuclear receptors, with each pathway characterized by unique properties. GPCRs are sophisticated transmembrane proteins that transform prostaglandin binding into precise intracellular responses through molecular events. When prostaglandins bind to their specific receptors, they trigger conformational changes in the GPCR they bind to, which activates the receptor's guanine nucleotide exchange factor activity. This activation prompts the exchange of GDP for GTP on the associated G protein α subunit, causing it to dissociate from the βγ complex. The separated G protein α subunit and the βγ complex initiate distinct downstream signaling cascades, primarily through two major pathways: the cAMP and phosphatidylinositol. The specificity of these responses depends on which G protein alpha subunit is coupled to the receptor. Gs proteins stimulate adenylyl cyclase to increase cAMP, Gi proteins inhibit this enzyme, and Gq proteins activate phospholipase C to trigger calcium signaling (Woodward et al., 2011). These diverse G protein-mediated signaling pathways are accessed through specific prostaglandin receptors, each with distinct coupling preferences and tissue distributions (Sugimoto et al., 2015).

Nuclear receptors represent another significant pathway through which prostaglandin mediates their biological effects (Hirata and Narumiya, 2011). These ligand-activated transcription factors belong to a superfamily of proteins that regulate gene expression by binding to specific DNA sequences in response to various molecular signals. PGI2 exemplifies a unique dual signaling mechanism, operating through GPCR (IP) and nuclear receptor PPARδ pathway (Lim

et al., 1999a). As a PGI2-activated transcription factor within the nuclear hormone receptor superfamily, PPARδ functions by forming heterodimers with the retinoid X receptor (RXR) and binding to specific DNA response elements (Lim et al., 1999a). The receptor can be activated by both endogenous and synthetic ligands, leading to transcriptional activation of target genes that modulate various cellular responses, including differentiation and metabolism (Gupta et al., 2000; Scherle et al., 2000).

The PGI2-PPARδ signaling axis plays crucial roles in multiple physiological and pathological processes. In reproduction, this pathway is essential for embryo implantation, decidualization, and early pregnancy success (Lim et al., 1999a). Additionally, PPARδ signaling has been implicated in colorectal cancer development and inflammatory responses (Casado et al., 2001; Gupta et al., 2000). The receptor shows increased expression during various pathological conditions and notably colocalizes with PTGS2 in specific tissues (Gupta et al., 2000), suggesting coordinated regulation of prostaglandin synthesis and signaling. The diverse functions of the PGI2-PPARδ pathway and its tissue-specific regulation make it an attractive target for therapeutic interventions in multiple contexts, including cancer treatment (Gupta et al., 2000), reproductive medicine, and inflammatory conditions (Daikoku et al., 2005).

Pathways activated by prostaglandin signaling

Prostaglandins exert their biological effects primarily through specific G-protein coupled receptors, activating various downstream signaling pathways that manage the complex aspects of pregnancy (Hirata and Narumiya, 2011; Sugimoto et al., 2015).

PGE2 receptors (EP1-EP2)

PGE2, an essential mediator during pregnancy, interacts with four receptor subtypes (EP1-4), each with specific spatiotemporal expression in the peri-implantation uterine environment (Yang et al., 1997) and distinct signaling pathways depending on the G-protein subunit each receptor is bound to (Sugimoto et al., 2015). The EP1 receptor is intricately linked to the Gαq protein, which activates phospholipase C-β. This enzyme plays a critical role in

catalyzing the hydrolysis of phosphatidylinositol 4,5-bisphosphate (PIP2), yielding inositol 1,4,5-trisphosphate (IP3) and diacylglycerol (DAG). Through this biochemical process, IP3 is responsible for promoting the release of calcium ions from intracellular reserves. In contrast, DAG serves to activate protein kinase C (PKC), which subsequently leads to the phosphorylation of a spectrum of target proteins (Sugimoto and Narumiya, 2007).

EP2 and EP4 receptors are associated with Gs proteins, which facilitate the activation of adenylate cyclase, leading to an increase in intracellular levels of cyclic adenosine monophosphate (cAMP) (Sugimoto et al., 2015; Sugimoto and Narumiya, 2007). The elevation in cAMP activates protein kinase A (PKA), which phosphorylates several substrates, including the transcription factor cAMP response element-binding protein (CREB). The phosphorylated form of CREB interacts with the coactivator CBP/p300 and binds to cAMP response elements (CRE) located in the promoters of target genes, thereby regulating the expression of genes implicated in implantation processes, such as PTGS2, amphiregulin, and decidual prolactin (Sugimoto and Narumiya, 2007; Wang and Dey, 2006).

Beyond these classical signaling pathways, EP receptors also engage in intricate signaling crosstalk. EP4, and to a lesser degree EP2, which couples to Gi, can activate PI3K/AKT signaling through a Gβγ-dependent mechanism that includes the scaffold protein β-arrestin (Sugimoto and Narumiya, 2007). Additionally, EP4 can induce transactivation of the epidermal growth factor receptor (EGFR), which activates the Ras/Raf/MEK/ERK cascade. This EGFR transactivation is a crucial intersection between prostaglandin and growth factor signaling during implantation (Hata and Breyer, 2004).

EP3 is coupled with Gi and primarily inhibits adenylyl cyclase (AC) activity, thereby reducing cAMP levels and affecting downstream signaling pathways, including calcium ion mobilization. Separately, EP3 activation can increase the entry and mobilization of calcium ions via alternative signaling mechanisms (Hata and Breyer, 2004). Due to its diverse C-terminal tails and alternative mRNA splicing, there are multiple variants of EP3 in humans and cattle (Sugimoto

and Narumiya, 2007). These isoforms are capable of activating signaling pathways, including PI3K and PKA/β-catenin, which are also subject to regulation by other EP receptors. Nevertheless, the distinct downstream effects are specifically mediated by the coupling mechanisms associated with the EP3 receptor (Sugimoto et al., 2015; Sugimoto and Narumiya, 2007).

PGI2 receptors (IP and PPARδ)

Prostacyclin (PGI2) transmits signals via the membrane receptor IP and the nuclear receptor peroxisome proliferator-activated receptor delta (PPARδ) pathways. The IP receptor primarily associates with Gs, consequently elevating cyclic adenosine monophosphate (cAMP) levels. Also, PGI2 signals through the PPARδ nuclear receptor. PPARδ receptor, but IP receptor, is the primary receptor that PGI2 acts on to stimulate its effect on implantation and decidualization (Lim et al., 1999a). Once activated, PPARδ forms heterodimers with RXRα in decidual cell nuclei to regulate genes that are essential for decidualization and angiogenesis (Lim et al., 1999a). The signaling capacity through the membrane and nuclear receptors allows PGI2 to regulate immediate cellular responses and longer-term transcriptional changes.

PGF2α (FP receptor)

The FP receptor is associated with the Gq protein, which activates phospholipase C-β. This activation initiates the production of inositol trisphosphate (IP3) and diacylglycerol (DAG), leading to the subsequent release of calcium ions (Hata and Breyer, 2004). Moreover, stimulation of the FP receptor via PGF2α may enhance cell contractility and promote cytoskeletal rearrangement by activating the small G-protein Rho, utilizing a Gq-independent mechanism (Hata and Breyer, 2004). Additionally, analogous to the EP2 receptor, intercommunication between the FP receptor and epidermal growth factor (EGF) has been documented (Hata and Breyer, 2004; Pierce et al., 1999). Activation of the FP receptor triggers the epidermal growth factor receptor (EGFR) and extracellular signal-regulated kinase (ERK) pathway, which is linked to increased proliferation of adenocarcinoma (Hata and Breyer, 2004).

The coordinated activation of these diverse signaling mechanisms allows prostaglandin to regulate both rapid cellular responses through GPCR-mediated pathways and longer-term adaptations via transcriptional changes. This complexity in signaling facilitates precise control of reproductive processes, with disruptions in these pathways potentially leading to various pregnancy complications (Black et al., 2019; Chen et al., 2013; Sugimoto et al., 2015; Wang and Dey, 2006).

1.4.5: Prostaglandins' role in pre-implantation events (ovulation and fertilization)

To investigate the role of prostaglandin in pregnancy events, researchers have employed genetic and pharmacological approaches. Genetic models include mice deficient in PTGS1, PTGS2, or prostaglandin receptors (EP2, EP3, FP), while pharmacological approaches use non-steroidal anti-inflammatory drugs (NSAIDs) as either non-selective inhibitors (indomethacin, ibuprofen) or selective inhibitors (Aspirin for PTGS1; DUP-697, celecoxib for PTGS2). These complementary approaches have revealed stage-specific roles for prostaglandin signaling throughout reproduction. The following section reviews studies from the literature that have evaluated prostaglandin function across various aspects of pregnancy, including ovulation, fertilization, embryo implantation, decidualization, and parturition.

PTGS1 and PTGS2 expression during ovulation

Wang et al. 2004, reports that in preovulatory follicles in mice, PTGS1 is found only in mural granulosa cells, while PTGS2 is present in both mural and cumulus granulosa cells. Following hCG stimulation, PTGS2 is induced at 4 hours, with C57BL/6J/129 mice maintaining expression until 12 hours, while CD1 mice exhibit a decline at 8 hours, followed by re-expression. PTGS1 regulation also differs by mouse strain; CD1 mice show early induction at 4 hours, while C57BL/6J/129 mice are delayed until 8 hours post-hCG. Notably, the presence of either PTGS1 or PTGS2 in mural granulosa cells from 4 to 8 hours before ovulation is vital for successful ovulation, and PTGS2 expression in cumulus cells is critical for optimal oocyte maturation and fertilization (Wang et al., 2004a). The observed strain-specific differences suggest that genetic

background significantly influences the regulation of prostaglandin, which may affect reproductive success rates (Lim et al., 1997; Wang et al., 2004a). Similar genetic variations in PTGS expression and activity have been reported in humans, where polymorphisms in the PTGS2 gene are associated with variations in fertility outcomes and a higher incidence of miscarriage among affected individuals (Salazar et al., 2010).

PTGS2 shows a complex expression pattern regulated during ovulation in the human ovarian system. Following hCG administration, it displays a biphasic profile primarily in granulosa cells, where several genes related to prostaglandin synthesis, such as PLA2G4A and PTGES, are upregulated (Jo et al., 2025). In human granulosa-lutein cells (hGLCs), PTGS2 expression initially rises significantly between 6 and 12 hours after hCG stimulation. The subsequent increase of PTGS2 expression in vivo likely requires additional signals, likely from leukocytes, highlighting the intricate communications involved in regulating ovulation (Jo et al., 2025). Furthermore, in primates, such as monkeys, PTGS1 protein, but not PTGS2, is expressed in the ovarian surface epithelium at baseline levels and at 36 hours post-hCG stimulation. However, Ptgs2 mRNA expression is detectable at baseline and after hCG stimulation. This suggests that PTGS1, not PTGS2, is essential for producing PGE2 during ovulation in monkeys (Cabrera et al., 2006).

PTGS1 and PTGS2 role during ovulation across multiple species

Numerous studies have shown that PTGS2, rather than PTGS1, plays a vital role in ovulation and follicle rupture. In one study, women were administered 25 mg of rofecoxib, a selective inhibitor of PTGS2, orally once a day for nine consecutive days during the ovulatory phase, specifically when the dominant follicle reached a diameter of 14-16 mm. This treatment delayed follicle rupture by over 48 hours following the LH peak, while the placebo group experienced follicle rupture 36 hours after the LH peak. Notably, this treatment did not alter serum levels of steroid hormones, suggesting that while PTGS2 inhibition affects the ovulatory process, it does not impact the concentrations of steroid hormones in peripheral serum (Pall et al., 2001). A study involving rhesus monkeys reports that a single administration of indomethacin, PTGS1,

and PTGS2 inhibitor directly into the pre-ovulatory follicle, either on the day before or the day of the LH surge, can prevent the release of oocytes without affecting follicle rupture. This effect was reversed when PGE2 was administered alongside indomethacin, indicating the critical role of PGE2 in the process of oocyte release in primates (Duffy and Stouffer, 2002).

In rodents, such as rats, indomethacin treatment during proestrus leads to rapid and extensive tissue degradation, resulting in follicle rupture at multiple sites in the follicle wall instead of just at the apex, which causes ovulation failure (Gaytán et al., 2002). Additionally, treatment with NS-398, a PTGS2-selective inhibitor, treatment in rats results in reduced PGE2, PGF2α, and 6-keto-PGF1α production and thus 60% ovulation failure without affecting steroidogenesis (Mikuni et al., 1998).

In a study involving mice, 600 mg/kg of celecoxib, a PTGS2-specific inhibitor, was administered twice daily for four days before the onset of superovulation and for an additional four days afterward. This regimen reduced the number of recovered and fertilized eggs compared to control mice. Although the difference was insignificant compared to the control, the PTGS2 inhibition affected ovulation and fertilization in the treated mice (Reese et al., 2001). However, the drug's effect was not as severe as reported in the *Ptgs2*$^{-/-}$, which displayed both ovulation and fertilization failures (Lim et al., 1997). These findings suggest that the effects of celecoxib were less significant than the deficiencies observed in the PTGS2-deficient mice. These results highlight that prostaglandins are also substantial for oocyte fertilization. The ovulatory defects reported in *Ptgs2*$^{-/-}$ were mainly attributed to the abnormal cumulus expansion observed, which was also noted in the *EP2*$^{-/-}$ mice, suggesting that PGE2 signaling is critical for mouse ovulation success (Matsumoto et al., 2001). However, the ovulatory defects in the *Ptgs2*$^{-/-}$ mice are more evident in adults than in immature mice, suggesting that with aging, prostaglandin becomes compromised upon PTGS2 ablation (Matsumoto et al., 2001). PTGS2 deficiency results in fertilization defects in *Ptgs2*$^{-/-}$ and *EP2*$^{-/-}$ mice (Davis et al., 1999; Lim et al., 1997). However, this may be due to a disruption in the microenvironment of the oviduct, which is essential for the

fertilization process, alongside issues with ovulation and oocyte maturation (Davis et al., 1999; Lim et al., 1997).

1.4.6: Prostaglandins' role in implantation and decidualization

Research on implantation suggests that women who experience spontaneous abortions or recurrent implantation failures after in vitro fertilization (IVF) typically have lower levels of PTGS2 and its derived prostaglandins, such as PGI2, in their endometrium (Achache et al., 2010; Wang et al., 2010). This implication highlights the critical role of PTGS2 in successful implantation. Furthermore, women with a polymorphism in the PTGS2 gene exhibit an increased risk of implantation failure (Salazar et al., 2010). No studies have established a link between PTGS1 deficiency and implantation issues. In animal studies, specifically with *Ptgs1*$^{-/-}$ mice, reproductive problems are not apparent, apart from prolonged parturition, which can result in the death of the pups. Concerning PTGS2, research indicates that wild-type blastocysts fail to implant in *Ptgs2*$^{-/-}$ mice, and stimulation with oil does not trigger a decidualization response in these mice (Lim et al., 1999a; Lim et al., 1997). This evidence underscores the importance of PTGS2 for both embryo implantation and decidualization. Research has demonstrated that while PTGS2 can compensate for the absence of PTGS1 during early pregnancy, PTGS1 cannot fulfill this role when PTGS2 is absent, leading to reproductive complications (Li et al., 2018b; Reese et al., 1999). This was shown in studies with mice deficient in these genes. Additional experiments indicated that inhibiting PTGS2 or PGI synthase (responsible for producing PGI2) resulted in a decreased success rate of embryo implantation (Pakrasi and Jain, 2008). However, the reintroduction of PGI2 restored implantation rates to normal levels. Furthermore, blocking PGIS in the uterus on day 3 of pregnancy caused the embryos to deteriorate, preventing any implantation by day 4 (Pakrasi and Jain, 2008). These findings underscore the crucial role of PGI2, produced through the PTGS2 pathway, in enabling successful embryo implantation.

Research findings have sparked interesting debates about PTGS2's exact role in uterine function and embryo implantation in mice (Cheng and Stewart, 2003; Lim et al., 1997). One

revealing study found that normal embryos could successfully implant and grow to full term when placed in surrogate mothers lacking PTGS2, suggesting this enzyme isn't required for implantation, embryo growth, and pregnancy success. Yet, there was still evidence of PTGS2's importance. These surrogate mothers showed a one-day delay in the initial development of decidual tissue after implantation, aligning with earlier research about PTGS2's role in the uterine response (Cheng and Stewart, 2003; Lim et al., 1997). Adding another layer of complexity, the genetic makeup of different mouse strains appears to influence these outcomes significantly. For instance, while mice with a C57BL/6J/129 background completely failed to reproduce without PTGS2, CD1 strain mice lacking PTGS2 maintained some fertility, though at reduced levels - showing drops of more than 50% in various reproductive measures including fertilization, early embryo development, implantation, and litter size. This better reproductive performance in CD1 mice was traced to their ability to increase PTGS1 production to partially compensate for the missing PTGS2 - an adaptation that depends on their genetic background (Wang et al., 2004a). Despite these varying results across different mouse strains, the overall evidence still points to PTGS2 signaling as a crucial component for normal reproduction in living organisms (Kennedy et al., 2007).

Vascular remodeling

Prostaglandin synthesis is necessary for the increased vascular permeability and uterine angiogenesis associated with early pregnancy. Prostaglandins, such as PGE2, PGI2, and PGF, are vasoactive factors that are synthesized by PTGS enzymes (Chakraborty et al., 1996; Funk, 2001). PTGS2-derived prostaglandins (PGE and PGI2) are elevated in the implantation sites in several mammalian species (Kennedy, 1977; Kennedy, 1985; Kennedy and Zamecnik, 1978; Lim et al., 1999a; Matsumoto et al., 2002; Pakrasi and Dey, 1982). In rodents, genetic or pharmacological depletion of prostaglandin function during pre-implantation is associated with abnormal post-implantation events including implantation failure or decreased vascular permeability and impaired decidualization, resulting in embryo growth restriction observed

between GD5 – GD7 (Boshier, 1970; Deanesly, 1967; Kennedy, 1985; Keys et al., 1986; Lau et al., 1973; Lim et al., 1999a; Lim et al., 1997; Sookvanichsilp and Pulbutr, 2002). *Ptgs2*$^{-/-}$ mice also show defects in implantation and vascular permeability, and daily intraperitoneal administration of carbaprostocyclin (a stable analogue of PGI2) to *Ptgs2*$^{-/-}$ mice starting at GD3.75 improves implantation at GD5 and GD7. VEGF and VEGFR2 expression, along with the number of blood vessels, was also restored (Lim et al., 1999a; Lim et al., 1997; Matsumoto et al., 2002), suggesting that prostaglandin depletion phenotypes are partly associated with disrupted VEGF signaling. Despite the observations that prostaglandin and VEGF signaling is associated with increased vascular permeability in early pregnancy (Kennedy, 1979; Kennedy, 1985; Matsumoto et al., 2002), the impact of prostaglandins and VEGFs on vessel structure around the site of embryo attachment is not entirely understood.

1.4.7: The role of prostaglandin in later pregnancy (parturition)

During the final stages of pregnancy, a precisely orchestrated series of molecular events involving prostaglandin guides the birth process. During later stages of pregnancy, uterine decidual cells produce PGF2α, which peaks as delivery approaches (Olson and Ammann, 2007). This prostaglandin travels to the ovaries, where it binds to FP receptors on luteal cells, triggering luteolysis (breaking down of the corpus luteum) and the subsequent shutdown of progesterone production (Sugimoto et al., 2015). The resulting drop in progesterone levels enables the uterine muscle tissue to activate crucial labor-associated genes, particularly PTGS1, thereby initiating labor-associated changes (Gross et al., 1998; Olson and Ammann, 2007).

Two key prostaglandins, PGF2α and PGE2, emerge as central regulators in the tissues surrounding the developing fetus (Yang et al., 1997). These prostaglandins act as natural stimulants of myometrial contractility through their specific receptors, FP and EP3 respectively (Myatt and Lye, 2004). Numerous lines of evidence indicate the critical role of prostaglandin in parturition: prostaglandin levels significantly increase during labor, and administering exogenous prostaglandin can also stimulate labor (Olson and Ammann, 2007; Sugimoto et al., 2015).

Furthermore, blocking prostaglandin synthesis with NSAIDs can delay labor onset (Reese et al., 2000). This understanding has critical clinical applications, as NSAIDs are routinely used to postpone preterm labor in both human and veterinary medicine. While the use of NSAIDs to delay labor is clinically relevant in both human and veterinary medicine, it is crucial to exercise caution when administering these drugs. For example, PTGS2-specific inhibitors, which are effective at postponing labor, can interfere with the closure of the ductus arteriosus at birth. This risk may lead to neonatal mortality in animal studies, such as those involving mice (Reese et al., 2000). In contrast, PTGS1-specific inhibitors do not carry these risks and can effectively delay labor with fewer adverse effects on maternal and fetal health (Loftin et al., 2002).

The critical role of prostaglandin signaling in parturition is further demonstrated through genetic studies. Mice deficient in PTGS1 experience prolonged and difficult labor with increased perinatal mortality (Gross et al., 1998; Langenbach et al., 1995), confirming that PTGS1-derived prostaglandins are essential for normal parturition. While the maternal decidual cells are the primary source of prostaglandins during labor, both maternal and fetal tissues contribute to the prostaglandin pool necessary for a successful delivery (Gross et al., 1998). Nonetheless, it is the maternal PTGS1-derived prostaglandins that ultimately regulate the timing of delivery (Gross et al., 1998).

1.5: Clinical relevance and therapeutic implications

Prostaglandin and reproductive health

Understanding prostaglandin signaling holds considerable implications for reproductive medicine, particularly concerning fertility and the management of pregnancy. Both naturally occurring conditions and therapeutic interventions underscore the clinical significance of these pathways.

Clinical evidence from human studies

Pregnancy success depends on precisely orchestrated molecular events during implantation and early pregnancy, with prostaglandin signaling playing a crucial regulatory role in

embryo movement and implantation (Chen et al., 2013). The clinical significance of prostaglandin in human reproduction has been a subject of ongoing debate, particularly regarding the impact of NSAIDs on pregnancy outcomes (Black et al., 2019). While some studies report an 80% increased risk of miscarriage with NSAID consumption during early pregnancy (Li et al., 2003), others find no significant association between NSAID use and adverse pregnancy outcomes (Daniel et al., 2014). These conflicting findings suggest that the effects of prostaglandin inhibition may depend on specific timing, dosage, or individual patient factors that remain poorly understood (Black et al., 2019). Furthermore, defective prostaglandin signaling has been observed in patients experiencing spontaneous pregnancy loss and recurrent miscarriage following in-vitro fertilization procedures (Achache et al., 2010; Wang et al., 2010). Notably, PTGS2-derived prostaglandins exhibit downregulation in endometrial samples obtained from these individuals (Achache et al., 2010; Wang et al., 2010). Genetic variations within the PTGS2 gene correlate with an increased risk of implantation failure (Salazar et al., 2010). These studies underscore the clinical significance of prostaglandin signaling, particularly during early pregnancy.

The controversy surrounding the role of PTGS2 in early pregnancy based on studies in mice

Similar controversies exist in animal models studying prostaglandin function in reproduction. Initial studies showed that PTGS2-deficient mice are completely infertile, with defects in ovulation, fertilization, implantation, decidualization response (Lim et al., 1997; Matsumoto et al., 2002). However, subsequent research demonstrated that when wild-type embryos were transferred to PTGS2-deficient pseudo-pregnant mice, while there was a 24-hour delay in decidualization, the mice successfully maintained pregnancy and delivered live pups (Cheng and Stewart, 2003). This apparent discrepancy has been partially explained by studies showing that the effects of PTGS2 deficiency can vary with genetic background, where mixed background mice show compensatory upregulation of PTGS1 that maintains fertility (Wang et al., 2004a). Also, PTGS2 from wild-type embryos might play a role in the success of implantation and pregnancy. These conflicting findings highlight the complexity of prostaglandin regulation in

reproduction and the need for a more precise understanding of cell-type-specific requirements and temporal regulation.

Research questions

The divergent findings underscore the intricate nature of prostaglandin regulation within reproductive processes and the necessity for a more nuanced comprehension of cell-type-specific requirements and temporal dynamics. Several pivotal inquiries persist: Which particular endometrial cell types require PTGS2 for the successful establishment of pregnancy? In which ways do various PTGS inhibitors impact discrete phases of early gestation? Furthermore, how do these molecular phenomena alter the three-dimensional architecture of the peri-implantation uterine environment?

Chapter 2: Materials and methods

2.1: Animals

Ptgs2-/- used in this study were the same mice used in previous studies (Dinchuk et al., 1995; Lim et al., 1997) (**Table 2.1**). We generated the *Ptgs2* conditional deletion mice by breeding C57/bl6 *Ptgs2*$^{f/f}$ (Ishikawa and Herschman, 2006) with C57/bl6 *Ltf*$^{cre/+}$ (Daikoku et al., 2014), mixed genetic background *Pax2*$^{cre/+}$ (Ohyama and Groves, 2004), or C57/bl6 *Pgr*$^{cre/+}$ (Soyal et al., 2005) mice (**Table 2.1**). For NSAIDs, we used adult CD1 mice aged between 6 and 10 weeks (**Table 2.1**). For pregnancy studies, we set adult females at 6-10 weeks to mate with fertile males. For *Ltf*$^{cre/+}$*; Ptgs2*$^{f/f}$, we mated them between 10-12 weeks, as PTGS2 deletion occurs in the adult females (Daikoku et al., 2014). To create pseudopregnancy, we mated females with vasectomized males. The appearance of a vaginal plug was identified as a gestational day (GD) GD0 1200h. We euthanized mice at several stages, including GD3 1200h and GD3 1800h, GD4 1800h, GD5.5, GD8.5, and GD12.5. For the NSAID studies, GD3.75 time point, dissections were performed on GD3 between 1800h and 2100h. For GD4.5, GD5.5, GD7.5, and GD12.5, dissections were conducted on the respective days between 1200h and 1500h. Alternatively, some mice were allowed to go to term to evaluate litter size, and the litter was sacrificed immediately after assessment. To induce an artificial decidualization, we used a non-surgical embryo transfer (NSET) device, where we transferred 1 µl sesame oil and 3 µl PBS to a pseudopregnant mouse on either pseudopregnancy day 2 1800h or day 3 0800h. We euthanized the oil-stimulated pseudopregnant mice at pseudopregnancy day 3 1200h or day 5.5. For GD4 and GD5 dissections, we euthanized the animals 10 minutes after 0.15 ml intravenous injection of 1.5% of Evans blue dye (MP Biomedicals, ICN15110805). The uteri from GD4.5-GD12.5 time points were photographed under white light to observe implantation and decidual sites. All mice were maintained on a 12-hour light/dark cycle, and all mouse studies and protocols were approved by the Institutional Animal Care and Use Committee at Michigan State University.

Model	Compartment	Deletion time
***Ptgs2*$^{-/-}$**	Global deletion	Gene targeting (Dinchuk et al., 1995)
***Ltf*$^{cre/+}$*; Ptgs2*$^{f/f}$**	Uterine epithelium (LE, GE)	Adult (> 8.5 weeks) (Daikoku et al., 2014)
***Pax2*$^{cre/+}$*; Ptgs2*$^{f/f}$**	Uterine epithelium (LE, GE) and endothelium	Embryonic (GD11.5) (Ohyama and Groves, 2004)
***Pgr*$^{cre/+}$*; Ptgs2*$^{f/f}$**	Ovarian granulosa cells, oviductal epithelium and myometrium, uterine epithelium (LE, GE), circular smooth muscle and stroma	Neonatal (P5 epithelium, stroma, P21 circular muscle) (Madhavan and Arora, 2022; Soyal et al., 2005)
6mg/kg Indomethacin	Systemic inhibition of PTGS1 and PTGS2	During embryo implantation on GD3 (Lau et al., 1973)
700 nmol Aspirin	Systemic inhibition of PTGS1	During embryo implantation on GD3 (Lim et al., 1997)
600 nmol Dup-697	Systemic inhibition of PTGS2	During embryo implantation on GD3 (Lim et al., 1997)

Table 2.1: Mouse models used to study PTGS2 function in the murine reproductive tract. The table outlines the models utilized in the study, along with the corresponding tissues and times of deletion or inhibition for PTGS2 or PTGS1, or both. *Ptgs2*$^{-/-}$ deletes PTGS2 constitutively in all body tissues. *Ltf*$^{cre/+}$*; Ptgs2*$^{f/f}$ deletes PTGS2 in the uterine luminal and glandular epithelium in adult mice > 10 weeks. *Pax2*$^{cre/+}$*; Ptgs2*$^{f/f}$ deletes PTGS2 in the uterine luminal, glandular epithelium, and uterine endothelium at the embryonic stage. *Pgr*$^{cre/+}$*; Ptgs2*$^{f/f}$ deletes PTGS2 in the ovary, oviduct, and uterine epithelium (luminal and glandular epithelium), circular smooth muscle, and stroma during neonatal stages. In addition to pharmacological models, indomethacin (PTGS1 and PTGS2 inhibitor), Aspirin (PTGS1-specific inhibitor), and Dup-697 (PTGS2-specific inhibitor). LE: Luminal Epithelium, GE: Glandular Epithelium.

2.2: Drugs

Indomethacin (Sigma-Aldrich, I7378-5G) was dissolved in 0.01% Dimethyl sulfoxide (DMSO) in PBS to a final concentration of 1mg/ml, and mice were intraperitoneally injected with either 150 ul or 50 ul (6mg/kg or 2mg/kg) on gestational day 3 (GD3) at 0800h and 1400h. Aspirin (Sigma-Aldrich) was dissolved in 0.01% ethanol in PBS to a final concentration of 7 mM, and 100 µl (700 nmol) (Lim et al., 1997) of this solution was intraperitoneally injected in CD1 mice on GD3 at 0800h and 1400h. Dup697 (Sigma-Aldrich) (PTGS2 specific inhibitor) was dissolved in 0.1% DMSO in PBS to a final concentration of 6 mM. Mice were intraperitoneally injected with 100 µl

(600 nmol) (Lim et al., 1997) intraperitoneally on GD3 at 0800h and 1400h. The drug doses were selected based on previous studies (Lau et al., 1973; Lim et al., 1997). Control mice for all drug treatments received only vehicle treatment (0.01% DMSO in PBS, 0.01% ethanol in PBS, or 0.1% DMSO in PBS, respectively) on GD3 at 0800h and 1400h. The twice-daily dosing schedule was chosen based on the pharmacokinetic properties of these compounds (Bindu et al., 2020).

2.3: Whole-mount immunofluorescence staining

As described previously (Arora et al., 2016; Flores et al., 2020; Madhavan et al., 2022) for whole-mount staining, we fixed dissected uteri in a mixture of cold DMSO: Methanol (1:4). We hydrated the samples in a (1:1) methanol: PBST (PBS, 1% triton) solution for 15 minutes, followed by a 15 minutes wash in 100% PBST. We then placed the samples in a blocking solution (PBS, 1% triton, and 2% powdered milk) for 1 hour at room temperature, followed by incubation with primary antibodies (**Table 2.2**) in the blocking solution for seven nights at 4°C. After washing with 100% PBST solution for 2X15 minutes and 4X45 minutes, we incubated the samples with Alexa Flour-conjugated secondary antibodies for three nights at 4°C (**Table 2.2**). Following the incubation, we washed the samples with 100% PBST for 2X15 minutes and 4X45 minutes and incubated the samples at 4°C overnight with 3% H2O2 diluted in methanol. Finally, we washed the samples with 100% methanol for 3X30 minutes and cleared the tissues overnight with benzyl alcohol: benzyl benzoate (1:2) (108006, B6630, Sigma-Aldrich).

2.4: Cryo-embedding, cryo-sectioning, and immunostaining

As described previously (Granger et al., 2024) we fixed uterine tissues in 4% PFA (paraformaldehyde) for 20 minutes and then incubated the samples with fresh 4% PFA overnight at 4˚C. The tissues were then washed with 100% PBS for 3X5 minutes and then incubated in 10% sucrose/PBS at 4°C overnight. We then transferred the samples to 20% and 30% sucrose solutions in PBS for 2-3 hours each at 4°C. Then we embedded the samples in tissue-Tek OCT (Andwin Scientific, 45831) and stored at -80°C. Cryo-sections of 7µm thickness were mounted on glass slides (Fisher, 1255015). For the immunofluorescent staining, we allowed the slides to air

dry for 15 minutes and then washed with 100% PBS for 3X5 minutes, and blocked with PBS + 2% powdered milk + 1% triton solution for 20 minutes. After additional 100% PBS for 3X5 minutes washes, we stained the slides with primary antibodies (**Table 2.2**) and incubated them at 4°C overnight. The next day, slides we washed the slides with 100% PBS for 3X5 minutes and incubated the sections with secondary antibodies and Hoechst (**Table 2.2**) for 1 hour at room temperature. Finally, after PBS washes, we added 2 drops of 20% glycerol in PBS to the slides followed by sealing the sections with glass coverslips.

2.5: In situ hybridization

We performed in situ hybridization on uterine sections using the RNAscope 2.5 HD Assay-RED kit (ACD Bio, 322350), which also has immunofluorescence capabilities, as described previously (Granger et al., 2024). We aimed to detect *Lif* mRNA associated with the uterine glands at GD3 1800h. To detect *Lif*, we used the Mm-Lif probe (ACD Bio, 475841), and to label uterine glands, we included immunostaining for FOXA2 (**Table 2.2**). The entire 3-day protocol was carried out according to the protocols provided by ACD Bio (322360-USM, MK 51-149 TN).

Primary antibody	Dilution	Stained tissues
Rat-anti-CDH1 (M108, 108006, B6630)	1:500	Luminal epithelium
Rabbit anti-FOXA2 (Abcam, ab108422)	1:500 (WM) 1:200 (sections)	Glandular epithelium
Rabbit anti-PTGS2 (Abcam, ab16701)	1:500	PTGS2-positive cells
Armenian-hamster anti-CD31 (DSHB, AB_2161039)	1:200	Endothelial cells
Secondary antibody	**Dilution**	
Goat anti-Armenian hamster 647 (Invitrogen, A78967)	1:500	
Goat anti-rat 647 (Invitrogen, A21247, CA, USA)	1:500	
Donkey anti-rabbit 555 (Invitrogen, A31572)	1:500	
Donkey anti-rat 488 (Invitrogen, A21208)	1:500	
Nuclear marker	Dilution	
Hoechst (Sigma Aldrich, B2261)	1:500	

Table 2.2: Primary and secondary antibodies used in the study.

2.6: Serum progesterone measurement

After euthanizing the mouse, we collected 200-500 µl of blood samples and left them at room temperature for 30 minutes. Then, we centrifuged the samples for 15 minutes at 2000 g, carefully separated the supernatant, and immediately saved the samples at -20°C. Following sample collection and preservation, we sent the samples to a Ligand Assay and Analysis Core Laboratory in Charlottesville, VA, to determine progesterone levels. Samples were diluted at a ratio of 1:4, tested in triplicate to ensure accuracy, and the results were reported in ng/ml.

2.7: Oviduct flush and in vitro embryo culture

For oviduct flush at GD1 1200h, we euthanized the female mice, excised both oviducts and placed them in warm (37°C) M2 medium (Sigma-Aldrich). We flushed each oviduct with approximately 300 – 500 ul of pre-warmed (37°) M2 medium using a blunted 30-gauge needle attached to a 1ml syringe. We collected embryos and unfertilized eggs using a mouth pipette with a pulled glass capillary. After washing them 2 to 3 times in warm (37°C) KSOM medium (CytoSpring), we incubated them in 400-600 µl drop of KSOM media and placed them in a 37°C jacketed incubator. We monitored embryonic development daily for 72 hours and recorded the number of embryos reaching 4-cell, 8-cell, morula, and blastocyst stages (Frum and Ralston, 2019).

2.8: RNA isolation, cDNA synthesis, and quantitative PCR

We isolated uterine decidual tissues at GD5.5, snap-froze, and stored the samples at -80 °C. We isolated total RNA from tissues using the Trizol reagent (Invitrogen, Thermo Fisher Scientific, 15596019). Briefly, we homogenized the tissues in 1 ml TRIzol solution using the Bead Mill 4 homogenizer (Thermo Fisher Scientific). Following phase separation with 500 µl chloroform, RNA was precipitated with isopropanol and washed with 75% ethanol. Then, we suspended the RNA in 50-100 µl RNase-free water (Invitrogen, Thermo Fisher Scientific, AM9922). We measured the RNA concentration and purity using a NanoDrop 2000 spectrophotometer (Mettler Toledo) with a concentration of at least 250 ng/µl. We performed first-strand cDNA synthesis from 1 ug RNA using reverse transcriptase enzyme. For qRT-PCR, we designed the primers using the primer3Plus and NCBI website (**Table 2.3**). We carried the qRT-PCR reactions in triplicate for each sample using the Quantstudio 5 Real-Time PCR system (Applied Biosystems) with a total reaction volume of 20 µl (10 µl SYBER Green, 7.4 µl Rnase and Dnase free water, 1.6 µl primer, and 1 µl cDNA). We used the comparative CT (ΔΔCt) method for gene expression analysis. We calculated the ΔCt for each sample by subtracting the Ct value of the *Rpl19* gene from the Ct value of the target gene. We calculated ΔΔCt by subtracting the mean ΔCt of the control group from the ΔCt of each sample. Fold change reported as 2^(-ΔΔCt) (Livak and Schmittgen, 2001).

Gene	Forward	GC%	TM	Reverse	GC%	TM	Product size
Bmp2	TCCCTCGGACAGAGCTTTT	48%	60.3	AAGCAGCAACACTAGAAGACAGC	53%	59.9	133
Wnt4	ACTGGACTCCCTCCCTGTCT	50%	60.1	TCACAGCCACACTTCTCCAG	55%	60	144
Igfbp1	GATCAGCCCATCCTGTGG	61.1%	60	GTTGGGCTGCAGCTAATCTC	55%	60	136
Prl3c1	ACCAAGATGTGCCAAACCA	47.4%	60	CTGCAGGTATGAGCATTTTCAG	45.5%	59.9	118

Table 2.3: Primers sequences for Quantitative real-time polymerase chain reaction (PCR). Forward and reverse primer sequences for decidualization genes (*Bmp2*, *Wnt4*, *Igfbp1*, *Prl3c1*). TM: melting temperature.

2.9: Confocal microscopy

We used a Leica SP8 TCS white light laser confocal microscope utilizing 10x air to image whole uterine tissues or 20X water objective and a 7.0 um Z stack or system-optimized Z stack to image the samples (Madhavan et al., 2022). Upon imaging, we imported the files (.LIF format) into Imaris v9.2.1 (Bitplane; Oxford Instruments, Abingdon, UK) 3D surpass mode. We created 3D renderings using surface modules.

2.10: Image analysis

Implantation chamber, luminal epithelium, and embryo visualization

We used the CDH1 fluorescent signal for the luminal epithelium surface and the FOXA2 fluorescent signal for uterine glands to visualize the implantation chamber. We isolated the luminal epithelium by subtracting the FOXA2-specific signal from the CDH1 signal. We used the Hoechst signal to locate embryos based on the inner cell mass (ICM) signal, and we used the 3D rendering surface in IMARIS software to create the embryo surfaces. We used the measurement function in Imaris to measure the length of the implantation chamber from the mesometrial to the anti-mesometrial pole.

Leukemia inhibitory factor (Lif) quantitation

As described (Granger et al., 2024), we used the FOXA2 signal to generate 3D surfaces of the glands' nuclei via the 3D surface function within the IMARIS software. Subsequently, we used the IMARIS masking function to produce a distinct channel for the *Lif* signal that lies beneath the previously established uterine gland 3D surface. Based on the new channel for the *Lif* signal, we created a new 3D surface of *Lif*. Following the creation of the 3D surfaces, we used the statistics function of Imaris to determine the 3D surface volume of both the glands and *Lif*. We used Microsoft Excel to calculate the *Lif* volume per uterine gland volume and plotted the results as *Lif* volume per uterine gland volume (FOXA2 signal) with normalized units.

Vessel density around the anti-mesometrial pole of the implantation chamber

We created a 3D rendering surface of blood vessels using a CD31 fluorescent signal and generated a channel in Imaris software to mask the surface of the blood vessels. For image segmentation, we imported 14 µm of the masked channel of vessels to ImageJ after adjusting the scale and applying the threshold function. Using vessel analysis and Mexican Hat Filter Plugins in ImageJ (https://imagej.net/), we calculated the density and diameter of the blood vessels in the embryo implantation and inter-implantation site. For vessel density the data is reported as the percentage of area occupied by blood vessels.

Embryo location

To perform a comprehensive analysis of embryo locations, we initiated the process by creating detailed 3D renderings of several key anatomical features: the oviductal-uterine junction, the embryos themselves, and the uterine horns as described previously (Flores et al., 2020). This step was accomplished using the Surface module, which allowed us to visualize these structures in three dimensions effectively. Following the creation of these renderings, we utilized the Measurements module to identify and meticulously record the three-dimensional Cartesian coordinates for the center of each surface. By projecting these coordinates onto the x-y plane, we were able to calculate several important distances: the distance between the oviductal-uterine

junction and each embryo (referred to as OE), the distances between adjacent embryos (designated as EE), and the overall length of the uterine horn. To address the natural variations in uterine horn lengths observed among the different mice, we normalized all measured distances to the respective horn length. This approach allows us to present the mean values for OE, EE, and other distance measurements as ratios, ensuring they are unitless and comparable across samples.

2.11: Statistical analysis

We used Graph Pad Prism (Dotmatics; GraphPad, La Jolla, CA, USA) and Microsoft Excel to analyze the statistical differences between the treatment groups and plot our graphs. To analyze the difference between the two treatment groups, we employed the unpaired parametric two-tail t-test. First, we tested the data for homogeneity of the variance between the two treatments. If the variances were equal, we proceeded with a parametric two-tailed t-test. If the variances differed, we used the Mann-Whitney U-test to compare the two treatment groups. We considered the data statistically different for P value < 0.05 or less.

Chapter 3: Uterine stromal but not epithelial PTGS2 is critical for murine pregnancy success

Noura Massri, Ripla Arora

3.1: Abstract

The use of non-steroidal anti-inflammatory drugs that target prostaglandin synthase (PTGS) enzymes has been implicated in miscarriage. Further, PTGS2-derived prostaglandin is reduced in the endometrium of patients with a history of implantation failure. However, in the mouse model of pregnancy, peri-implantation PTGS2 function is controversial. Some studies suggest that *Ptgs2*$^{-/-}$ mice display deficits in ovulation, fertilization, and implantation, while other studies suggest a role for PTGS2 only in ovulation but not implantation. Further, the uterine cell type responsible for PTGS2 function and the role of PTGS2 in regulating implantation chamber formation are not known. To address this, we generated tissue-specific deletion models of Ptgs2. We observed that PTGS2 ablation from the epithelium alone in *Ltf*$^{cre/+}$*; Ptgs2*$^{f/f}$ mice and in both the epithelium and endothelium of the *Pax2*$^{cre/+}$*; Ptgs2*$^{f/f}$ mice does not affect embryo implantation. Further, deletion of PTGS2 in the ovary, oviduct, and uterus using *Pgr*$^{cre/+}$*; Ptgs2* $^{f/f}$ does not disrupt pre-implantation events but instead interferes with post-implantation chamber formation, vascular remodeling, and decidualization. While all embryos initiate chamber formation, more than half of the embryos fail to transition from blastocyst to epiblast stage, resulting in embryo death and resorbing decidual sites at mid-gestation. Thus, our results suggest no role for uterine epithelial PTGS2 in early pregnancy but instead highlight a role for uterine stromal PTGS2 in modulating post-implantation embryo and implantation chamber growth. Overall, our study provides clarity on the compartment-specific role of PTGS2 and provides a valuable model for further investigating the role of stromal PTGS2 in post-implantation embryo development.

3.2: Introduction

According to the American College of Obstetricians and Gynecologists, approximately 26% of pregnancies end in miscarriage, and only 10% of these losses are clinically recognized

(Bulletins—Gynecology, 2018). Additionally, 1-2% of women experience recurrent pregnancy loss due to undetermined causes (Turesheva et al., 2023). Given the ethical considerations, human pregnancies cannot be studied directly. Thus, mice are often utilized as a model system to understand the early events of pregnancy. Recent advancements in 3D imaging methodology have been successfully applied to the pre-implantation stages of a mouse pregnancy, revealing phenomena that are challenging to uncover using traditional 2D histology. 3D imaging has revealed that embryo clusters enter the uterine environment at gestational day (GD) 3, ~72 hours after the mouse mating event. These embryos initially move together as clusters towards the middle of the uterine horn and then they undergo a bidirectional scattering movement followed by embryo spacing along the oviductal-cervical axis (Chen et al., 2013; Flores et al., 2020). At GD4, once the embryo arrives in the center of a flat peri-implantation region of the uterine lumen, a V-shaped embryo implantation chamber begins to form (Madhavan et al., 2022). This is concurrent with increased vascular permeability and sprouting angiogenesis at the embryo implantation sites at GD4 1800h (Madhavan et al., 2022; Massri et al., 2023). The proper formation of the embryo implantation chamber is critical as it facilitates embryo alignment along the mesometrial-anti-mesometrial axis, where the blastocyst's inner-cell mass faces the uterine mesometrial pole (Madhavan et al., 2022). Following embryo implantation, decidualization occurs, where stromal cells in the uterus become epithelialized, and embryos grow to the epiblast stage at GD5. Aberrations in events surrounding embryo implantation and decidualization can lead to a cascade of events that negatively impact subsequent pregnancy development, ultimately resulting in miscarriage and pregnancy loss (Cha et al., 2012).

Successful embryo implantation and maintenance of early pregnancy rely on a delicate interplay of numerous molecular mechanisms (Chen et al., 2013). Among these, prostaglandin, including PGE_2, PGI_2, and $PGF_{2,}$ have emerged as critical mediators of reproductive success (Clark and Myatt, 2008; Psychoyos et al., 1995; Wang and Dey, 2006). Prostaglandin is synthesized by the action of PTGS enzymes (Funk, 2001). Numerous studies have found

evidence of PTGS1 and PTGS2 expression in human uterine compartments during implantation (Marions and Danielsson, 1999). PTGS1 is expressed at a constant level in the human endometrium, while PTGS2 is expressed explicitly in the glandular epithelial cells and the endothelial cells (Marions and Danielsson, 1999), and the stromal cells (Stavreus-Evers et al., 2005). Additionally, there is evidence for both PTGS1 and PTGS2 expression in the uteri of various species, including mice (Chakraborty et al., 1996), western spotted skunks (Das et al., 1999), baboons (Kim et al., 1999), and hamsters (Evans and Kennedy, 1978; Wang et al., 2004b). PTGS2 is expressed in the luminal epithelium and sub-epithelial stroma surrounding the blastocyst attachment site in the anti-mesometrial pole, and its expression is induced by the presence of the embryo (Chakraborty et al., 1996). Post embryo implantation, PTGS1 is expressed in the secondary decidual zone; however, PTGS2 expression is localized at the mesometrial pole (Chakraborty et al., 1996).

Non-steroidal anti-inflammatory drugs (NSAIDs) that block PTGS1 and PTGS2 function are amongst the most common over-the-counter medications that women take during pregnancy (Thorpe et al., 2013). There is evidence for an 80% increased risk of miscarriage with the consumption of NSAIDs during pregnancy (Jackson-Northey and Evans, 2002; Li et al., 2018a; Li et al., 2003). PTGS1 has not been shown to have a role in pregnancy in women, and PTGS1-deficient mice do not display significant reproductive issues during pregnancy, except for prolonged parturition (Langenbach et al., 1995). On the other hand, studies in pregnant women who experience recurrent pregnancy loss or implantation failure after in-vitro fertilization procedures demonstrate dysregulation in endometrial PTGS2 (Achache et al., 2010), and its derived prostaglandin PGI2 (Wang et al., 2010). Furthermore, genetic variations in the PTGS2 gene are associated with an increased risk of implantation failure among women going through assisted reproductive procedures (Salazar et al., 2010). In rodents, Lim et. al determined that PTGS2-deficient mice are infertile due to ovulation, fertilization, and implantation deficits (Lim et al., 1997). While ovulation and fertilization defects are widely accepted, there is a controversy

regarding the role of PTGS2 during embryo implantation (Cheng and Stewart, 2003; Lim et al., 1997). Chang et. al reported that when wild-type blastocysts are transferred into PTGS2-deficient pseudo pregnant uteri, a 24-hour delay in decidualization is observed, but pregnancy proceeds to birth normally (Cheng and Stewart, 2003). These data suggest that PTGS2 may not be essential for implantation, decidualization, and overall pregnancy success. To explain the discrepancy between these studies it has been proposed that mixed mouse genetic background allows the upregulation of PTGS1 in PTGS2-deficient animals and this PTGS1 may compensate for the loss of PTGS2 (Wang et al., 2004a).

To resolve the controversy surrounding the function of PTGS2 in embryo implantation and to determine the compartment in which PTGS2 function is essential, we utilized the cre-lox recombinase system (Kim et al., 2018a). We deleted PTGS2 in the adult uterine epithelium using *Ltf*$^{cre/+}$ (Daikoku et al., 2014), in the embryonic uterine epithelium and endothelium using *Pax2*$^{cre/+}$ (Granger et al., 2024; Ohyama and Groves, 2004), and in the epithelial and stromal compartment of the uterus using *Pgr*$^{cre/+}$(Madhavan and Arora, 2022; Soyal et al., 2005) (**Table 2.1**). We determine that PTGS2 function in the uterine epithelium and endothelium is not critical for implantation or pregnancy success. However, stromal PTGS2 is critical for post-implantation embryo and implantation chamber growth for continued pregnancy progression.

3.3: Results

3.3.1: Peri-implantation PTGS2 expression in embryo mediated and in oil-stimulated pregnancy

To determine which uterine cells might contribute to PTGS2 expression during peri-implantation stages we performed expression analysis of PTGS2 in the uterine tract during peri-implantation stages utilizing natural and artificial pregnancy models. At GD3 1600h, when embryos are present in the uterus, PTGS2 is not expressed in the uterine luminal epithelium (Fig. 3.1 A, A', B). mRNA expression of *Ptgs2* has been reported in the luminal epithelium when a pseudopregnant uterus is stimulated with oil (Lim et al., 1997). We also observed PTGS2 protein

expression in the uterine luminal epithelium four hours after intraluminal oil stimulation of the pseudopregnant uterus at GD3 1200h (Fig. 3.1 C, C', D). At GD4 1200h, when the embryo is at the center of the peri-implantation region, PTGS2 is expressed only in the luminal epithelium but not in the stroma (Madhavan et al., 2022). Following embryo implantation at GD4 1800h, PTGS2 is observed in the uterine sup-epithelial stroma surrounding the embryo implantation chamber (Fig. 3.1 E, E', F), as reported previously (Chakraborty et al., 1996; Madhavan et al., 2022). At GD5.5, PTGS2 is expressed at the mesometrial pole surrounding the embryo implantation chamber as reported previously (Chakraborty et al., 1996) and uterine glands at the implantation chamber (Fig. 3.1 G, G', H).

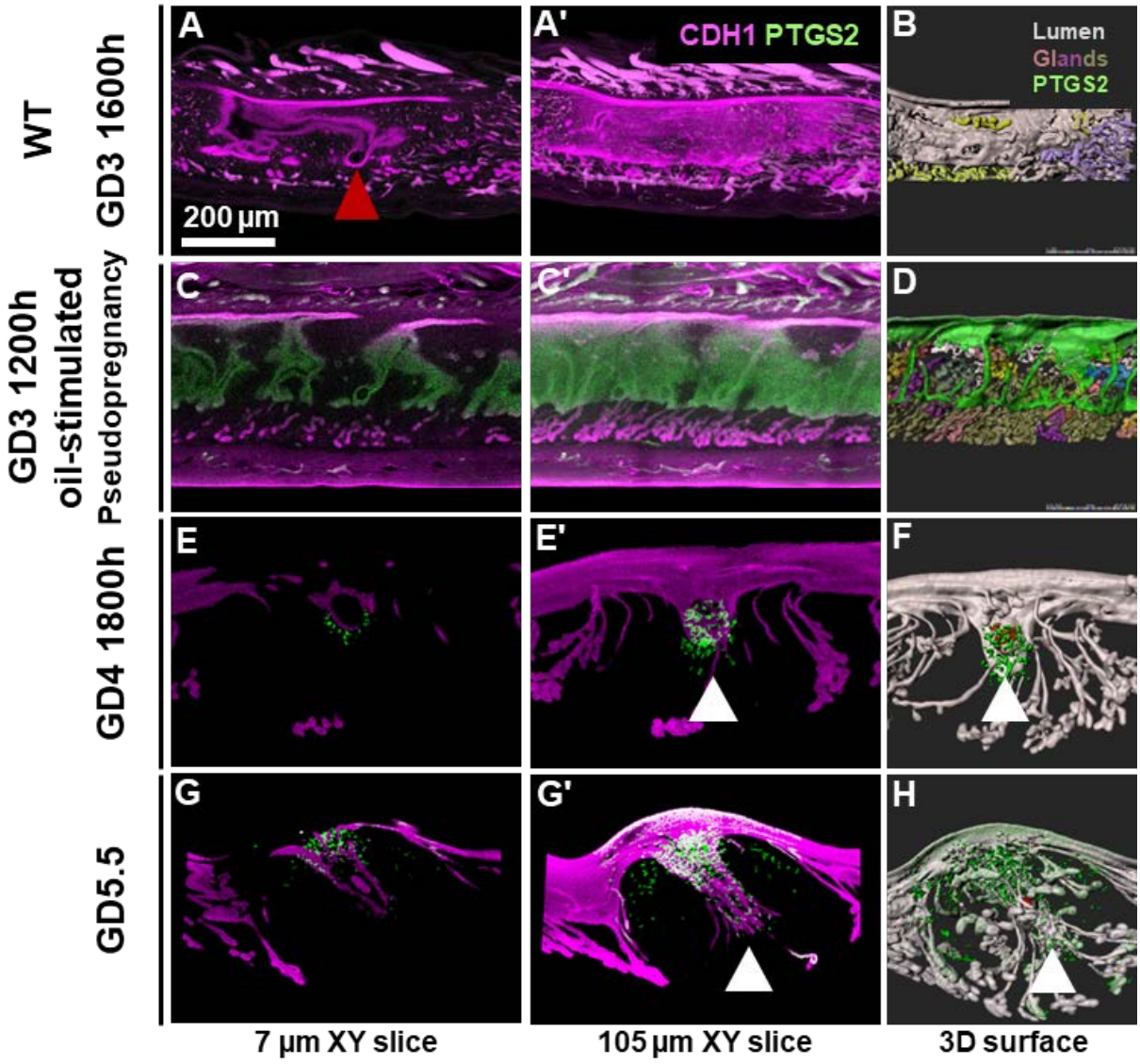

Figure 3.1. Timeline of uterine PTGS2 expression during peri-implantation stages and in an oil-stimulated pseudopregnancy. CDH1 and PTGS2 expression in pregnant wild-type uteri at GD3 1600h (**A, A'**). PTGS2 expression in CDH1 positive cells in oil-stimulated pseudo pregnant uteri at GD3 1200h, 4h after oil stimulation (**C, C'**). 3 different regions from at least 8 uterine horns were evaluated. PTGS2 expression in the subepithelial stroma surrounding the embryo implantation chamber at GD4 1800h (**E, E'**). PTGS2 expression in the mesometrium pole and the uterine glands of the embryo implantation chambers at GD5.5 (**G, G'**). 3D rendering surfaces (**B, D, F, H**) At least 2 implantation sites from at least 3 uterine horns were analyzed. 7µm XY slice (**A, C, E, G**). 105 µm XY slice (**A', C', E', G**'). Scale bar: 200 µm. GD: gestational day; Red arrowhead: embryo; White arrowheads: embryo implantation chamber.

3.3.2: PTGS2 deletion in the uterine luminal epithelium and endothelium does not affect embryo implantation, embryo growth, and pregnancy progression

To determine if the uterine epithelium is responsible for pre-implantation PTGS2 function, we generated tissue-specific deletion models of PTGS2 using cre-lox recombinase methodology (Kim et al., 2018a) (Fig. 2.2 A, B). For adult uterine epithelial deletion, we used *Ltf*$^{cre/+}$ *; Ptgs2*$^{f/f}$ mice (Daikoku et al., 2014), and for embryonic uterine epithelium and endothelial deletion, we used *Pax2*$^{cre/+}$*; Ptgs2*$^{f/f}$ mice (Ohyama and Groves, 2004). To confirm PTGS2 depletion in the CDH1 positive uterine epithelial cells we used oil-stimulated pseudopregnancies for both *Ltf*$^{cre/+}$*; Ptgs2*$^{f/f}$, and *Pax2*$^{cre/+}$*; Ptgs2*$^{f/f}$ models (Fig. 2.3 A, A', B, B', C, C'). At GD4 1800h, we observed the formation of the V-shaped embryo implantation chamber and stromal PTGS2 expression in control, *Ltf*$^{cre/+}$*; Ptgs2*$^{f/f}$, and *Pax2*$^{cre/+}$*; Ptgs2*$^{f/f}$ mice (Fig. 2.3 D, D', E, E', F, F'). At GD4 1800h, we observed no defects in the development of the blastocyst in the *Pax2*$^{cre/+}$*; Ptgs2*$^{f/f}$ uteri (Fig. 2.3 G, H, and Table 3.2). Epithelial-specific and epithelial and endothelial-specific PTGS2-deficient mutants displayed normal embryo spacing and increased vessel permeability at embryo implantation sites, as observed by the blue dye reaction at GD4 (Fig. 2.3 I, J, K). At GD12.5, we observed that uteri from both mutants displayed embryos that had developed similar to embryos from control uteri (Fig. 2.3 J, L). Further, both *Ltf*$^{cre/+}$*; Ptgs2*$^{f/f}$ and *Pax2*$^{cre/+}$*; Ptgs2*$^{f/f}$ mice were able to go to term with no significant effect on the duration of the pregnancy or the number of the pups born (Fig. 2.3 K, L). Overall, our data suggest that the uterine epithelium and endothelium are not the sources of PTGS2-derived prostaglandin synthesis critical for implantation and pregnancy progression.

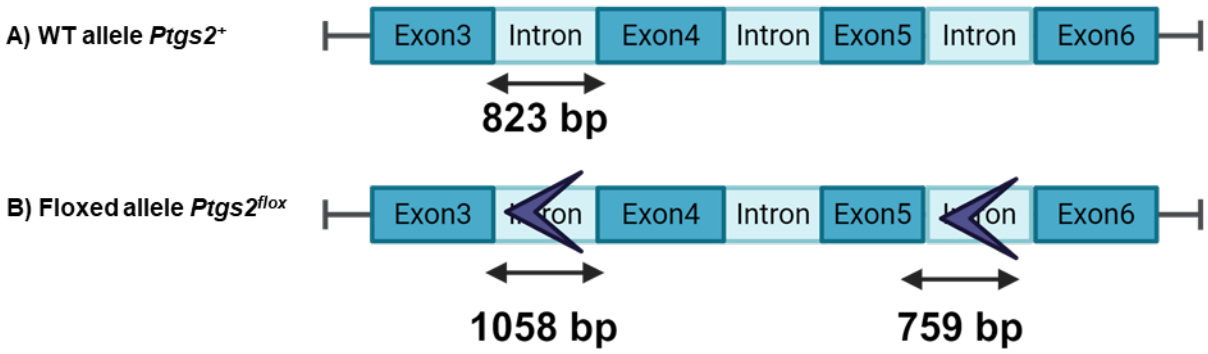

Figure 3.2. Utilizing the cre-lox recombinase system to specifically delete PTGS2 from the murine reproductive tract. The diagram displays the wild-type allele of *Ptgs2* (**A**) and the floxed allele of *Ptgs2* with the lox-p sites inserted in introns 3 and 5 (**B**).

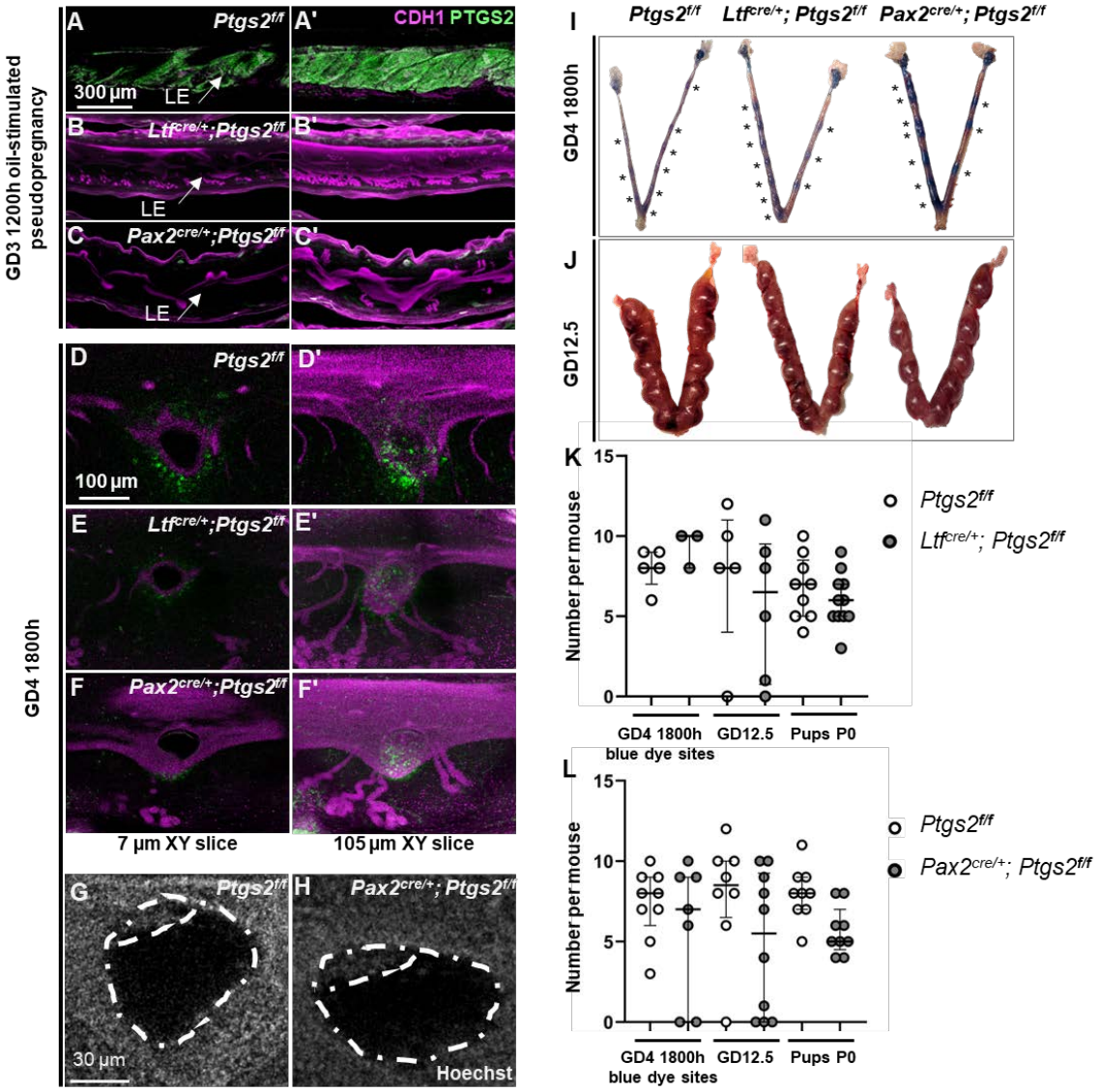

Figure 3.3. Conditional deletion of PTGS2 in the uterine epithelium and endothelium does not affect embryo implantation and pregnancy success. PTGS2 expression in CDH1 positive cells in oil-stimulated pseudopregnant *Ptgs2*$^{f/f}$ uteri (**A**), *Ltf*$^{cre/+}$*; Ptgs2*$^{f/f}$ uteri (**B**) and *Pax2*$^{cre/+}$*; Ptgs2*$^{f/f}$ uteri (**C**) at at pseudopregnancy day3 1200h, 4h after intraluminal oil stimulation. 3 different regions from at least 4 uterine horns were evaluated. 7µm XY slice (**A, B, C**). 105µm XY slice (**A', B', C'**). PTGS2 expression in the subepithelial stroma in *Ptgs2*$^{f/f}$ (D), *Ltf*$^{cre/+}$*; Ptgs2*$^{f/f}$ (**E**), and *Pax2*$^{cre/+}$*; Ptgs2*$^{f/f}$ uteri (**F**) at GD4 1800h. 7µm XY slice (**D, E, F**). 105µm XY slice (**D', E', F'**). At least 2 implantation sites from 3 different uterine horns were analyzed. The top of the images represents the mesometrial pole, while the bottom represents the anti-mesometrial pole. Blastocyst stage embryos in *Ptgs2*$^{f/f}$ (**G**) and *Pax2*$^{cre/+}$*; Ptgs2*$^{f/f}$ mice (**H**) at GD4 1800h. White dashed lines: blastocyst. Uteri with blue dye sites at GD4 1800h (**I**). Black asterisks: bluedye sites. Uteri with embryo sites at GD12.5 (J). Quantitation of blue dye sites at GD4 1800h, live embryos at GD12.5, and P0 pups in *Ltf*$^{cre/+}$*; Ptgs2*$^{f/f}$ mice (**K**), and in *Pax2*$^{cre/+}$*; Ptgs2*$^{f/f}$ (**L**) with their respective controls. Each dot represents one mouse analyzed. Median values shown. Data analyzed using unpaired parametric t-test. No significant differences were observed due to lack of evidence. Scale bars, A-C': 300 µm, D-F': 100 µm, G, H: 30 µm. LE: Luminal epithelium.

3.3.3: Stromal deletion of PTGS2 results in mid-gestation decidual resorption

To delete *Ptgs2* in the granulosa cells of the pre-ovulatory follicle and the corpus luteum, the epithelium, and the myometrium of the oviduct (Soyal et al., 2005), and the circular smooth muscle, epithelium, and stroma of the uterus (Madhavan and Arora, 2022; Soyal et al., 2005) we utilized the Progesterone-Receptor-driven Cre (*Pgr^{cre})* mouse line (Table 2.1, and Fig. 3.4 A, A', B, B', and Fig. 3.5). We observed normal embryo spacing in *Pgr$^{cre/+}$; Ptgs2$^{f/f}$* mice; however, embryo implantation was delayed as observed using the blue dye reaction at GD4 1800h (Fig. 3.4 C, D, G) (median blue dye sites in controls: 10, *Pgr$^{cre/+}$; Ptgs2$^{f/f}$*: 7, $P<0.05$). 24 hours later at GD5.5, a similar number of decidual sites was observed in controls and *Pgr$^{cre/+}$; Ptgs2$^{f/f}$* uteri (Fig. 3.4 D, G). Complete loss of PTGS2 expression was observed in *Pgr$^{cre/+}$; Ptgs2$^{f/f}$* implantation chamber at GD4 1800h (Fig. 3.4 A, B) and at GD5.5 (Fig. 3.5). To determine the cause for delayed implantation in the mutant mice, we determined the mRNA expression of a critical glandular cytokine, *Leukemia inhibitory factor* (*Lif*) at GD3 1800h. We observed reduced levels of *Lif* mRNA in FOXA2+ glandular epithelial uterine cells in *Pgr$^{cre/+}$; Ptgs2$^{f/f}$* uteri (Fig. 3.6 A, B, C). However, we observed no differences in the serum progesterone levels between control and mutant mice at GD3 and GD4 1800h (Fig. 3.6 D). Similar to GD5.5, at GD8.5, we observed no significant difference in the number of decidual sites between control and *Pgr$^{cre/+}$; Ptgs2$^{f/f}$* uteri; however, we started to observe a few resorption sites in the mutants (Fig. 3.4 E, H). At GD12.5, the number of decidual sites was similar; however, we observed a significant number of resorbing decidua (50%) in the mutant uteri (median live embryo number in control: 9, *Pgr$^{cre/+}$; Ptgs2$^{f/f}$*: 4, $P<0.01$) (Fig. 3.4 F, H). Commensurate with the resorptions at mid-gestation, we observed a significant reduction in pups born to *Pgr$^{cre/+}$; Ptgs2$^{f/f}$* females (48% pups loss) in comparison with control (median live pup number in controls: 8, *Pgr$^{cre/+}$; Ptgs2$^{f/f}$*: 4, $P<0.05$) (Fig. 3.4 I).

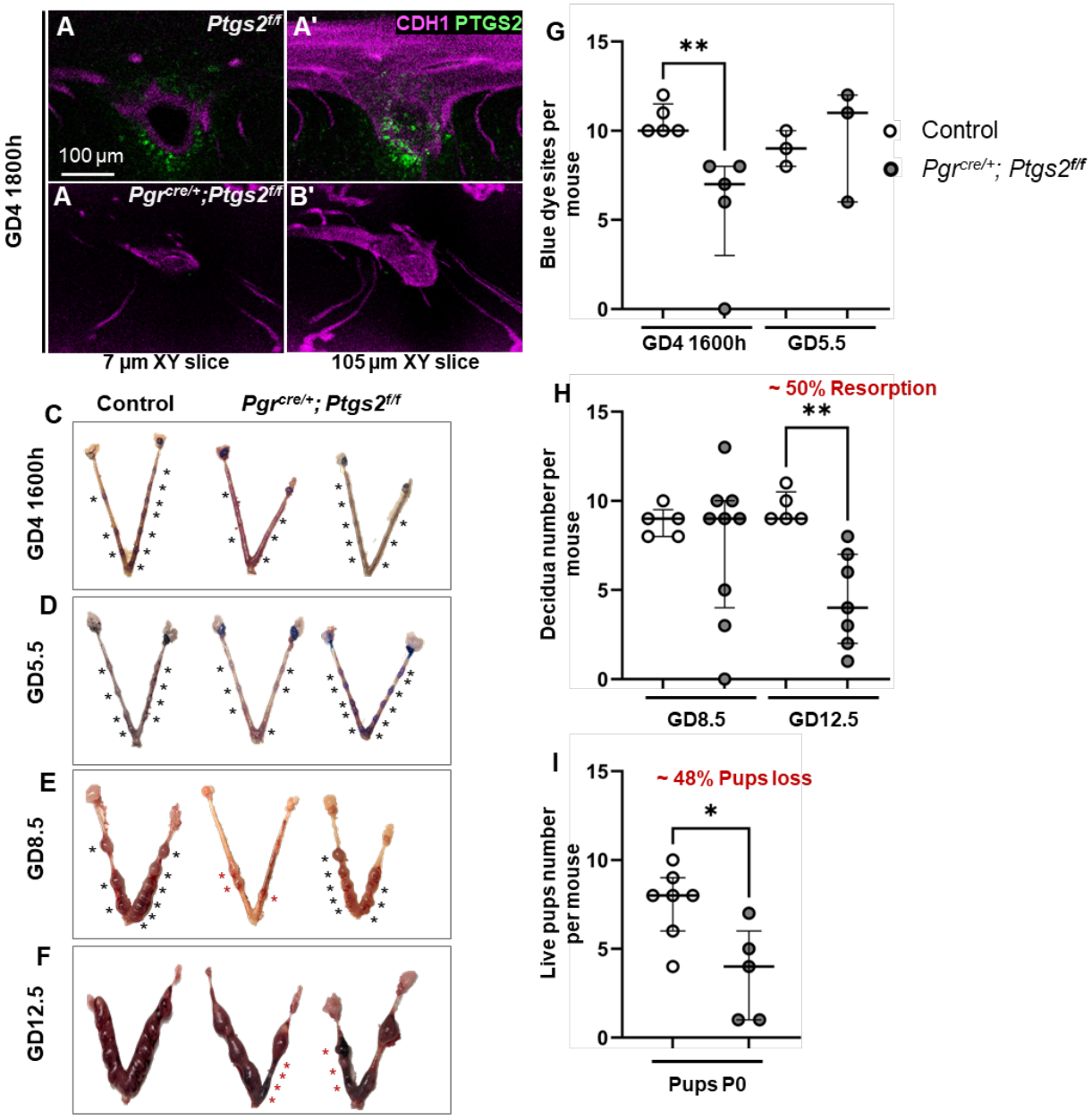

Figure 3.4. *Pgr*$^{cre/+}$*; Ptgs2*$^{f/f}$ mice display a delay in embryo implantation, mid-gestation decidual resorption, and pregnancy loss. PTGS2 expression in the subepithelial stroma surrounding the embryo implantation chamber in *Ptgs2*$^{f/f}$ (**A**) and *Pgr*$^{cre/+}$*; Ptgs2*$^{f/f}$ (**B**) uteri at GD4 1800h. At least 9 implantation sites were evaluated in at least 2 mice. 7µm XY slice (**A, B**). 105µm XY slice (**A', B'**). The top of the images represents the mesometrial pole, while the bottom represents the anti-mesometrial pole. Blue dye sites at GD4 1800h (**C**) and GD5.5 (**D**). Decidual sites at GD8.5 (**E**), and GD12.5 (**F**) in control and *Pgr*$^{cre/+}$*; Ptgs2*$^{f/f}$ uteri. Black asterisks: blue dye sites. Orange arrowheads: resorbed deciduae sites. Quantification of blue dye sites at GD4 1800h and GD5.5 (**G**), decidual sites number at GD8.5 and at GD12.5 (**H**) and live pups at P0 (**I**) in both groups. At least n=3 mice were evaluated per genotype for each pregnancy stage. Each dot represents one mouse. Median values shown. Data analyzed using unpaired parametric t-test. * $P < 0.05$, ** $P < 0.01$. Scale bar for A-B': 100 µm.

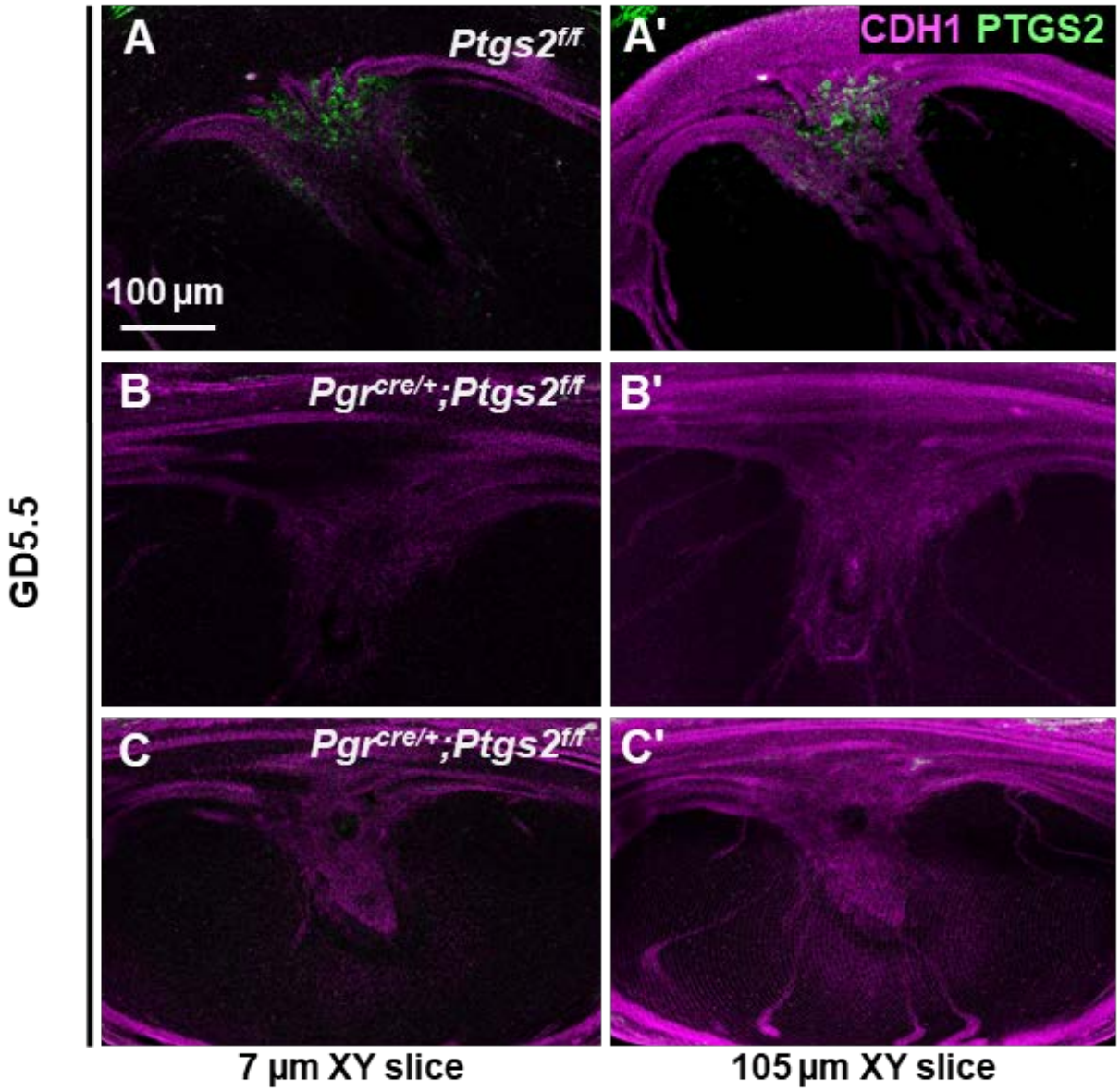

Figure 3.5. *Pgr*$^{cre/+}$*; Ptgs2*$^{f/f}$ uteri display ablation of PTGS2 expression in the mesometrial pole. PTGS2 expression in the mesometrial pole surrounding the embryo implantation chamber in *Ptgs2*$^{f/f}$ (A, A') and *Pgr*$^{cre/+}$*; Ptgs2*$^{f/f}$ (B, B', C, C') uteri at GD5.5. At least 10 implantation sites were evaluated in at least 2 mice. 7µm XY slice (A, B, B). 105µm XY slice (A', B', B'). The top of the images represents the mesometrial pole, while the bottom represents the anti-mesometrial pole. Scale bar: 100 µm.

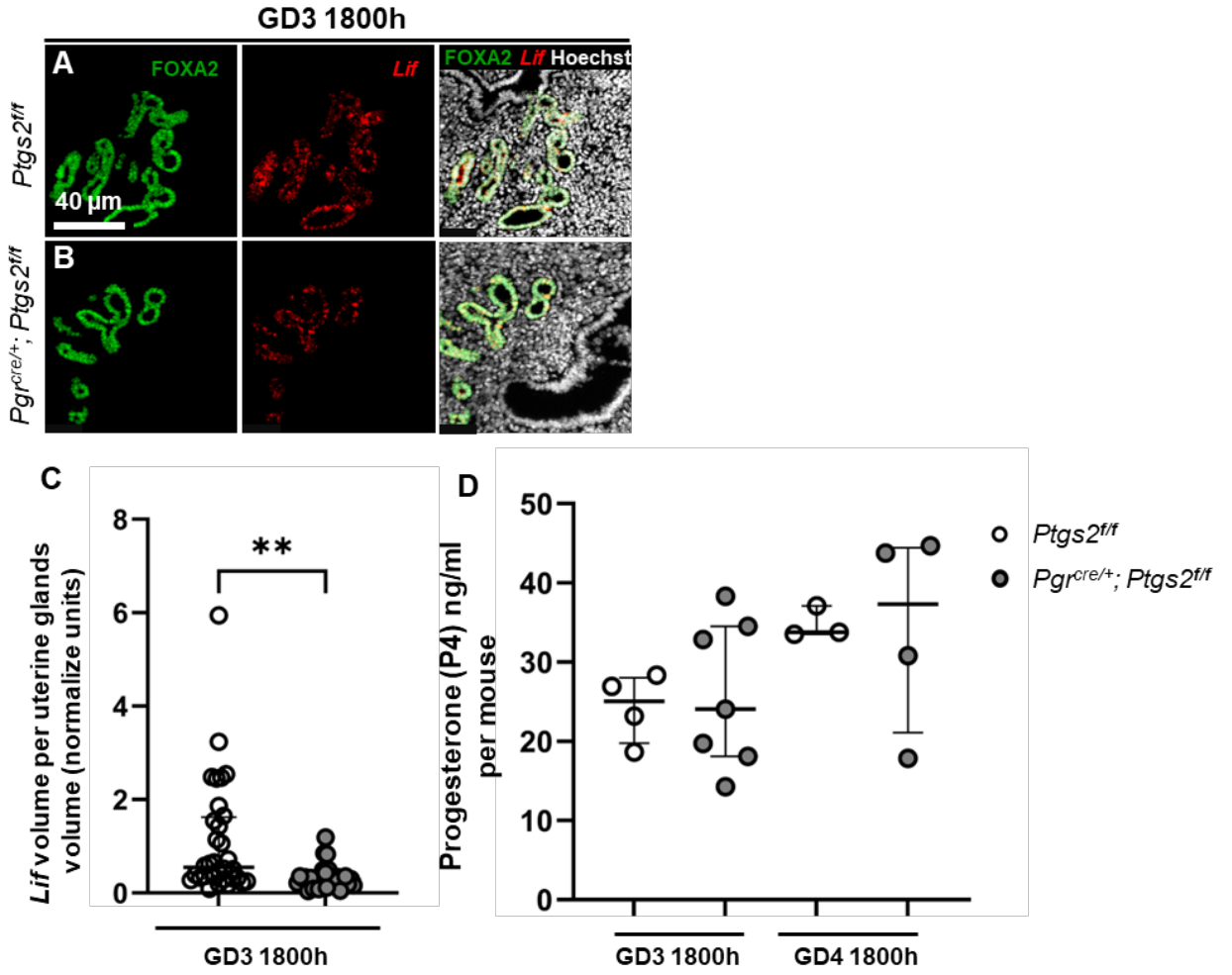

Figure 3.6. *Pgr$^{cre/+}$; Ptgs2$^{f/f}$* uteri display a reduction in preimplantation *Leukemia Inhibitory Factor*. *Leukemia inhibitory factor* (*Lif) expression in* FOXA2+ glandular epithelium cells in *Ptgs2$^{f/f}$* and *Pgr$^{cre/+}$; Ptgs2$^{f/}$* at GD3 1800h (A, B). Quantification of *Lif* volume normalized to FOXA2+ glandular epithelium volume at GD3 1800h per uterine section in the two groups (C). At least 4 mice and 28 sections were analyzed for each group. Each dot represents one uterine section. Median values shown. Data analyzed using unpaired parametric t-test.** $P < 0.01$. Progesterone serum levels in *Ptgs2$^{f/f}$* and *Pgr$^{cre/+}$; Ptgs2$^{f/f}$* at GD3 1800h and GD4 1800h (D). At least n=3 mice per genotype were analyzed. Each dot represents one mouse. Median values shown. Data analyzed using unpaired parametric t-test. No significant difference observed. Scale bar, A-B: 40 µm.

3.3.4: Abnormal embryo development in the post-implantation chamber of PTGS2-deficient uteri

To determine the first-time point when embryo development is affected in the *Pgr*$^{cre/+}$*; Ptgs2*$^{f/f}$ uteri, we examined embryo morphology at different time points during gestation. *Ptgs2*$^{-/-}$ mice display a ~30% reduction in the number of eggs ovulated per mouse and a complete failure of fertilization (Lim et al., 1997) Thus, we first examined the fraction of fertilized eggs in the *Pgr*$^{cre/+}$*; Ptgs2*$^{f/f}$ mice. We performed an oviductal flush at GD1 1200h and cultured the embryos in vitro for 72 hours. In control mice, we observed that 97.5% of the embryos were at the 2-cell stage at the time of the oviductal flush. After 72 hours of in-vitro embryo culture, 18/39 (45%) embryos reached the morula stage, and 21/39 (52.5%) reached the blastocyst stage (Table 3.1 and Fig. 3.7 A, C, E, G, I, J). With *Pgr*$^{cre/+}$*; Ptgs2*$^{f/f}$ mice, we observed 12/56 (21.42%) unfertilized eggs, 4/56 (7.14%) 1-cell stage embryos, and 40/56 (71.42%) 2-cell stage embryos at the time of oviductal flush. After 72 hours of in-vitro embryo culture, 8/56 (14.28%) embryos reached the morula stage, and 36/56 (64.28%) embryos reached the blastocyst stage. The 12/56 (21.42%) unfertilized eggs remained as such with no extrusion of polar body and cell division (Table 3.1 and Fig. 3.7 B, D, F, H, I, J). Thus, *Pgr*$^{cre/+}$*; Ptgs2*$^{f/f}$ mice show a substantially improved fertilization rate compared to *Ptgs2*$^{-/-}$ mice (Lim et al., 1997; Matsumoto et al., 2001). Overall, in our *Pgr*$^{cre/+}$*; Ptgs2*$^{f/f}$ model, we noted that once fertilization occurs, these embryos develop normally to the morula/blastocyst stage in vitro.

Next, we evaluated embryo development in our *Pgr*$^{cre/+}$*; Ptgs2*$^{f/f}$ model in vivo. We observed that for uteri with embryos, at GD3 1800h, 95% of the embryos reached the blastocyst stage (Table 3.2 and Fig. 3.7 K, L). However, at post-implantation stages at GD4 1800h, we observed that ~62.5% of the embryos displayed embryo morphology that deviated from the typical elongated blastocyst (Table 3.2 and Fig. 3.7 M, N). At GD5.5, we observed that 85% of the decidual sites had degrading embryos suggestive of pregnancy arrest (Table 3.2 and Fig. 3.7 O, P). Since some embryos displayed normal embryo development at GD5.5, we determined if there

was compensatory upregulation of PTGS1 in the *Pgr*$^{cre/+}$*; PTgs2*$^{f/f}$ uteri. PTGS1 was robustly expressed in the secondary decidual zone stroma around the embryo, in the glands at the anti-mesometrial pole and in the glands and stroma in the inter-implantation region at GD5.5. No differences were observed between control and *Pgr*$^{cre/+}$*; PTgs2*$^{f/f}$ decidua (Fig. 3.8) Our data suggests that embryonic growth restriction begins soon after implantation in *Pgr*$^{cre/+}$*; Ptgs2*$^{f/f}$ mice (Table 3.2 and Figure 3.7 Q).

	Day of collection/ oviduct flush			**After 72 hours of culture**		
Genotype /Mice number	**Unfertilized eggs n (%)**	**1-Cell embryos n (%)**	**2-cell embryos n (%)**	**Unfertilized eggs n (%)**	**Morula n (%)**	**Blastocyst n (%)**
Ptgs2$^{f/f}$ n= 5	1 (2.5%)	0 (0%)	39 (97.5%)	1 (2.5%)	18 (45%)	21 (52.5%)
Pgr$^{cre/+}$*; Ptgs2*$^{f/f}$ n=8	12 (21.43%)	4 (7.14%)	40 (71.43%)	12 (21.43%)	8 (14.28%)	36 (64.28%)

Table 3.1: In-vitro-embryo culture in *Ptgs2*$^{f/f}$ and *Pgr*$^{cre/+}$*; Ptgs2*$^{f/f}$ mice. The percentage of 2-cell stage embryos we obtained from *Ptgs2*$^{f/f}$ mice flush is 97.5% in (n=3 mice), and after 72 hours of embryo culture, 52.5% of embryos reached the blastocyst stage, and 45% reached the morula stage, while the remaining egg remain unfertilized with no extrusion of the polar body (A). The percentage of 2-cell stage embryos in the mutant**,** *Pgr*$^{cre/+}$*; Ptgs2*$^{f/f}$ mice is 71.43%, with the remaining 21.43% and 7.14% being unfertilized eggs and 1-cell stage embryos, respectively. After 72 hours of culture, 64.28% of embryos reached the blastocyst stage, 14.28% reached the morula stage, and 21.42% remained in the unfertilized eggs stage with no polar body extrusion (B).

Stage	Genotype	Mice Number No.	Uterine horns No.	Avg Embryo sites (observed by blue dye)	Embryo sites (Examined by 3D)	Blastocyst or Epiblastn (%)	Abnormal n (%)
GD3	***Ptgs2$^{f/f}$***	N = 5	5	NA	20	18 (90)	2 (10)
	Pgr$^{cre/+}$; Ptgs2$^{f/f}$	N = 4	5	NA	19	18 (95)	1 (5)
GD4	***Ptgs2$^{f/f}$***	N = 4	4	10.6	14	14 (100)	0 (0)
	Pgr$^{cre/+}$; Ptgs2$^{f/f}$	N = 5	5	5.8	24	9 (37.5)	15 (62.5)
	Pax2$^{cre/+}$; Ptgs2$^{f/f}$	N = 4	5	5.85	32	29 (90.6)	3 (9.4)
GD5	***Ptgs2$^{f/f}$***	N = 3	3	9	9	8 (88.88)	1 (11.11)
	Pgr$^{cre/+}$; Ptgs2$^{f/f}$	N = 5	5	9.6	20	3 (15)	17 (85)

Table 3.2: Percentage of embryo development to the blastocyst or epiblast stage at GD3 1600h, GD4 1600h, and GD5 1600h in *Ptgs2$^{f/f}$* and *Pgr$^{cre/+}$; Ptgs2$^{f/f}$* mice. At GD3 1600h, 90% of the embryos in control (n=5 mice) reach the blastocyst stage (A), and 96% of mutant embryos (n=4 mice) (B). At GD4 1600h, 100% of embryos in the control (n=5 mice) are in the blastocyst stage (C), while only 37.5% of embryos in the mutant (n=4 mice) are in the blastocyst stage, and the remaining 62.5% of embryos have growth restriction (D). At GD4 1600h, 90.6% of embryos in the *Pax2$^{cre/+}$; Ptgs2$^{f/f}$* mutant (n=4 mice) are in the blastocyst stage, and the remaining 9.4% of embryos have growth restriction (E). AT GD5 1600h, 88.88% of the control embryos (n= 3 mice) are in the epiblast stage (F), while only 15% of mutant embryos (n=6 mice) reached the epiblast stage and the remaining 76% have growth restriction (G). No.: Number.

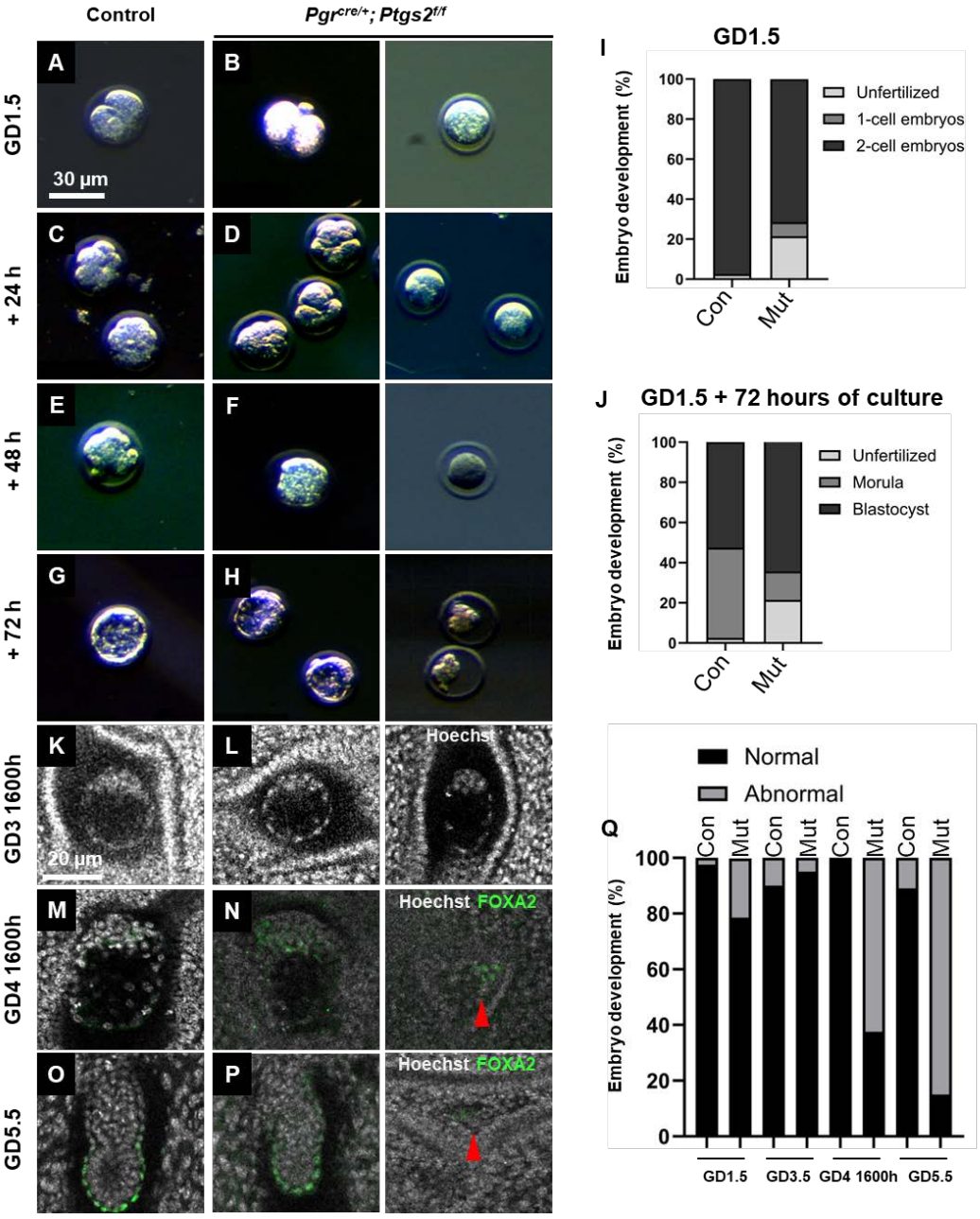

Figure 3.7. Stromal ablation of PTGS2 restricts embryo growth at post-implantation stages. Oviductal flush at GD1 1200h revealed 2-cell stage embryos in control (A), and 2-cell stage embryos and unfertilized eggs in *Pgr*$^{cre/+}$*; Ptgs2*$^{f/f}$ mice (B). 24, 48, and 72 hours culture of flushed embryos/eggs in control (C, E, G) and *Pgr*$^{cre/+}$*; Ptgs2*$^{f/f}$ mice (D, F, H). Embryo development percentage at GD1 1200h (I) and at GD1 1200h + 72 hours of culture (J). Blastocyst stage embryos in control (K) and *Pgr*$^{cre/+}$*; Ptgs2*$^{f/f}$ mice (L) at GD3 1800h. Blastocyst stage embryos in control (M), and blastocyst and abnormal embryos in *Pgr*$^{cre/+}$*; Ptgs2*$^{f/f}$ mice at GD4 1800h (N). Epiblast stage embryos in control mice (O); and epiblast and abnormal embryos in *Pgr*$^{cre/+}$*; Ptgs2*$^{f/f}$ mice at GD5.5 (P). Red arrowheads: resorbing embryos. Comparison of embryo development percentage across GD1.5 - GD5.5 (Q). Analysis was performed in uteri with embryos. At least n=3 mice were analyzed per time point. Scale bars, A-H: 30 µm , K-P: 20 µm. Con: Control; Mut: mutant *Pgr*$^{cre/+}$*; Ptgs2*$^{f/f}$.

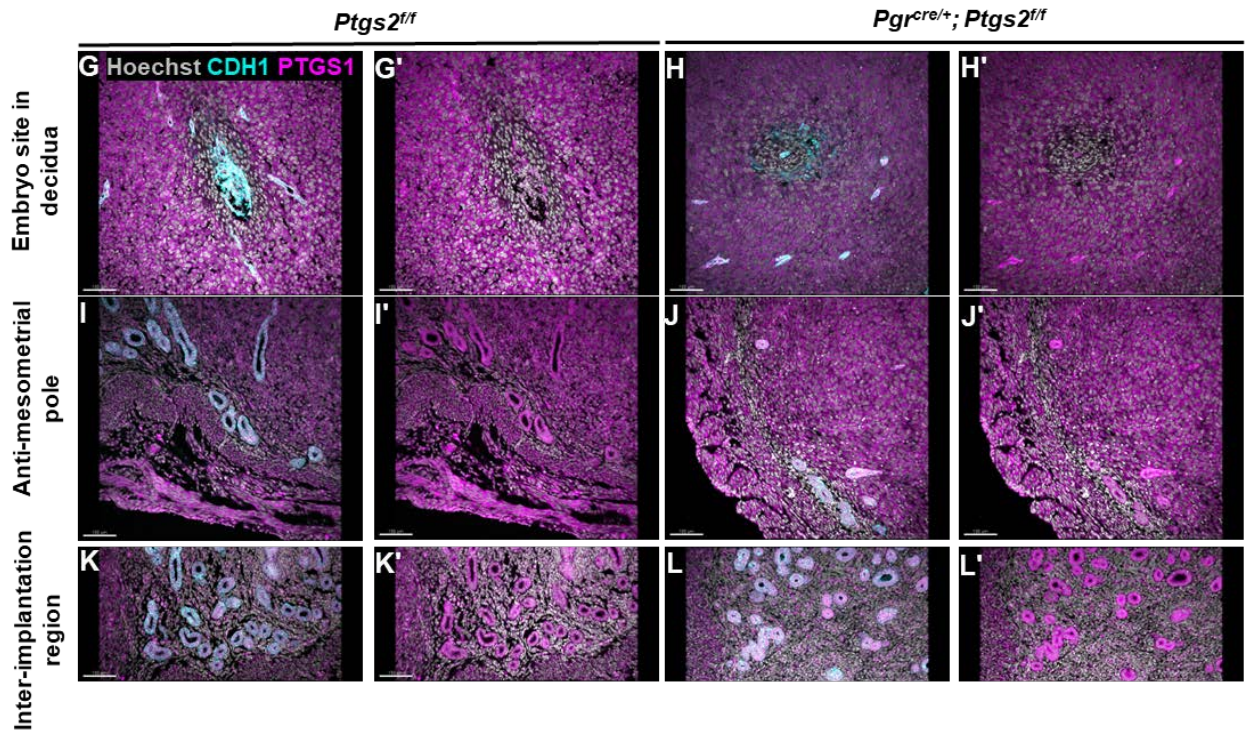

Figure 3.8. *Pgr*$^{cre/+}$*; Ptgs2*$^{f/f}$ uteri do not display upregulation of PTGS1 at GD5.5. PTGS1 expression in the decidua sites surrounding the embryo (A, A', B, B'), anti-mesometrial region (C, C, D, D'), and inter-implantation region (E, E', F, F') in control and Pgrcre/+; Ptgs2f/f deciduae at GD5.5. Scale bar 100 µm.

3.3.5 Loss of stromal PTGS2 results in an abnormal implantation chamber, reduced implantation site vascular remodeling, and a poor decidualization response

Since we observed defects in the post-implantation embryo, we hypothesized that implantation chamber and decidualization were the critical processes affected by the loss of PTGS2. We reconstructed the implantation chamber at GD4 1800h and GD5.5 using 3D confocal imaging and image segmentation. At GD4 1800h, 13/14 embryos in control mice displayed a V-shaped chamber; however, in *Pgr*$^{cre/+}$*; Ptgs2*$^{f/f}$ mice, only 6/24 implantation chamber displayed a V-shape while the remaining 18/24 embryos displayed either an asymmetric or an abnormal V-shaped chamber (Fig. 3.9 A, B, C). At GD5.5, control mice displayed continued elongation of the V-shape chamber while the chambers in the *Pgr*$^{cre/+}$*; Ptgs2*$^{f/f}$ uteri appeared shorter (Fig. 3.9 D, E, F). The length of the implantation chamber in *Pgr*$^{cre/+}$*; Ptgs2*$^{f/f}$ mice was significantly lower than control at both GD4 1800h (median chamber length in controls: 575.5µm, *Pgrcre/+; Ptgs2f/f*: 425.5µm, $P < 0.001$) and GD5.5 (median chamber length in controls: 1007µm, *Pgrcre/+; Ptgs2f/f*: 589.5µm, $P < 0.0001$) (Fig. 3.9 G).

We also evaluated vascular development in the implantation and inter-implantation regions of the uterine horn at GD4 1800h. We observed a drastic decrease in vessel density surrounding the embryo implantation chamber in the mutant uteri compared to controls; however, the vessel density in the inter-implantation site remained comparable (Fig. 3.10 A, B, C, D). Vessel diameter was similar in controls and mutants across both implantation and inter-implantation sites (Fig. 3.10 A, B, D). CD31-positive cells accumulate around the implantation chamber (Govindasamy et al., 2021), and this expression overlaps with the PTGS2 expression domain. We observed that 8/8 implantation sites in control mice showed this CD31 signal around the implantation chamber (Fig. 3.10 E, E'), while only 4/10 implantation sites in the mutant showed a CD31 signal around the chamber (Fig. 3.10 F, F', G, G', H).

Given the defects in the implantation chamber, we evaluated the expression of classic decidualization markers. Using qPCR we observed a reduction in *Bmp2* ($P = 0.052$) and *Wnt4* (P

< 0.05) transcripts at GD5.5 in *Pgr*$^{cre/+}$*; Ptgs2*$^{f/f}$ deciduae compared to controls (Fig. 3.11 A). We also tested the decidual response of pseudo-pregnant control and mutant mice to an oil stimulus. We observed in comparison to the control uteri intraluminal oil stimulation of the *Pgr*$^{cre/+}$*; Ptgs2*$^{f/f}$ uteri at pseudopregnancy day 2 1800h completely failed to elicit a decidualization response at pseudopregnancy day 5.5 as reported in *Ptgs2*$^{-/-}$ (Fig. 3.11 B) (Dinchuk et al., 1995; Lim et al., 1997). Taken together, our data suggests that stromal PTGS2 is crucial for post-implantation chamber growth, vessel remodeling surrounding the implantation chamber, and the initiation of decidualization, all of which are critical processes for successful pregnancy.

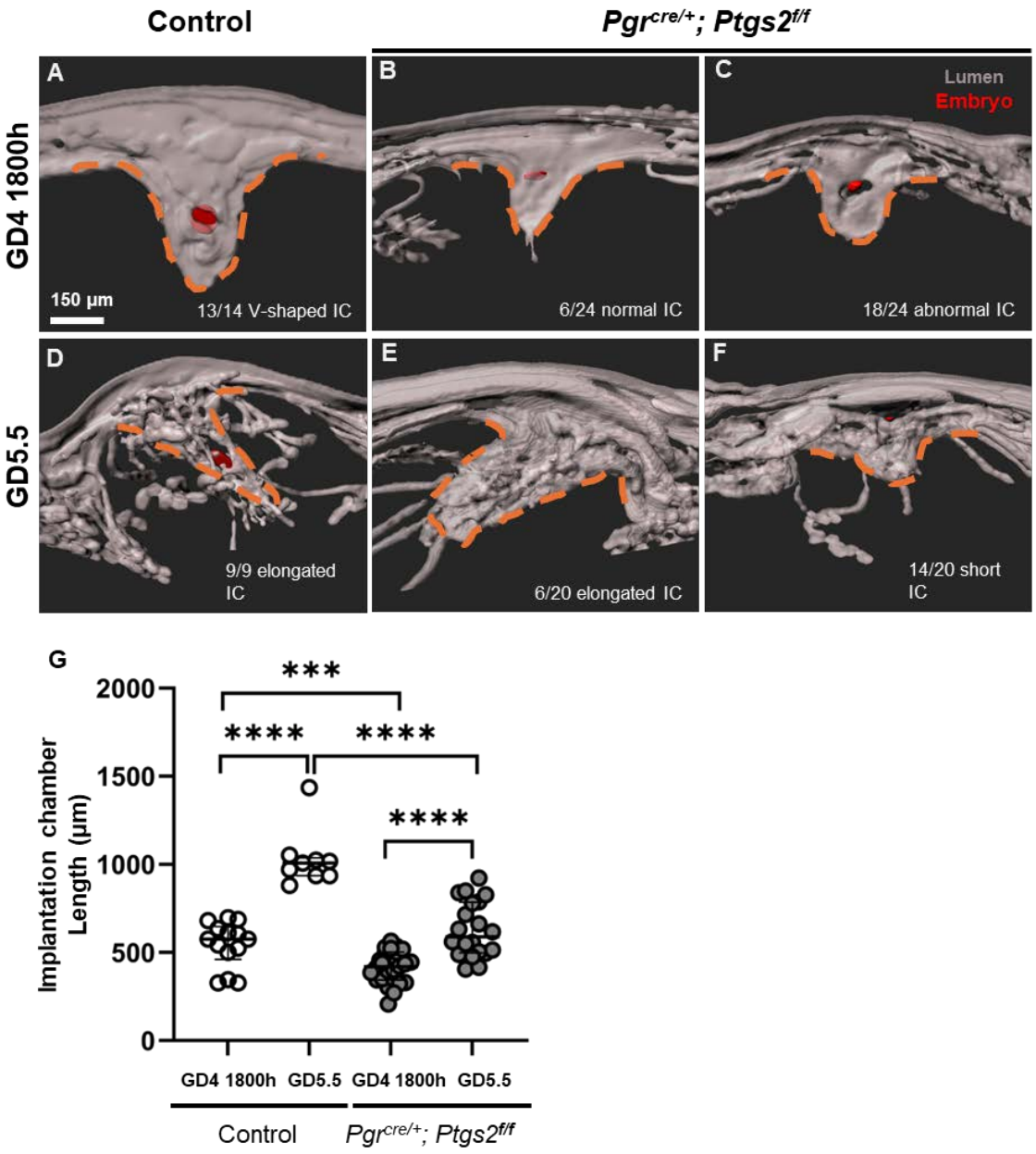

Figure 3.9. Abnormal embryo implantation chamber structure in *Pgr$^{cre/+}$; Ptgs2$^{f/f}$* mice. At GD4 1800h, V-shaped implantation chambers (13/14) are observed in control mice (A) and 6/24 normal V-shaped implantation chambers (B) and 18/24 abnormally shaped implantation chambers (C) are observed in *Pgr$^{cre/+}$; Ptgs2$^{f/f}$* mice. At GD5.5, elongated embryo implantation chambers (9/9) are observed in control mice (D) and 6/20 elongated (E) and 14/20 short implantation chambers (F) are observed in *Pgr$^{cre/+}$; Ptgs2$^{f/f}$* mice. The top of the images represents the mesometrial pole, while the bottom represents the anti-mesometrial pole. Quantitation of implantation chamber in control and *Pgr$^{cre/+}$; Ptgs2$^{f/f}$* mice at GD4 1800h and GD5.5 (G). At least n=3 mice were evaluated per time point. Each dot represents one implantation chamber. Median values are shown. Data was analyzed using an unpaired parametric t-test. *** $P < 0.001$, **** $P < 0.0001$. Scale bar, A-F: 150 µm. Orange dashed lines: embryo implantation chamber; IC: Implantation Chamber.

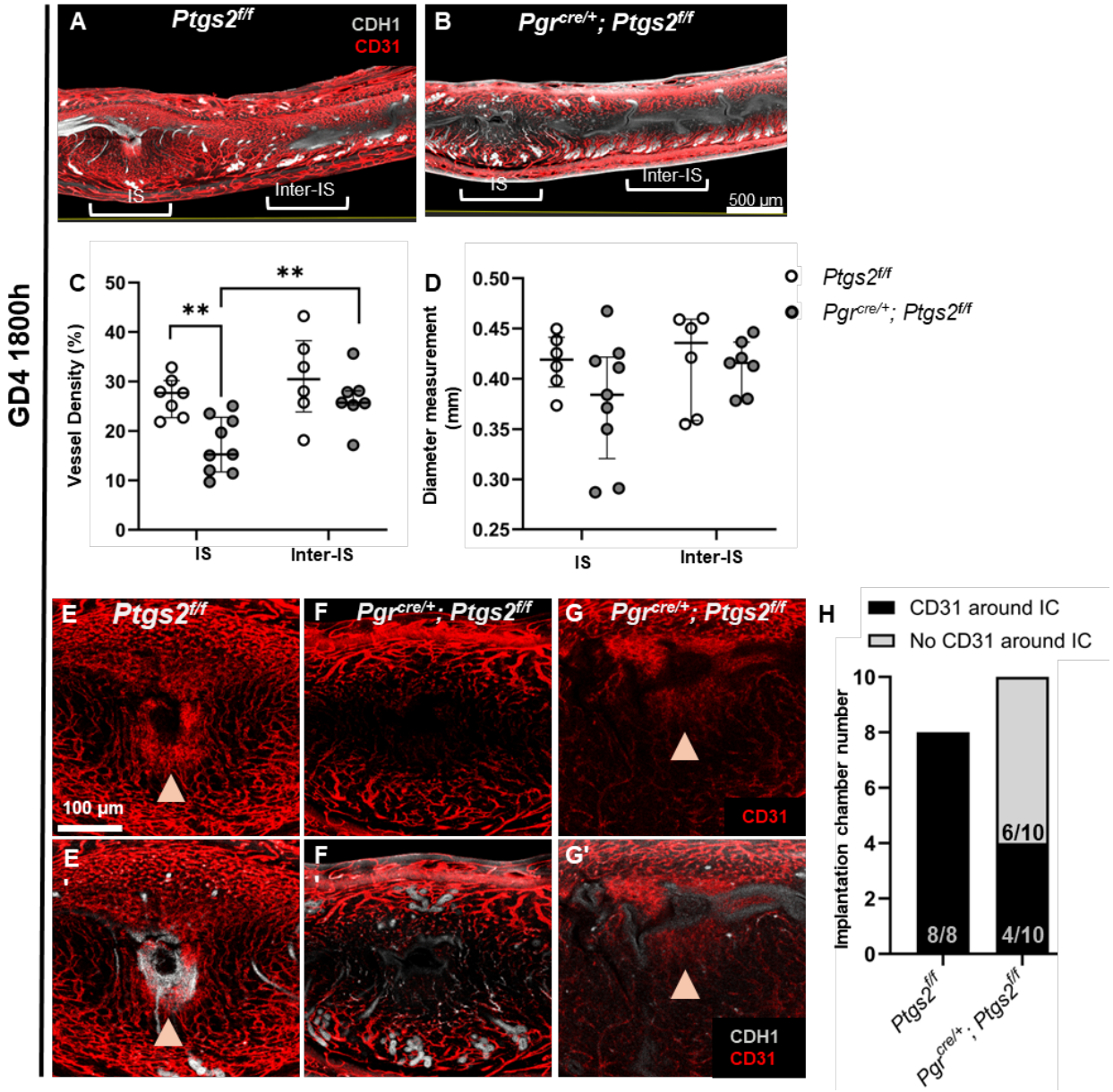

Figure 3.10. Abnormal vascular development at implantation site in *Pgr$^{cre/+}$; Ptgs2$^{f/f}$*. CD31 expression in *Ptgs2$^{f/f}$* (A) and *Pgr$^{cre/+}$; Ptgs2$^{f/f}$* (B) mice at GD4 1800h. Quantitation of vessel density (C) and vessel diameter (D) at embryo implantation sites and in inter-implantation sites (region between two implantation sites). CD31 expression around the embryo implantation chamber in *Ptgs2$^{f/f}$* (E, E') and *Pgr$^{cre/+}$; Ptgs2$^{f/f}$* mice (F, F', G, G'). The top of the images represent the mesometrial pole while the bottom represent the anti-mesometrial pole. Quantification of embryo implantation chamber with and without CD31 expression (H). n=3 mice were evaluated per genotype. Each dot represents one implantation or inter implantation site. Median values shown. Data analyzed using unpaired parametric t-test. ** P < 0.01. Scale bar, A-B: 200 µm, E-G': 100 µm. IS: Implantation site; Inter-IS: inter-implantation site; IC: implantation chamber.

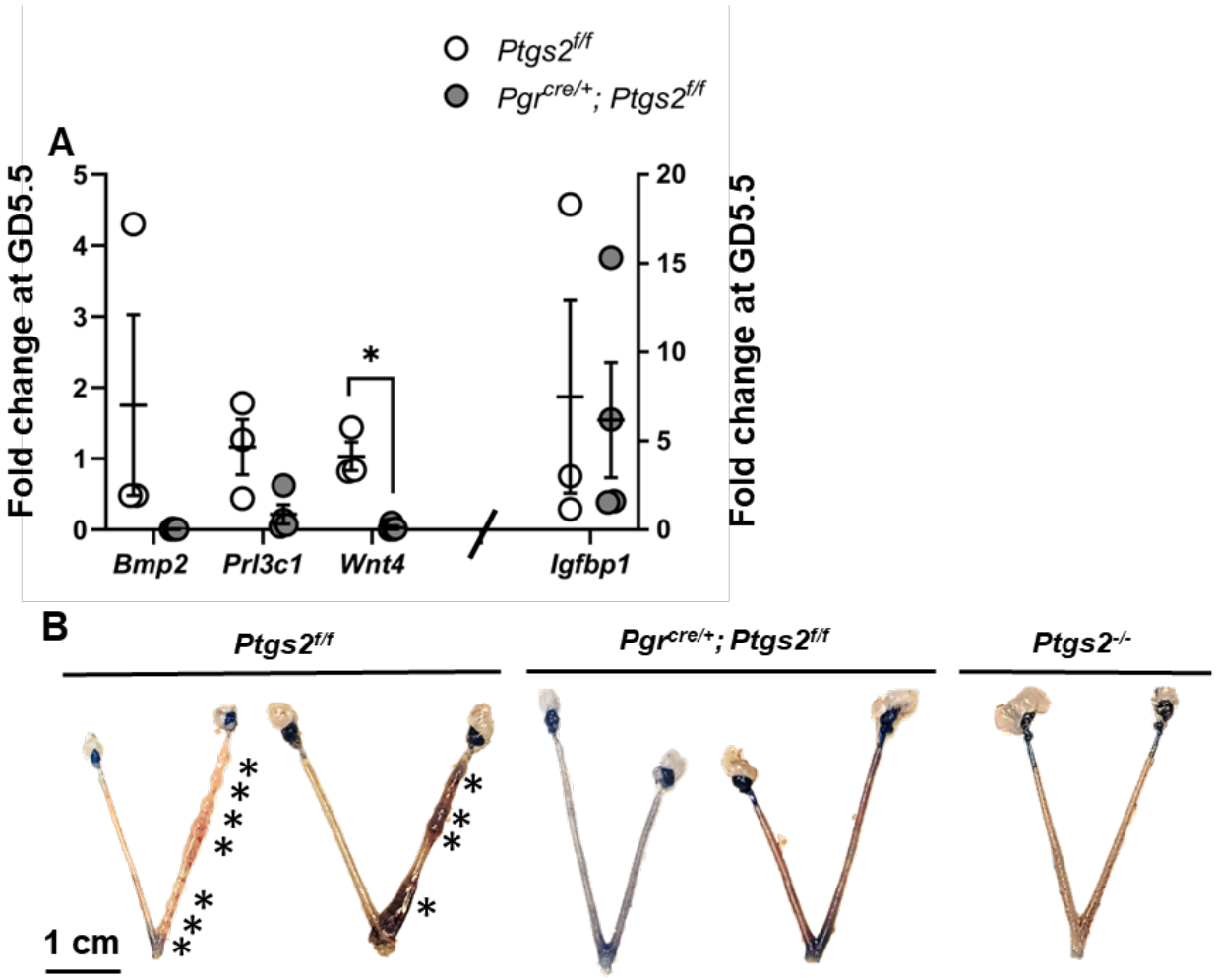

Figure 3.11. Decidualization failure in stromal deletion model of PTGS2. Expression of decidualization markers measured by qRT-PCR at GD5.5 (A). Artificial decidualization induced by oil-stimulation for pseudopregnant mice at pseudopregnancy day 2 1800h and analyzed at pseudopregnancy day 5.5 (B). At least 3 mice for each condition were analyzed. Each dot represents one mouse. Median values shown. Data analyzed using unpaired parametric t-test. * $P < 0.05$. Scale bar, B: 1cm. Black asterisks: decidual sites.

3.4: Discussion

PTGS2-derived prostaglandin is functionally implicated in reproductive processes, including ovulation, fertilization, embryo implantation, and decidualization (Kennedy, 1977; Lim et al., 1999a; Lim et al., 1997; Matsumoto et al., 2001). Despite these studies, there is still a debate in the literature regarding the role of PTGS2 in embryo implantation (Cheng and Stewart, 2003). In this study, we used different tissue-specific ablation models of PTGS2. We do not observe a statistically significance difference in pregnancy success when PTGS2 is deleted in the uterine epithelium and endothelium. In contrast, deleting PTGS2 from the stroma results in post-implantation embryonic growth restriction, defective implantation chamber growth, and mid-gestation resorption. Our results highlight a role for uterine stromal PTGS2 in post-implantation stages of embryo development and initiation of decidualization but no critical role for PTGS2 in pre-implantation processes. During the drafting of this manuscript (Aikawa et al., 2024) published their observations using $Pgr^{cre/+}$; $Ptgs2^{f/f}$ mice, and their results are consistent with ours, suggesting a role for stromal PTGS2 at the maternal-fetal interface. Given the debate on the role of PTGS2 function in murine pregnancy, consistent results with the tissue-specific deletion highlight a role for PTGS2 function independent of mouse genetic background. The discussion below considers our study, as well as those by Aikawa et. al (Aikawa et al., 2024).

Our data demonstrates differences between epithelial and combined epithelial and stromal deletion of PTGS2. However, it does not clearly distinguish between stromal cell-specific synthesis of prostaglandin and a requirement for a threshold level of prostaglandin at the embryo implantation site. Although implantation is delayed at GD4.5, embryo degradation is only observed at GD5.5 when PTGS2 is exclusively expressed in the stroma. This is highly suggestive of a critical role for stromal PTGS2 in post-implantation pregnancy progress. The phenotype in $Pgr^{cre/+}$; $Ptgs2^{f/f}$ mice also supports previous data highlighting unique contributions of stromal PTGS2. PTGS2-derived prostaglandin, particularly PGI2 and PGE2, are crucial regulators of vascular permeability and decidualization, with PGI2 working through the activation of PPARδ

and IP (Lim et al., 1999a). Chromatography/mass spectrometry analysis has revealed that PGI2 is the most abundant prostaglandin at embryo implantation sites, and PGI2 is primarily produced by stromal cells surrounding these implantation sites (Lim et al., 1999a; Wang et al., 2007). In addition to PGI2, recent reports have highlighted other prostaglandins, such as PGD2, which function through its receptor located in the mesometrial region of stromal cells, and PGE2, which functions through its EP4 receptor located in the stromal anti-mesometrial region. The spatial and temporal regulation of these PTGS2-derived prostaglandins remains high during the decidualization process, suggesting that prostaglandin plays a critical role in the decidualization process (Sakamoto et al., 2024).

The delay in embryo implantation observed with combined epithelial and stromal PTGS2 deletion could be due to a greater reduction in local prostaglandin synthesis in the combined deletion compared to the epithelial-only deletion. This is supported by previous studies that demonstrate a need for threshold levels of prostaglandin for successful embryo implantation. For instance, pharmacological studies with PTGS2-specific inhibitor Dup-697 demonstrate progressively severe effects on the implantation process with an increase in inhibitor dose (Lim et al., 1997). Kennedy et al. also report a direct relationship between prostaglandin concentration and vascular permeability (Kennedy, 1979). Further, Wang et al. demonstrate that PTGS1 can rescue fertility in PTGS2-deficient mice in CD1 mouse background, possibly suggesting that total prostaglandin levels must be maintained at a certain threshold to rescue fertility (Wang et al., 2004a). Further studies are needed to distinguish between these possibilities of threshold levels of prostaglandin compared to stromal contributions of prostaglandin synthesis. The development of stromal cell-specific Cre lines, complemented with quantitative assessment of compartment-specific prostaglandin, would help address these questions.

3.4.1: Granulosa cell-specific deletion of PTGS2 does not produce ovulation and fertilization defects

PTGS2 is active in the ovaries during follicular development (Liu et al., 1997; Park et al., 2020a), suggesting its importance during ovulatory processes. Clinical observations have reported luteinized unruptured follicle syndrome, characterized by the failure of follicle wall rupture despite a normal ovulatory cycle, in women who consume non-steroidal anti-inflammatory drugs such as indomethacin or selective PTGS2 inhibitors (Micu et al., 2011). This condition results in infertility (Qublan et al., 2006). In rodents, indomethacin treatment during proestrus disrupts the follicle rupture process, resulting in ovulation failure (Gaytán et al., 2002). Furthermore, both in vitro and in vivo studies have demonstrated that PTGS2 inhibition through indomethacin and NS-398 treatment inhibited LH hormone induction of PGE2 production and thus decreased ovulation rates in rats (Mikuni et al., 1998). *Ptgs2*$^{-/-}$ mice failed to produce prostaglandin in response to gonadotropin stimulation and could not ovulate due to compromised cumulus expansion (Davis et al., 1999). This phenotype of failed ovulation occurs irrespective of mouse genetic background. These diverse lines of studies underscore the indispensable role of PTGS2 in ovulation. PGR and PTGS2 are co-expressed in the mural granulosa cells of the pre-ovulatory follicle following hCG stimulation (Zhang et al., 2023) and LH stimulation (Park et al., 2020a). However, despite PTGS2 deletion in granulosa cells of the pre-ovulatory follicle and the corpus luteum of the ovary (Soyal et al., 2005), *Pgr*$^{cre/+}$*; Ptgs2*$^{f/f}$ mice did not exhibit any ovulation failure. It is possible that *Pgr*^{cre} may fail to delete *Ptgs2* in all granulosa cells, resulting in residual PTGS2 expression and function during ovulation. Alternatively, serum prostaglandin synthesized outside the ovary, oviduct, and uterus may be responsible for the pro-inflammatory response resulting in ovulation. This will be a subject of future investigations.

3.4.2: Uterine epithelial PTGS2 does not contribute to embryo spacing and on-time embryo implantation

The endometrial epithelium has been recognized as a source of the inducible PTGS2 and

associated prostaglandins, especially in the context of menstruation (Lundström et al., 1979). In addition, the epithelial and endothelial prostaglandins are thought to regulate smooth muscle contraction and relaxation (Félétou et al., 2011; Ruan et al., 2011). Inhibiting prostaglandin synthesis results in embryo crowding in pregnant rats (Kennedy, 1977), and prostaglandin plays a critical role in parturition (Aiken, 1972; Reese et al., 2000), highlighting a possible link between epithelial PTGS2 and muscle contractility for embryo spacing and parturition. Our expression studies did not detect epithelial or endothelial PTGS2 during the pre-implantation stage, although we did observe that PTGS2 is expressed in the luminal epithelium shortly after intraluminal stimulation with oil (Lim et al., 1997) and in the glands at the implantation chamber at GD5.5. Despite this, epithelial-only and epithelial and endothelial deletion of PTGS2 did not affect embryo spacing or on-time embryo implantation. Further, deletion of PTGS2 in the circular muscle in the *Pgr*$^{cre/+}$*; Ptgs2*$^{f/f}$ did not affect embryo spacing, supporting that PTGS2 synthesized in the circular muscle, epithelium or endothelium is dispensable for uterine contractility critical for the initial phases of embryo movement.

3.4.3: Uterine stromal PTGS2 is critical for decidualization success

Previous literature suggests that implantation and decidualization failure in *Ptgs2*$^{-/-}$ are not related to disruption in ovarian steroid levels or genes related to implantation success, such as *Leukemia inhibitory factor* (*Lif)* (Lim et al., 1997). Although progesterone levels were normal, we observed a significant reduction in *Lif* mRNA levels in our *Pgr*$^{cre/+}$*; Ptgs2*$^{f/f}$ model. Reduced levels of *Lif* can explain the delay in implantation and may also contribute to the absence of decidualization response with an oil stimulus in this mutant. Delayed implantation may also explain the deviation of the embryo's morphology compared to an elongated blastocyst at GD4 1800h. However, the absence of stromal PTGS2 at the anti-mesometrial pole of the implantation chamber in the *Pgr*$^{cre/+}$*; Ptgs2*$^{f/f}$ model is the most likely cause of poor elongation of the implantation chamber and degradation of the embryos at GD5.5. A defective chamber likely results in a ripple effect of decreased vascular remodeling in the decidua surrounding the

implantation chamber and reduction in the amount of decidualized stroma, leading to growth arrest in the embryo and failure of pregnancy progression. Our results suggest that elongation of the implantation chamber is critical for the transition of the embryo from an elongated blastocyst to an epiblast stage, highlighting a critical role for stromal PTGS2 in embryo-uterine communication at this stage of pregnancy.

Our results also highlight that once chamber formation begins and decidualization is initiated, the embryo is no longer needed for continuous expansion of the decidua. Even though 85% of embryos displayed severe growth retardation at GD5.5, decidual expansion continued until beyond GD8.5, and resorptions were only observed at a significant level at GD12.5 when extraembryonic tissue contributions are required for the formation of the placenta. These data are in line with other models of decidualization where oil and beads (Chen et al., 2011; Herington et al., 2009) can stimulate the initiation of decidualization, and the decidua continues to expand in the absence of embryonic contributions until mid-gestation. It has been proposed that decidualization with a bead or oil is different from embryo-induced decidualization (Herington et al., 2009). The *Pgr*$^{cre/+}$*; Ptgs2*$^{f/f}$ mouse may be a good model to compare the growth of the decidua with and without a growing epiblast to explore the similarities and differences between the two decidualization processes.

Our data also highlights that even with complete ablation of stromal PTGS2 ~50% of the embryos in the *Pgr*$^{cre/+}$*; Ptgs2*$^{f/f}$ uteri continue to develop beyond mid-gestation and are also born. PTGS2 may permit implantation chamber growth beyond a certain length. If the chamber is stochastically able to grow beyond this length (due to PTGS1 upregulation or other factors such as the expanding decidua), then PTGS2 in the stroma may no longer be required. It is also possible that the embryos that display a delay in implantation are susceptible to the absence of stromal PTGS2 during the elongation of the chamber. However, these different hypotheses need to be tested to determine why some embryos continue to grow despite the absence of stromal PTGS2.

3.4.4: Overlapping roles for PTGS1 and PTGS2 in murine implantation success and the role of mouse genetic background

Ptgs1$^{-/-}$ mice on a 129/B6 mouse background have 32% lower vascular permeability and significantly lower prostaglandin levels (specifically 6-keto-PGF1α and PGE_2). These mice also display an upregulation of PTGS2 expression during the pre-implantation stage (Reese et al., 1999). This indicates that PTGS2 can compensate for the function of PTGS1 (Reese et al., 2000). When *Ptgs2* is inserted into the *Ptgs1* locus, PTGS2 can compensate for PTGS1 loss and rescue the parturition defect observed in *Ptgs1*$^{-/-}$ mice (Li et al., 2018b). However, on a C57Bl6 mouse background, when *Ptgs1* was placed in the *Ptgs2* locus, PTGS1 failed to compensate for PTGS2 function resulting in mice with implantation phenotypes similar to the *Ptgs2*$^{-/-}$ mice (Li et al., 2018b; Lim et al., 1997). It has been previously reported that on a mixed mouse genetic background, PTGS1 is upregulated in the *Ptgs2*$^{-/-}$ mice, and these mice exhibit improved fertility compared to *Ptgs2*$^{-/-}$ mice on a pure C57Bl6 mouse background (Wang et al., 2004a). In our studies (on a C57Bl6 background) we did not observe a post-implantation compensatory increase in PTGS1 expression. Further in our studies and those by Aikawa et al (Aikawa et al., 2024) (mouse background not specified), the *Pgr*$^{cre/+}$*; Ptgs2*$^{f/f}$ mice show ~50% number of pups at birth. This percentage is similar to that observed with *Ptgs2*$^{-/-}$ mice on a mixed-background (Wang et al., 2004a) suggesting that factors other than mouse background could be at play. Aikawa et. al also showed that depletion of both PTGS1 and PTGS2 (*Ptgs1*$^{-/-}$;*Pgr*$^{cre/+}$*; Ptgs2*$^{f/f}$ mice, mouse background unknown), results in a complete failure of embryo implantation with embryos floating in the uterus (Aikawa et al., 2024). Since embryos were presumably normal in these mice, the cause for a complete absence of implantation could be lack of *Lif*, however this needs to be tested. All of these studies highlight the interconnected roles of PTGS enzymes and suggest that both PTGS1 and PTGS2 are critical for processes such as implantation and decidualization.

3.5: Conclusion

Our study highlights that PTGS2-derived prostaglandin necessary for implantation does not come from uterine epithelial and endothelial sources. Our work also suggests that stromal PTGS2 at the base of the embryo implantation chamber is critical for both the growth of the embryo and the implantation chamber. Further work is needed to understand how stromal PTGS2 depletion affects the decidualization response and vascular remodeling and why a certain percentage of embryos can escape this requirement and go through gestation. Overall, this study distinguishes between the pre-implantation and post-implantation roles of PTGS2 and provides a valuable model for investigating the role of stromal PTGS2 without the need for embryo transfer to study the initiation of the decidualization process and how it relates to pregnancy success.

Chapter 4: Inhibition of PTGS1 and PTGS2 by indomethacin during embryo implantation disrupts embryo spacing and post-implantation uterine and embryonic development, leading to adverse pregnancy outcomes

Noura Massri, Savannah Wright, Michelle Lupa, Ripla Arora

4.1: Abstract

In patients experiencing recurrent implantation failure, unsuccessful in-vitro fertilization (IVF) is linked to impaired synthesis of prostaglandin. The peri-conceptional use of non-steroidal anti-inflammatory drugs (NSAIDs), which inhibit prostaglandin synthase (PTGS) enzymes PTGS1 and PTGS2, may pose risks to pregnancy. Significant knowledge gaps exist regarding how prostaglandin influences the three-dimensional organization and functionality of the uterine compartments. By employing advanced imaging techniques in conjunction with pharmacological inhibitors, we found that treatment with indomethacin (a dual PTGS1 and PTGS2 inhibitor at a dosage of 6 mg/kg) delayed embryo implantation and resulted in disrupted embryo spacing. Additionally, indomethacin treatment adversely affected the formation of the implantation chamber and impaired vascular permeability at the implantation sites. It led to decidual and embryo resorption, culminating in approximately a 50% reduction in live pups. Furthermore, indomethacin significantly reduced the expression of Leukemia Inhibitory Factor (Lif), a critical component for embryo attachment, prior to implantation, although it did not influence serum progesterone levels. Our findings indicate that the concurrent inhibition of PTGS1 and PTGS2 during the window of uterine receptivity produces detrimental effects on pregnancy, primarily by disrupting timely embryo implantation and causing embryo crowding issues. Moreover, our data reveals that the effects of indomethacin are dose-dependent. This study may help resolve existing discrepancies regarding NSAIDs and miscarriage risks, ultimately facilitating more informed decision-making regarding the use of pain medications during pregnancy.

4.2: Introduction

Non-steroidal anti-inflammatory drugs (NSAIDs), including indomethacin, Aspirin, naproxen, and ibuprofen, represent an important class of medications frequently prescribed for managing pain and inflammation (Funk, 2001). These drugs are used by approximately 2 to 15% of pregnant women in early pregnancy, and they can inhibit PTGS1 and/or PTGS2 with varying specificity, affecting prostaglandin synthesis critical for pregnancy establishment and maintenance (Black et al., 2019; Clark and Myatt, 2008). Although these medications offer effective pain relief for many pregnant women, their use during early pregnancy has raised significant medical concerns and research attention (Black et al., 2019). Population-based studies investigating NSAID use and adverse pregnancy outcomes, particularly spontaneous abortion, have yielded conflicting results. While some studies suggest that NSAID consumption during the early stages of pregnancy may be linked to an increased risk of miscarriage (Li et al., 2003; Nakhai-Pour et al., 2011; Nielsen et al., 2001), others have found no association between NSIAD use and miscarriage risks (Daniel et al., 2014; Edwards et al., 2012). An important exception is the use of indomethacin, which has been noted to have some associated risks (Daniel et al., 2014). These inconsistent findings are further complicated by methodological limitations, such as inadequate exposure measurement and a failure to consider over-the-counter NSAID use. Therefore, understanding the role and potential risks of NSAIDs during early pregnancy is crucial for healthcare providers and expectant mothers to make informed decisions about pain management strategies during this critical period of fetal development.

In rodent models, which have been instrumental in understanding reproductive impacts, NSAIDS profoundly affect multiple aspects of fertility and pregnancy, including ovulation, embryo implantation, decidualization, duration of gestation, and litter size (Aiken, 1972; Diao et al., 2007; Kennedy et al., 2007; Reese et al., 2000; Reese et al., 2001). Studies with specific NSAIDs have revealed timing and drug-dependent effects. For example, the selective PTGS2 inhibitors nimesulide and niflumic acid, have been shown to decrease ovulation rates in rats in a dose-

dependent manner (Diao et al., 2007). While nimesulide does not directly interfere with the implantation process or vascular permeability, it alters critical implantation markers such as PPARδ, HB-EGF, and vimentin, ultimately affecting reproductive outcomes through changes in litter size, birth weight, and gestational length (Diao et al., 2007). The timing of NSAID administration proves critical - celecoxib (PTGS2 inhibitor) and indomethacin (PTGS1 and PTGS2 inhibitor) significantly reduce pregnancy rates when given during days 3-5 of pregnancy in rats (Sookvanichsilp and Pulbutr, 2002), potentially due to the impact of indomethacin on embryo crowding in treated rats (Kennedy, 1977). Similarly, in mice, high doses of ibuprofen (PTGS1 and PTGS2 inhibitor) during the pre-implantation phase resulted in fewer implantation sites (Reese et al., 2001). Notably, concurrent inhibition of both PTGS1 and PTGS2 produces more severe reproductive effects than targeting either enzyme alone (Reese et al., 2001), as demonstrated by diclofenac's reduction of implantation rates to 35-41% compared to 72% in controls (Carp et al., 1988). Collectively, these findings across multiple species highlight the necessity of careful consideration when using NSAIDs during reproduction, as their effects can influence multiple stages of reproductive processes.

Given the ethical considerations in studying human subjects to address the NSAID risk in early pregnancy, rodents have become a viable model to address the risk of NSAID. While previous studies highlight the detrimental effects that NSAIDs have on pregnancy, a critical knowledge gap to be addressed includes how NSAIDs affect the uterine environment during peri-implantation stages, leading to adverse pregnancy outcomes. Thus, we hypothesize that using NSAIDs during early pregnancy can hinder the production of prostaglandin, which results in disrupting the 3D structure of the uterine environment at post-implantation stages, leading to adverse pregnancy outcomes.

To answer this question, we established an NSAID model using indomethacin. Indomethacin binds to the enzyme’s active site and prevents the interaction between the enzyme and its substrate, arachidonic acid. This pharmacological agent is utilized to investigate

prostaglandin function in rodent pregnancy and has been shown to lead to adverse pregnancy outcomes in both mice and rats (Kennedy, 1977; Lau et al., 1973; Snabes and Harper, 1984). Here, we used CD1 mouse model, and we utilized 6mg/kg, a previously used dose (Lau et al., 1973), of indomethacin treatment specifically during the receptivity period on GD3, and evaluated pregnancy outcomes throughout gestation. We also present the use of a selective inhibitor of PTGS1 or PTGS2: 700 nmol of Aspirin and 600 mg/kg of Dup-697.(Lim et al., 1997) in CD1 mouse models, to study how selective inhibition of PTGS enzymes affects implantation success in CD1 background mice. Our research indicates that the concurrent inhibition of PTGS1 and PTGS2 negatively impacts pregnancy. This detrimental effect is associated with several aspects of the implantation process, including delays in embryo implantation, disruptions in embryo spacing as reported in previous studies. Furthermore, pre-implantation inhibition of PTGS1 and PTGS2 alters the three-dimensional structure of the embryo implantation chamber, thus affecting embryo invasion and development. Together, these factors lead to a significant decrease in litter size among the treated group.

4.3: Results

4.3.1: Pre-implantation indomethacin treatment causes delayed embryo implantation, reduced vascular permeability, smaller and crowded decidua, embryo resorption, and litter size reduction

We wanted to determine how PTGS1 and PTGS2 inhibition during pre-implantation period affect pregnancy outcomes. To determine that, we performed an intraperitoneal injection of 6mg/kg indomethacin treatment on gestational day (GD) 3 at 0800h and 1400h (Fig. 4.1 A), the day of uterine receptivity where embryos enter the uterus (Flores et al., 2020). Our data shows that pre-implantation 6mg/kg indomethacin treatment significantly reduces the litter size compared to the vehicle treatment by ~56% (median pups number in the vehicle: 10, 6mg/kg: 4, $P<0.001$) (Fig. 4.2 A, G, H). In contrast, treatment with 2mg/kg indomethacin did not reduce the number of live pups born compared to the vehicle (Fig. 4.2 A). These results suggest that pre-

implantation indomethacin treatment affects pregnancy outcomes in a dose-dependent manner. To determine how 6mg/kg indomethacin treatment led to a significant decrease in live pups at postnatal day (P) 0, we evaluated indomethacin-treated uteri throughout gestation (Fig. 4.1 A). We found that the number of embryo implantation sites (EISs) present in indomethacin-treated mice, as observed by the blue dye sites, was ~49% lower than that in vehicle-treated mice on GD4.75 (median blue dye sites number in vehicle: 14, 6mg/kg: 8, $P<0.0001$) (Fig. 4.2 B, H), however no difference in embryo number between vehicle and 6mg/kg indomethacin treatment was observed on GD3.75 (Fig. 4.2 H), and at GD5.5 (Fig. 4.2 C, H), indicating that pre-implantation indomethacin treatment causes delayed embryo implantation on GD4.5 (Fig. 4.2 B, H). Furthermore, indomethacin treatment causes smaller and more crowded decidua on GD7.5, with no significant difference in decidual site numbers between vehicle and indomethacin-treated uteri (Fig. 4.2 D, H). Furthermore, pre-implantation indomethacin treatment results in embryo crowding and ~40% embryo resorption at GD12.5 (median live embryo number in the vehicle: 11, 6mg/kg: 7, $P<0.01$) (Fig. 4.2 E, F, H). However, such defects were absent in 2mg/kg indomethacin treatment (Fig. 4.3 A-E). In addition, no effect on embryo implantation, as observed by blue dye sites, was noted in aspirin (a PTGS1 inhibitor) and Dup-697 (a PTGS2 inhibitor) (Fig. 4.4 A-F). Despite the delay in embryo implantation observed by lower blue dye sites at GD4.5, we report that pre-implantation indomethacin treatment did not affect luminal closure on GD3.75 in 6mg/kg indomethacin-treated uteri (Fig. 4.5 A, B); However, we observed that indomethacin treatment leads to a significant decrease of Leukemia inhibitory factor (*Lif)* expression in uterine glands at the time of embryo attachment at GD3.75 compared to vehicle-treated uteri (median *Lif* volume associated with FOXA2-positive cells in vehicle: 1.35, 6mg/kg indo: 0.30, normalized unit, $P<0.0001$) (Fig. 4.5 C, D, E). However, despite the significant decrease in *Lif* expression, indomethacin treatment does not affect serum progesterone (P4) levels at GD3.75, indicating only a uterine effect but no ovarian effect of indomethacin treatment at GD3.75 (Fig. 4.5 F). Also, no effect was noted on hormone levels in Aspirin and Dup-697 treatment (Fig. 4.5 B, C, E, F). Thus,

our data illustrates that systemic inhibition of PTGS1 and PTGS2 during the phase of embryo implantation can interfere with uterine function, leading to the delay in embryo implantation and, thus, adverse pregnancy outcomes.

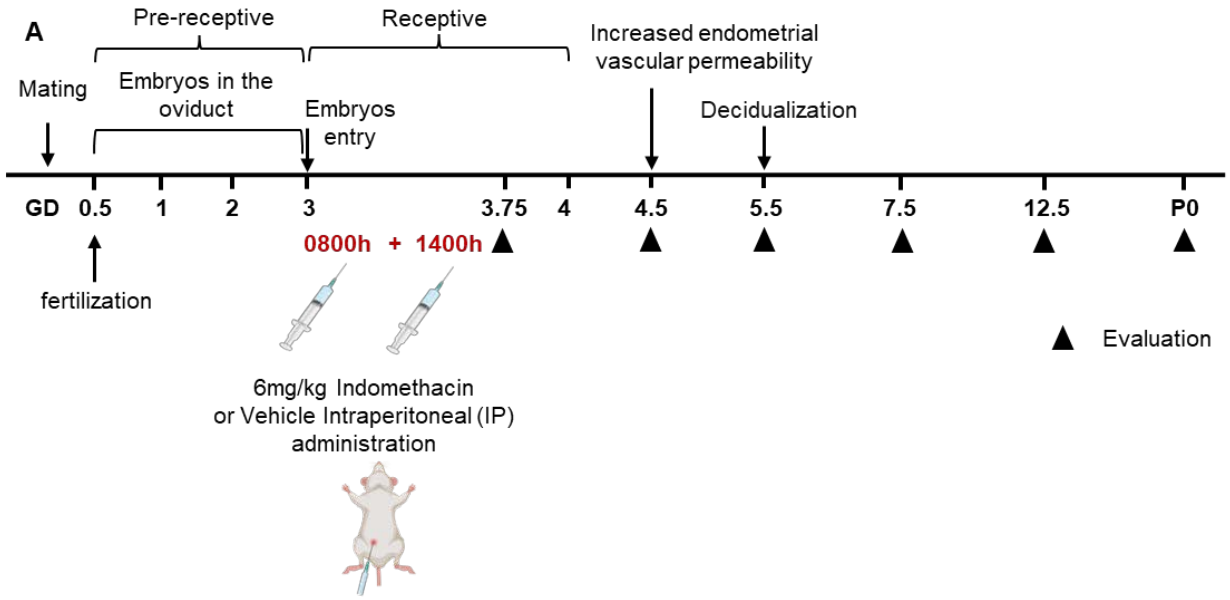

Figure 4.1. Schematic of early events in mouse pregnancy, pre-implantation NSAID treatment, and evaluation times throughout gestation. (**A**) Represent the timeline of mouse pregnancy, indicating the time of 6mg/kg indomethacin and vehicle treatment and uteri evaluation throughout pregnancy.

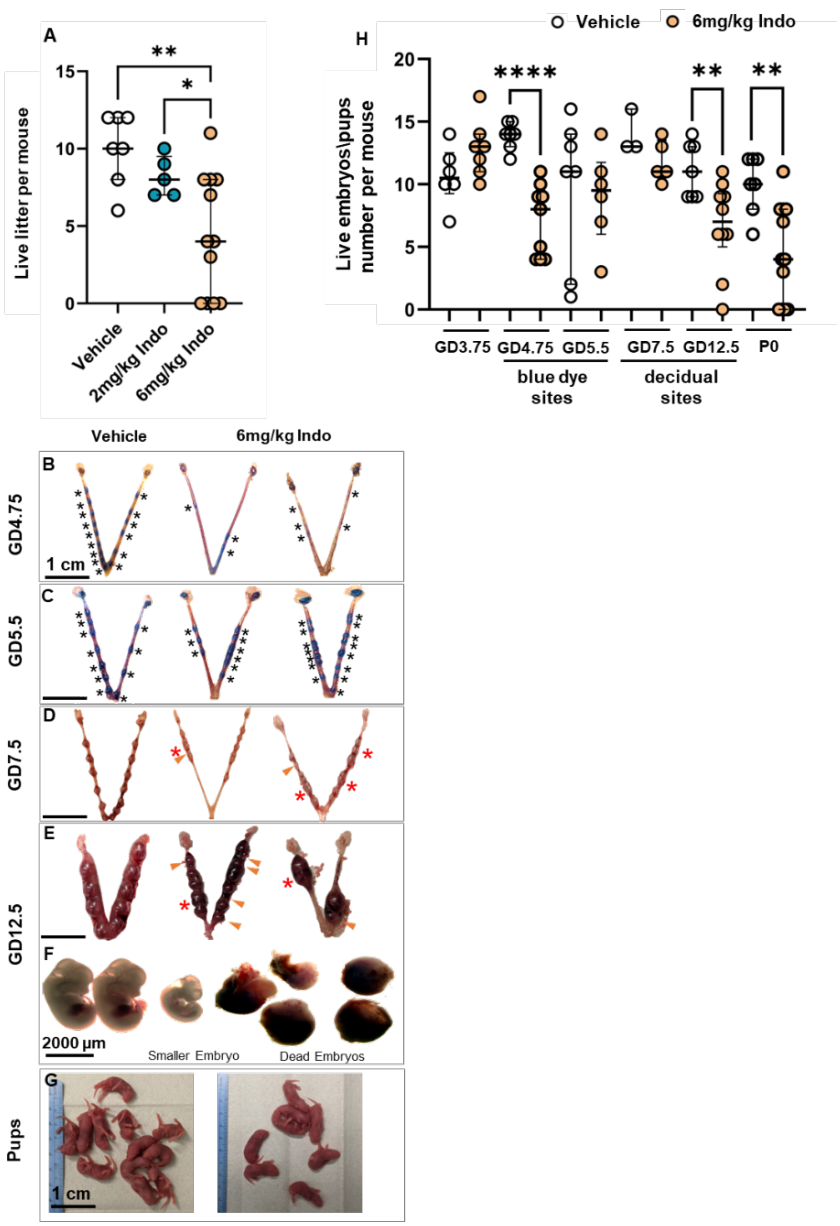

Figure 4.2. Pre-implantation 6mg/kg indomethacin treatment delays embryo implantation, causes mid-gestation decidual resorption, and reduces litter size. (**A**) Quantification of pups number at P0 in the vehicle, 2mg/kg Indo, and 6mg/kg Indo-treated mice. At least n=5 mice were evaluated per treatment group. Each dot represents one mouse. Median values are reported. Data was analyzed using an unpaired parametric t-test and ordinary one-way ANOVA. * $P < 0.05$, ** $P < 0.01$. (**B and C**) Blue dye sites at GD4.75 and GD5.5. (**D and E**) Decidual sites at GD7.5 and GD12.5. (**F**) Representation of embryos at GD12.5, illustrating the small and dead embryos in 6mg/kg indo-treated mice. And (**G**) Litter size at P0 in the vehicle and 6mg/kg Indo-treated uteri. Black asterisk: blue dye site, red asterisk: crowded decidua, orange arrowheads: resorbed decidua. Scale bar, B-E, G: 1 cm, F: 2000 µm. (**H**) Quantification of blue dye sites at GD4.75 and GD5.5, decidual sites number at GD8.5 and GD12.5, and live pups at P0 in both groups. At least n=3 mice were evaluated per group. Each dot represents one mouse. Median values are reported. Data was analyzed using an unpaired parametric t-test. ** $P < 0.01$, **** $P < 0.0001$.

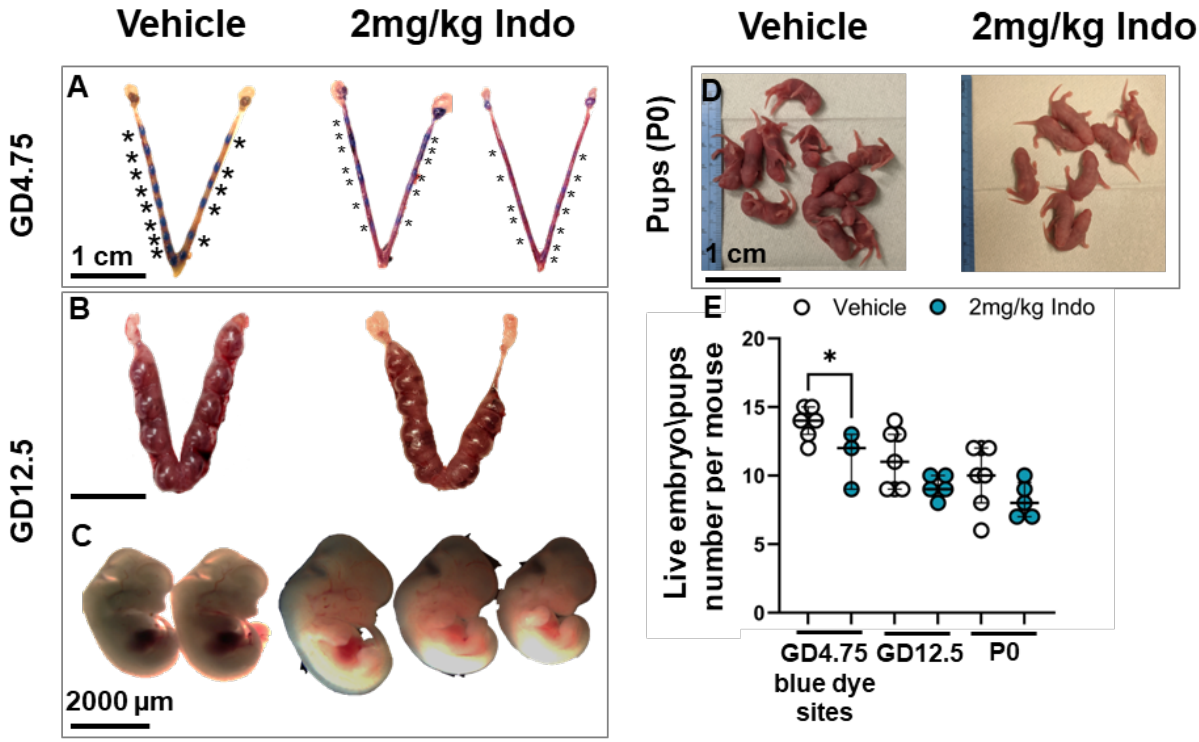

Figure 4.3. Pre-implantation treatment of 2mg/kg indomethacin does not affect overall pregnancy success. (**A**) Blue dye sites at GD4.75, (**B**) decidual sites at GD12.5, (**F**) representation of embryos at GD12.5, and (**G**) Litter size at P0 in the vehicle and 2 mg/kg Indo-treated uteri. Scale bar, A, B, D, 1 cm, C: 1 µm, F: 2000 µm. (**E**) Quantification of embryo number at GD4.75, GD12.5, and live pups number at birth in both vehicle and 2 mg/kg Indo-treated group. At least n=3 mice were evaluated per group. Each dot represents one mouse. Median values are reported. Data was analyzed using an unpaired parametric t-test. ** P < 0.01, **** P < 0.0001.

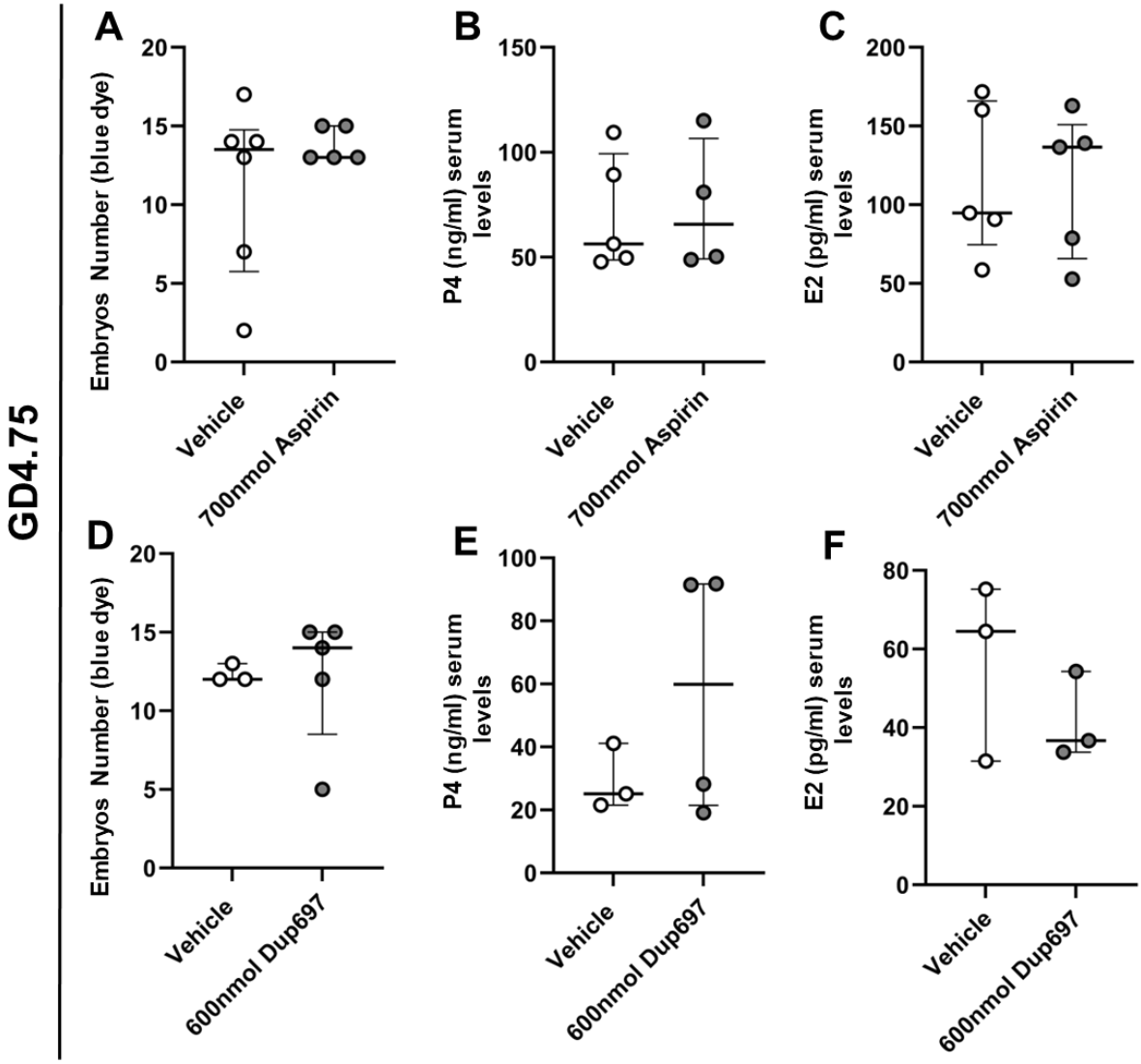

Figure 4.4. Pre-implantation treatment with 700 nmol Aspirin or 600 nmol Dup-697 does not affect implantation and steroid hormone levels. (**A**) Quantification of blue-dye sites, (**B**) progesterone serum levels, and (**C**) estradiol serum level at GD4.75 in Vehicle and 700 nmol Aspirin-treated mice. (**D**) Quantification of blue-dye sites, (**E**) progesterone serum levels, and (**F**) estradiol serum level at GD4.75 in Vehicle and 600 nmol Dup-697-treated mice. At least n = 3 mice were evaluated per group. Each dot represents one mouse. Median values are reported. Data was analyzed using the Mann Whitney T-test for blue due sites, and an unpaired parametric t-test for hormone levels data; $P > 0.05$ was considered non-significant.

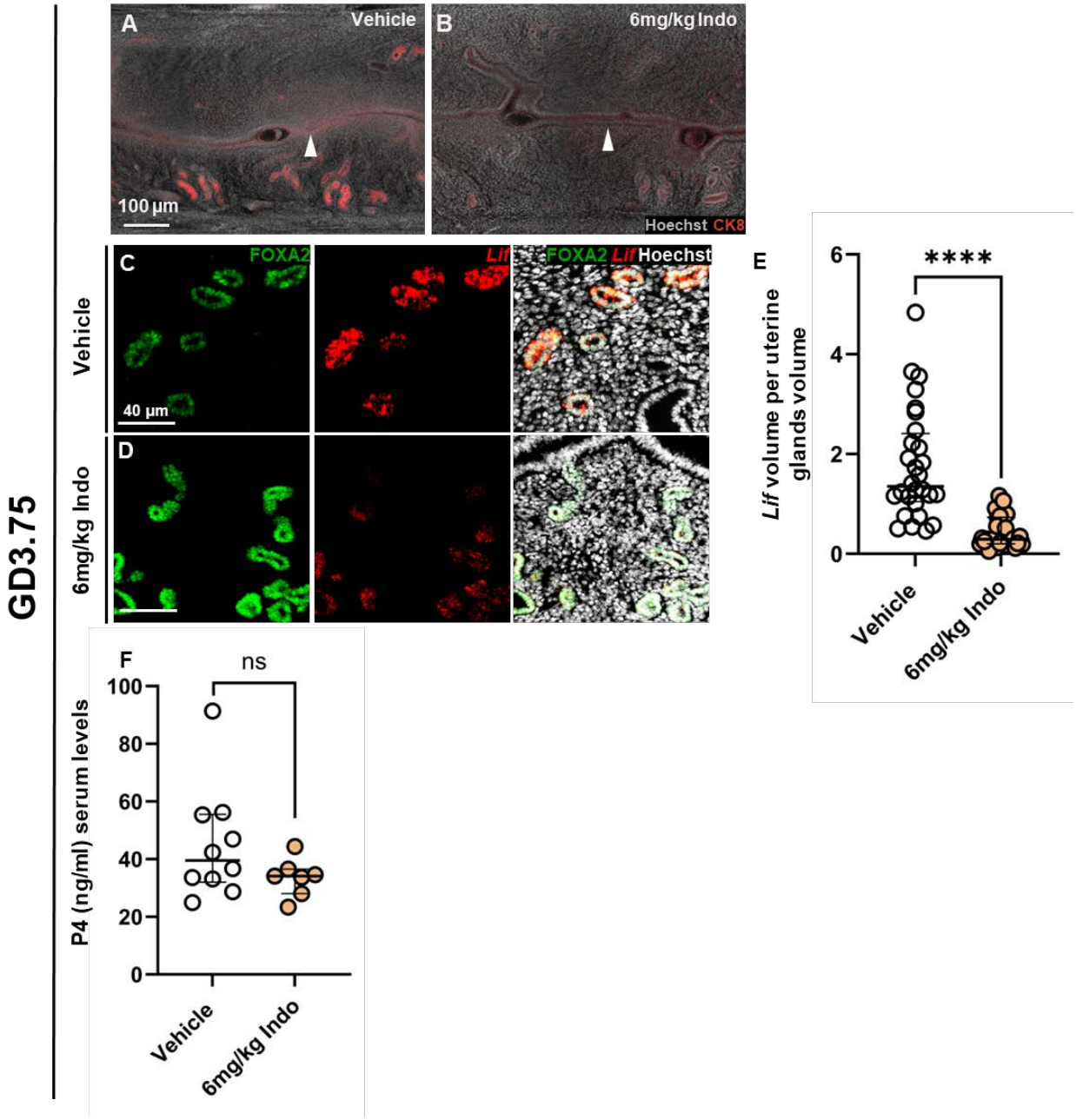

Figure 4.5. 6mg/kg indomethacin-treated uteri display a reduction in preimplantation *Leukemia Inhibitory Factor* with no effect on luminal closure or progesterone levels. Luminal closure representation in (**A**) Vehicle and (**B**) 6mg/kg Indo-treated mice at GD3.75. At least n = 3 mice were evaluated. Scale bar, A, B: 100µm. (**C and D**) *Leukemia inhibitory factor (Lif) expression in* FOXA2+ glandular epithelium cells in the vehicle and 6mg/kg indo-treated uteri at GD3.75. (**E**) Quantification of *Lif* volume normalized to FOXA2+ glandular epithelium volume at GD3.75 per uterine section in the two groups. At least n = 4 mice, and 28 sections were analyzed for each group. Each dot represents one uterine section. Median values are shown. Data was analyzed using the Mann-Witney test. **** $P < 0.0001$. (**F**) Progesterone serum levels in both groups at GD3.75. At least n=3 mice per genotype were analyzed. Each dot represents one mouse. Median values are shown. Data was analyzed using an unpaired parametric t-test. No significant difference was observed.

4.3.2: 6mg/kg indomethacin treatment delays embryo implantation and causes embryo crowding, leading to embryo resorption and, thus, pregnancy loss

Previous research from our group evaluated embryo movement patterns during peri-implantation stages and discovered three distinct movement patterns, including embryo entry to the uterus as a cluster, unidirectional movement, where embryos move as a cluster to the middle of the horn, and bidirectional movement, where the embryos separate from each other until they attach to the uterine epithelium at the end of GD3 (Flores et al., 2020). Using our established NSAIDs mouse model (Fig. 4.1 A), we show here the location of the embryos along the longitudinal oviductal-cervical axis in several treatment models, which include vehicle, 2mg/kg indomethacin, and 6mg/kg indomethacin treatments. We calculated the distance each embryo traveled from the oviduct (O-E) and the embryo-embryo (E-E) distance at GD4.5. We observed that in the 2mg/kg indomethacin treatment, the E-E and O-E distance is not significantly different from the E-E and O-E distance in comparison to the vehicle-treated uteri (Fig. 4.6 A, B, D, E). However, 6mg/kg indomethacin treatment did significantly disrupt the E-E distance in comparison to vehicle-treated uteri (median E-E distance in vehicle is: 1.17, in 6mg/kg indo: 0.73, $P < 0.0001$) (Fig. 4.6 A, C, D, E), with no effect on the O-E distance between the two treatments. Furthermore, the 6mg/kg indomethacin treatment significantly disrupted E-E distance compared to the 2mg/kg indomethacin treatment (median E-E distance in 2mg/kg is: 0.96, in 2mg/kg indo: 0.73, $P < 0.01$) (Fig. 4.6 B, C, D, E). Moreover, the 6 mg/kg indomethacin treatment significantly reduced litter size compared to the vehicle and 2 mg/kg indomethacin treatments, indicating that disrupted embryo spacing negatively impacts pregnancy success.

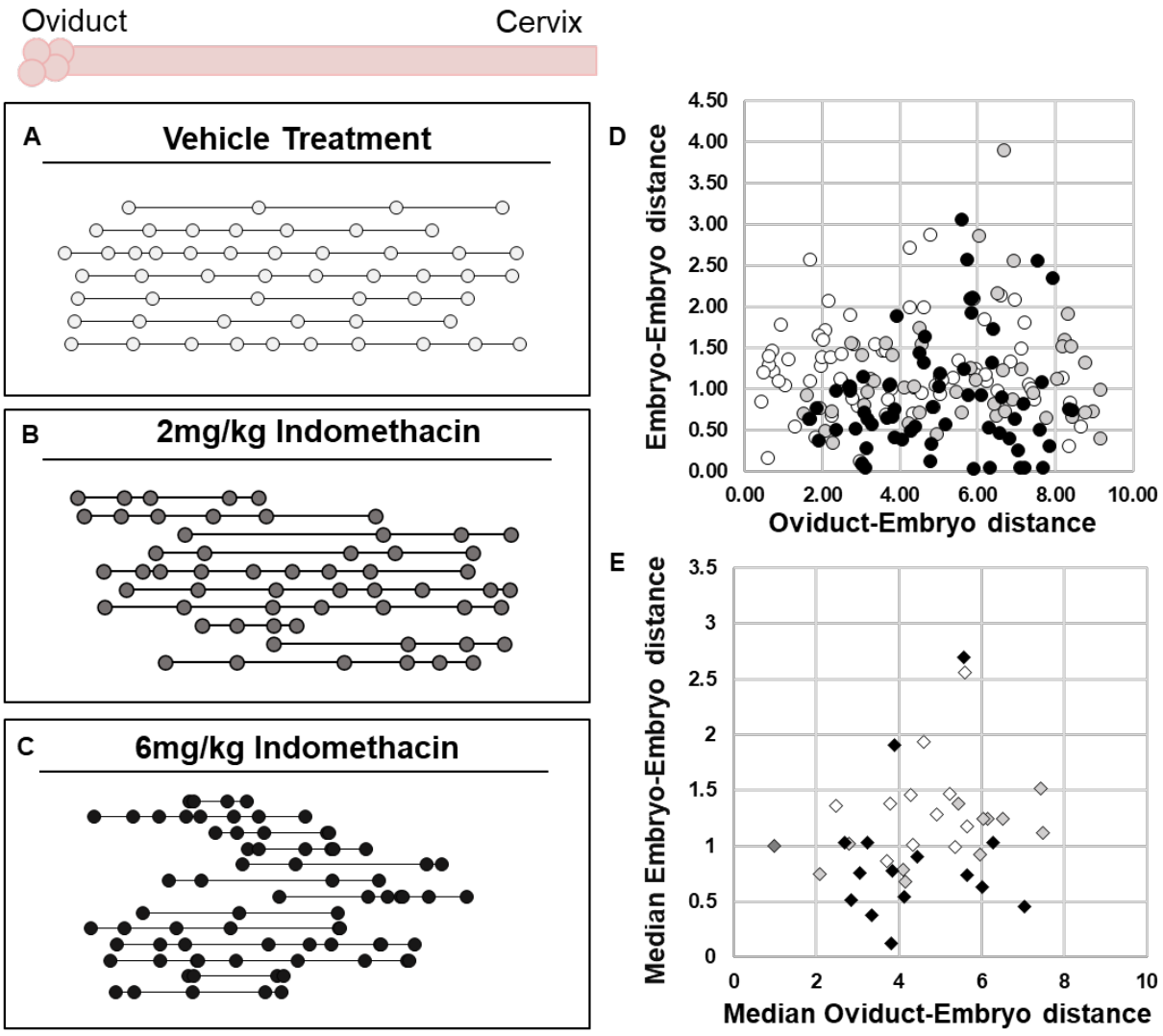

Figure 4.6. Uteri treated with 6mg/kg indomethacin shows a significant disturbance in embryo spacing compared to those treated with vehicle or 2mg/kg indomethacin. Representation of the placement of embryos along the oviduct and cervix axis in the vehicle group (**A**), the 2 mg/kg indo group (**B**), and the 6 mg/kg indo-treated uterine horns (**C**) at post-implantation stages on GD 4.5. Each circle represents an individual embryo, and circles connected by a line indicate embryos that are from the same uterine horn. The oviduct is on the left side, while the cervix is on the right side. A minimum of n = 5 mice and 7 uterine horns were analyzed for each treatment group. Classification of uterine horns based on individual data points representing the oviduct-embryo (OE) and embryo-embryo (EE) distance (**D**). Each circle on the graph represents an embryo. Data was analyzed by the Mann-Whiney test. ** $P < 0.01$, **** $P < 0.0001$. The graph represents the median OE and EE distance (**E**). Each symbol represents the median values of OE and EE distance from each uterine horn in the three treatment groups. (D, E) white color symbols represent vehicle, light gray color symbols represent 2mg/kg indo, and black color symbols represent 6mg/kg indo.

4.3.3: Pre-implantation indomethacin treatment at peri-implantation stages interferes with embryonic development to the epiblast stage at GD5

Our previous study suggests that PTGS2 depletion using *Pgr*$^{cre/+}$*; Ptgs2*$^{f/f}$ (Madhavan and Arora, 2022) from the uterine environment results in embryonic growth restriction and, thus, mid-gestation resorption and ~46% litter size reduction (Massri and Arora, 2025). Since we have ~40% embryo resorption at GD12.5 and ~56% litter size reduction at P0 with pre-implantation pharmacological inhibition of PTGS1 and PTGS2 using 6mg/kg indomethacin, we wanted to determine how PTGS1 and PTGS2 inhibition might affect embryonic development to the blastocyst stage at GD3.75 and GD4.5 and the epiblast stage at GD5.5. We report that pre-implantation indomethacin treatment (Fig. 4.1 A) did not affect embryonic development to the blastocyst stage on GD3.75 and GD4.5 (Fig. 4.7 A-E, I); however, indomethacin treatment did affect embryonic development to the epiblast stage at GD5.5, as approximately ~48% of the embryos did not develop to the proper epiblast stage some of these embryos are completely resorbed, others remain in the morula or the blastocyst stage and the rest did not reach the cylinder shape of the epiblast (Fig. 4.7 A-H, I). Since we reported crowding phenotype in our 6mg/kg indomethacin treatment and to determine if the crowding phenotype is the cause for abnormal embryonic development at GD5.5, we found that ~38% of the abnormal-looking embryos are in the crowded sites (in the same decidua), while around 58% of the abnormally shaped embryos are not. Embryos in the same decidual sites at GD5.5 were crowded (Fig. 4.7 J). Our data indicates that pre-implantation inhibition of PTGS1 and PTGS2 interferes with embryonic development to the epiblast stage at GD5.5.

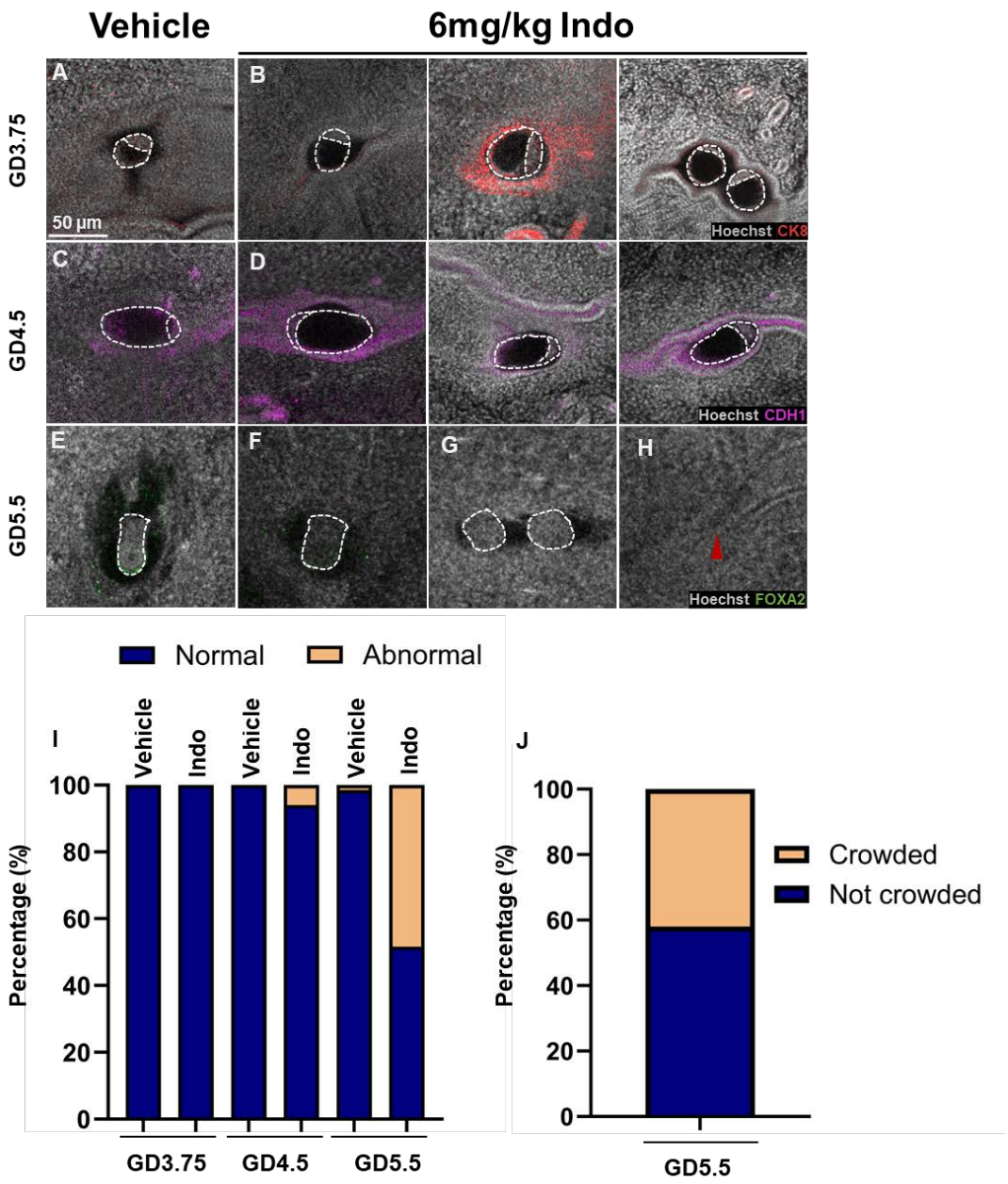

Figure 4.7. PTGS1 and PTGS2 inhibition restrict embryo growth at post-implantation stages on GD5.5. At gestational days 3.75 (GD3.75) and 4.5 (GD4.5), embryos in the blastocyst stage were observed in both vehicle-treated (**A and C**) and 6 mg/kg Indo-treated (**B and D**) mice. Additionally, epiblast-stage embryos were found in vehicle-treated mice (**E**). At the same time, in the 6 mg/kg Indo-treated uteri, there were epiblast and abnormal embryos, including those with abnormal epiblast-shape (**F**), morula-stage embryos (**G**) and wholly resorbed embryos (**H**) at GD5.5. Red arrowhead: resorbed embryo. A comparison was made of the percentage of embryo development across GD3.75 to GD5.5 (**I**). The percentage of abnormal embryos was compared between those located in crowded sites (within the same decidua) and those located in a single decidua at GD5.5 (**J**). At least n=6 mice for each group were analyzed per time point. Scale bars, A-H: 50 µm. The top of the images represents the mesometrial pole, while the bottom represents the anti-mesometrial pole.

4.3.4: Pre-implantation indomethacin treatment disrupts embryo implantation chamber formation and vascular remodeling around the embryo implantation chamber

PTGS1 and PTGS2 treatment interferes with post-implantation embryonic development, as we observed with our *Pgr*$^{cre/+}$*; Ptgs2*$^{f/f}$ model where embryos were resorbed during post-implantation stages at GD4 1800h (Massri and Arora, 2025). Meanwhile, in our indomethacin model, embryos are starting to be resorbed at GD5.5. Building on these findings, we employed similar methodologies and report that the formation and length of the embryo implantation chamber in our 6mg/kg indomethacin mouse model are disrupted compared to vehicle-treated uteri. Specifically, the length of the embryo implantation chamber is significantly shorter in indomethacin-treated uteri compared to those treated with the vehicle at both GD4.5 (median implantation chamber length in vehicle is: 544.0, in 6 mg/kg indo: 386.5, $P < 0.001$) and GD5.5 (median implantation chamber length in vehicle is: 885, in 6 mg/kg indo: 609, $P < 0.0001$) (Fig. 4.8. A-I). Additionally, the density of blood vessels surrounding the embryo implantation chamber in the indomethacin-treated uteri is significantly higher than that in the vehicle-treated uteri at GD4.5 (median blood vessel density around embryo implantation chamber in the vehicle is 21.03, in 6 mg/kg indo: 29.82, $P < 0.05$) (Fig. 4.9 A, B, C). Furthermore, CD31-positive cells can be observed clustering around the implantation chamber, and this distribution notably coincides with the area where PTGS2 is expressed (Massri and Arora, 2025). We observed that 22 out of 22 implantation sites in vehicle-treated mice displayed a CD31 signal around the implantation chamber (Fig. 4.9 D-D', G). In contrast, only 10 out of 14 implantation sites in the mutant showed a CD31 signal in the same area (Fig. 4.9 E, E', F, F', G). Thus, our data suggests that the pharmacological inhibition of PTGS1 and PTGS2 during pre-implantation stages at GD3 delays embryo implantation and disrupts the proper formation of the embryo implantation chamber and the remodeling of blood vessels around it. This disruption ultimately leads to mid-gestation embryo resorption and a reduction in litter size.

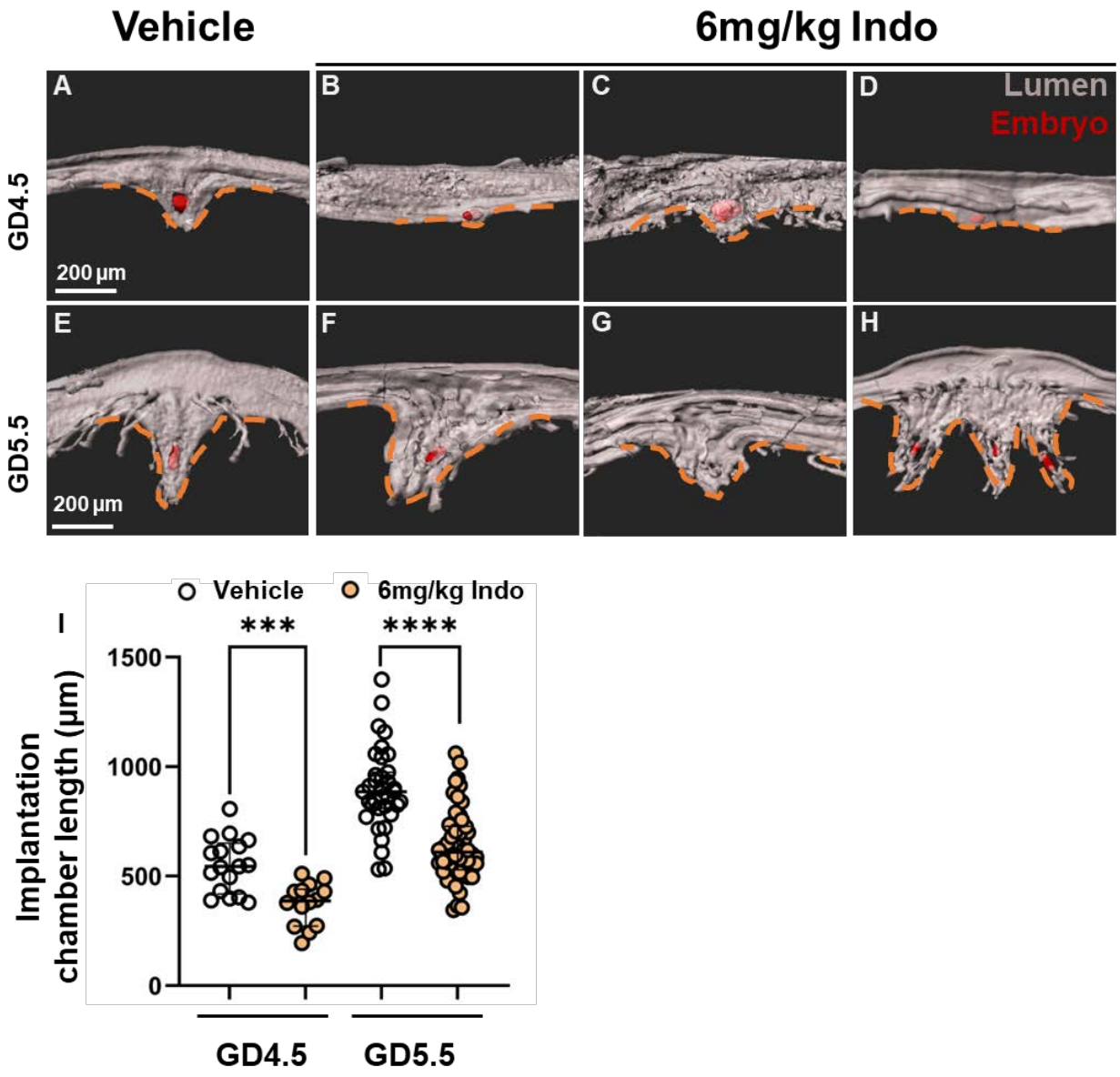

Figure 4.8. Abnormal embryo implantation chamber length and formation in 6mg/kg indomethacin-treated uteri. At GD4.5, V-shaped implantation chambers are observed in vehicle-treated mice (**A**), and abnormally shaped implantation chambers (**B, C, D**) are observed in 6mg/kg indo-treated mice. At GD5.5, elongated embryo implantation chambers are observed in control mice (**E**), and short implantation chambers (**F, G**) and elongated chambers (**H**) are observed in 6mg/kg indo-treated mice. Orange dashed lines: embryo implantation chamber. Scale bar, A-H: 200 µm. The top of the images represents the mesometrial pole, while the bottom represents the anti-mesometrial pole. Quantitation of implantation chamber in the vehicle and 6mg/kg indo-treated uteri at GD4.5 and GD5.5 (G). At least n=6 mice were evaluated per time point. Each dot represents one implantation chamber. Median values are shown. Data was analyzed using an unpaired parametric t-test and the Mann-Whitney test. *** $P < 0.001$, **** $P < 0.0001$.

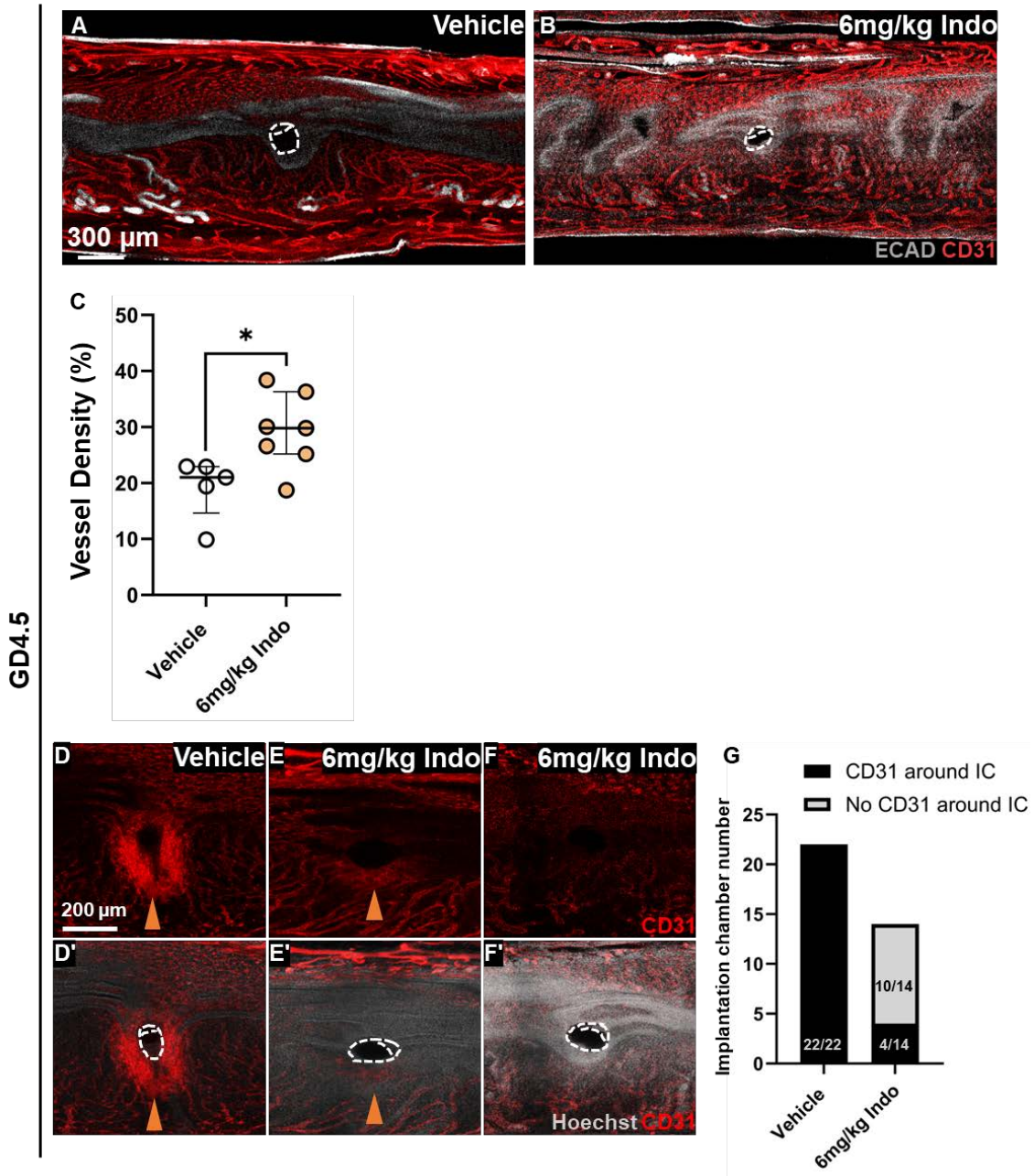

Figure 4.9. Abnormal vascular development at the embryo implantation sites in 6mg/kg indomethacin-treated uteri. Vessels architecture in vehicle-treated uteri (**A**) and 6mg/kg indo-treated uteri (**B**) at GD4.5. Scale bar, A-B: 300 µm. Quantitation of vessel density at embryo implantation sites in both groups at GD4.5 (**C**). Median values are shown. Each dot represents one implantation site. Data was analyzed using an unpaired parametric t-test, * $P < 0.05$. CD31 expression around the embryo implantation chamber in the vehicle (**D and D'**) and 6mg/kg indo-treated uteri (**E-F'**). Orange arrowhead: CD31 expression. Scale bar, D-F': 200 µm. The top of the images represents the mesometrial pole, while the bottom represents the anti-mesometrial pole. Quantification of embryo implantation chamber with and without CD31 expression (**G**). At least n=3 mice were evaluated per treatment group. IC: implantation chamber.

4.4: Discussion

Our findings indicate that systemic inhibition of PTGS1 and PTGS2 during the peri-implantation period, induced by indomethacin treatment, affects pregnancy outcomes in a dose-dependent manner. Treatment with 6 mg/kg of indomethacin significantly reduced the number of live pups compared to the 2 mg/kg dosage, suggesting a more pronounced negative impact of the higher dose on pregnancy success. Our data indicates that pre-implantation PTGS1 and PTGS2 inhibition caused by 6mg/kg indomethacin treatment results in delayed implantation and resorbed and crowded decidua, ultimately reducing litter size. Our data aligns with earlier observations regarding pre-implantation PG-depletion and adverse pregnancy outcomes in rodents (Kennedy, 1977; Kennedy, 1979; Kennedy et al., 2007; Lau et al., 1973).

Specifically, the 6 mg/kg indomethacin treatment resulted in the following observations: delayed embryo implantation, evidenced by significantly lower *Lif* expression at GD3.75, fewer blue dye sites in the 6 mg/kg group at GD4.75, but comparable numbers of implantation sites at GD5.5. Indomethacin led to the emergence of smaller and more crowded decidua at GD7.5, which led to embryo resorption at mid-gestation, culminating in a significant reduction in live pups born. The increased embryo resorption observed at birth may be attributed to the progressive resorption or demise of smaller embryos noted in the 6 mg/kg indomethacin treatment during mid-gestation. In addition, the 6mg/kg indomethacin treatment caused significant disruption in the embryo-embryo distance compared to the vehicle and 2mg/kg indomethacin treatment. Furthermore, indomethacin results in an abnormal development of the embryos to the epiblast stage at GD5.5. Moreover, this treatment disrupts the shape and length of the embryo implantation chamber and leads to abnormal vascular remodeling surrounding the embryo implantation sites at post-implantation stages.

4.4.1: Delayed embryo implantation and disrupted embryo spacing are detrimental to pregnancy success

Previous studies have highlighted that delayed embryo implantation and disrupted embryo

spacing can impair pregnancy success through distinct mechanisms (Diao et al., 2015; Song et al., 2002; Ye et al., 2005). Delayed embryo implantation may result in defective post-implantation development, which can manifest as retarded embryonic growth and a reduction in litter size (Diao et al., 2007; Song et al., 2002; Song and Fazleabas, 2021). Transferring blastocyst-stage embryos to wild-type mice outside the designated implantation window can result in significant anomalies and increased resorption rates (Song et al., 2002). This finding emphasizes the critical importance of embryo implantation within the specific uterine receptivity period. In humans, the timing of embryo implantation is vital. Implantation must occur within the window of 6 to 10 days after ovulation; otherwise, it may lead to early pregnancy loss (Su and Fazleabas, 2015).

In addition to delayed embryo implantation, embryo crowding leads to several adverse outcomes that significantly compromise pregnancy success. During normal pregnancy, embryos space themselves evenly along the uterine horn to ensure each has adequate room for placental development and access to maternal resources (Chen et al., 2013; Flores et al., 2020). However, when this spacing mechanism fails, as seen in Lpar3-deficient mice or Pla2g4a-deficient mice, multiple embryos cluster together at a single implantation site (Song et al., 2002; Ye et al., 2005). Studies have shown that 2 to 4 embryos can crowd into one location, with 44% of implantation sites showing this abnormal clustering by embryonic day 10.5 (Ye et al., 2005). This crowding event forces the embryos to compete for limited space and maternal resources, often resulting in shared placentas that cannot adequately support multiple embryos (Chen et al., 2013; Chen et al., 2011). The consequences cascade throughout development; embryos with shared placentas show significantly slower growth rates due to restricted nutrient and oxygen access. This compromised development frequently leads to embryo resorption, where some or all of the clustered embryos fail to survive. Even embryos that initially develop normally may ultimately fail due to the increasing demands for resources as gestation progresses. The impact extends beyond individual embryos to affect entire litter survival, making proper embryo spacing a critical determinant of successful pregnancy outcomes (Chen et al., 2011; Ye et al., 2005).

These defects in implantation might have led to the restricted embryonic development to the epiblast stage by GD5.5 in our indomethacin model. Among these restricted embryos, only 38% were located in crowded decidual sites, suggesting that embryo crowding was not the sole factor contributing to restricted embryonic development and, thus, substantially reduced live pups at birth. Importantly, our indomethacin treatment at a dose of 2 mg/kg did not affect the distance between embryos relative to those in vehicle-treated uteri, highlighting that the effects of indomethacin are dose-dependent.

4.4.2: PTGS1 and PTGS2 inhibition produced a more pronounced effect on pregnancy

Our results indicate that inhibiting both PTGS1 and PTGS2 leads to more significant defects in a dose-dependent manner. Although we did not assess the pregnancy outcomes related to Aspirin (PTGS1 specific inhibitor) and Dup-697 (PTGS2 specific inhibitor) treatments, data from the blue dye sites showed no signs of delayed implantation. Also, we did not observe any clustering of embryos on GD4.5 in the CD1 mice treated with either 700nmol Aspirin or 600 nmol of Dup-697 at pre-implantation stages. One factor that may contribute to the success of embryo implantation in cases of single isoform inhibition is a system of a backup mechanism that helps ensure reproductive success through supporting embryo implantation (Reese et al., 1999; Wang et al., 2004a). The strongest evidence for this comes from genetic studies showing dramatically different outcomes when one versus both PTGS isoforms are eliminated. Mice lacking PTGS2 displayed complete implantation failure in C57BL/6J/129 mice (Lim et al., 1997). However, in CD1 mice, PTGS2 deletion leads to only partial reproductive defects because PTGS1 compensates by becoming upregulated in a pattern that mimics regular PTGS2 expression (Wang et al., 2004a). In contrast, the deletion of PTGS1 resulted in only extended difficulties related to parturition (Loftin et al., 2002), indicating that PTGS2 plays a more crucial role in the early stages of pregnancy. Various molecular mechanisms may contribute to the compensatory upregulation of PTGS1 in PTGS2-null CD1 mice, a phenomenon absent in C57BL/6 mice. One possible explanation is that CD1 mice might possess polymorphisms in the regulatory regions of PTGS1,

enabling it to respond to transcription factors such as NF-κB, C/EBP, or CREB, which typically regulate PTGS2 (Harper and Tyson-Capper, 2008; Kang et al., 2007). Alternatively, the deficiency of prostaglandin resulting from PTGS2 deletion could activate feedback loops that stimulate signaling pathways capable of inducing PTGS1 transcription in ways that resemble PTGS2 expression in endometrial tissues during peri-implantation stages (Chakraborty et al., 1996; Ricciotti and FitzGerald, 2011; Wang et al., 2004a). Conducting ChIP-seq analysis (Esnault et al., 2014) to investigate transcription factors binding to PTGS1 enhancer regions in both CD1 and C57BL/6 mouse strains could provide further insight into the precise molecular basis of this intriguing regulatory mechanism.

The critical importance of having at least one functional PTGS isoform becomes clear when examining dual PTGS1/PTGS2 knockout mice. These animals experience complete reproductive failure with no embryo attachment, demonstrating that the presence of at least one PTGS enzyme is essential for implantation (Aikawa et al., 2024; Lim et al., 1997; Reese et al., 2001) Pharmacological studies support this conclusion: while selective inhibition of either PTGS1 or PTGS2 alone allows some reproductive function, simultaneous inhibition of both enzymes with non-selective NSAIDs like indomethacin or ibuprofen can prevent implantation (Kennedy, 1977; Lau et al., 1973; Reese et al., 2001). For instance, treating mice with ibuprofen can prevent successful implantation and decidualization (Reese et al., 2001). On the other hand, selectively inhibiting just one isoform with medications such as nimesulide or NS-398 typically results in less severe reproductive issues than blocking both isoforms. A key experiment demonstrating this principle used the selective PTGS2 inhibitor celecoxib at high doses (600 mg/kg twice daily) during days 3-7 of pregnancy. Even at these high doses, celecoxib alone only modestly reduced prostaglandin levels. However, when researchers combined this PTGS2 inhibition with the genetic deletion of PTGS1, they observed complete reproductive failure (Reese et al., 2001).

This suggests that while individual isoforms may have some redundant functions, the simultaneous loss of both PTGS1 and PTGS2 eliminates all alternative sources of prostaglandin

synthesis in the female reproductive tract, resulting in a complete failure in embryo attachment (Aikawa et al., 2024; Reese et al., 2001). This is significantly more severe than the phenotype observed with a single PTGS2 deletion (Massri and Arora, 2025) or a time-dependent inhibition of PTGS1 and PTGS2, where approximately half of the embryos can develop beyond mid-gestation since some prostaglandins are still functional at the implantation sites.

In our model, our indomethacin treatment was only on GD3, the uterine receptivity day, or during the embryo implantation window. This treatment delayed embryo implantation, resulting in an abnormal formation of the embryo implantation chamber and disrupted vascular remodeling around the embryo implantation sites. We predict that with sustained inhibition of PTGS1 and PTGS2 by indomethacin, complete embryo implantation failure might be observed, as shown in previous reports (Aikawa et al., 2024; Reese et al., 2001). Also, using the *Pgr*$^{cre/+}$*; Ptgs2*$^{f/f}$ model, we observed that PTGS2 is critical for on-time embryo implantation, the formation of the embryo implantation chamber, and the remodeling of blood vessels around the embryo implantation chamber (Massri and Arora, 2025).

4.4.3: Limitations of the study

Using a wide range of non-steroidal anti-inflammatory drugs (NSAIDs) at different doses and their respective controls is a valuable approach to studying prostaglandin function in early pregnancy. The NSAIDs included in these studies are 2 mg/kg and 6 mg/kg indomethacin, 700 nmol aspirin, and 600 nmol Dup-697. However, it is also crucial to identify which specific prostaglandins are inhibited during these drug treatments. This information is essential for understanding the prostaglandin associated with the adverse pregnancy outcomes observed in our studies. We can achieve this by measuring serum and tissue levels of prostaglandin during and after the treatment time using ELISA or mass spectrometry.

4.5: Conclusion

NSAIDs pose a risk during early pregnancy if taken at the time of conception(Black et al., 2019). Additionally, studies in rodents have further validated that the administration of NSAIDs

during early pregnancy can lead to adverse pregnancy outcomes (Kennedy et al., 2007). Our research demonstrates that treatment with 6 mg/kg indomethacin can cause delays in embryo implantation, disrupt embryo spacing, retard embryo growth, and interfere with the formation of the implantation chamber. These effects ultimately result in a significant reduction in litter size among the treated group. Our findings suggest that NSAID administration during the critical window of embryo implantation can lead to unfavorable pregnancy outcomes, substantially disrupting the three-dimensional structure of the uterine environment, which contributes to the reduction in litter size. Therefore, caution should be exercised when administering NSAIDs to women during early pregnancy, considering our results and other studies that indicate a significant disruption to the maternal environment that ultimately compromises its ability to support embryonic growth and development. Additionally, our findings have important clinical implications. The ability of PTGS1 to compensate for PTGS2 loss in certain genetic backgrounds suggests that individual responses to PTGS inhibitors may vary significantly based on genetics. This could help explain the variable efficacy of selective PTGS2 inhibitors across human populations and emphasize the importance of considering genetic factors when using these medications, particularly during pregnancy (Salazar et al., 2010).

Chapter 5: Summary, discussion, and translational application

5.1: Summary of major findings

Our study employs complementary genetic and pharmacological methods to offer new insights into the spatial and temporal dynamics of prostaglandin signaling during the early stages of pregnancy. We establish that stromal PTGS2 is critical for post-implantation development (chapter 3), while epithelial PTGS1 serves a distinct function in embryo spacing during the uterine receptivity period, and it does not compensate for the function of PTGS2 at post-implantation stages (Fig. 5.1) (Massri and Arora, 2025). These findings address longstanding questions regarding the tissue-specific roles of prostaglandin in reproduction and have significant implications for therapeutic strategies (Cheng and Stewart, 2003; Lim et al., 1997).

5.1.1: Stromal PTGS2 expression is critical for post-implantation development

We have gained critical insights into compartment-specific prostaglandin signaling during early pregnancy by analyzing multiple tissue-specific deletion models in the murine reproductive tract. Our studies reveal that stromal expression of PTGS2 is essential for successful post-implantation development, while epithelial and endothelial PTGS2 play less significant roles as evidenced by our data- a finding that addresses longstanding questions since initial studies with global *Ptgs2*$^{-/-}$ mice reported complete infertility (Lim et al., 1997). Normal fertility in both epithelial (*Ltf*$^{cre/+}$*; Ptgs2*$^{f/f}$) and epithelial/endothelial (*Pax2*$^{cre/+}$*; Ptgs2*$^{f/f}$) models challenged previous assumptions about epithelial PTGS2's role in implantation, while analysis of the stromal deletion model (*Pgr*$^{cre/}$+*; Ptgs2*$^{f/f}$) revealed critical temporal windows for PTGS2 function during peri-implantation stages. Although pre-implantation development proceeded normally despite progesterone-receptor-driven deletion in multiple reproductive tissues (Soyal et al., 2005), defects emerged specifically during implantation chamber formation and early post-implantation phases (Massri and Arora, 2025). Through advanced three-dimensional imaging, we demonstrated that stromal PTGS2 coordinates chamber morphogenesis, vascular remodeling processes, and decidualization response critical for post-implantation development (Fig. 5.2) (Massri and Arora,

2025). These findings align with recent studies highlighting the importance of stromal-derived factors in pregnancy success (Sakamoto et al., 2024) and provide a foundation for examining the downstream molecular mechanisms by which stromal PTGS2 regulates the implantation process.

5.1.2: Complementary insights from combined approaches – pharmacological approach

Our study used genetic and pharmacological methods to examine PTGS's role in early pregnancy. The genetic models provided insights into PTGS2 spatial requirements and revealed compensatory mechanisms that could mask protein function in early pregnancy. By integrating these findings with pharmacological methods, we managed to regulate the timing of prostaglandin inhibition, which helped to identify critical phases for PTGS1 and PTGS2 in reproduction. Furthermore, our pharmacological investigations reflect clinical contexts in which NSAIDs are utilized, enhancing the relevance of our findings for human medicine, especially in the care of pregnant women. We used selective and non-selective NSAIDs in CD1 mouse models to explore prostaglandin signaling during embryo implantation. Pre-implantation treatments with PTGS1 or PTGS2 inhibitors had minimal effects, but dual inhibition with 6 mg/kg indomethacin led to significant reproductive issues, reducing live pups by about 50%. This aligns with our genetic findings, suggesting that PTGS enzymes' compensatory mechanisms are crucial in early pregnancy. The timing effects of NSAIDs verify our genetic model results; just as stromal PTGS2 deletion affected post-implantation development, indomethacin impacted pre-implantation processes, resulting in poor pregnancy outcomes. This connection improves understanding of prostaglandin signaling in successful pregnancy, indicating that maintaining PTGS1 or PTGS2 in CD1 mice supports early pregnancy. NSAIDs also affect embryo implantation in a dose-dependent way; our indomethacin model showed that 6 mg/kg inhibited both PTGS1 and PTGS2, delaying embryo implantation, disrupting embryo movement, and restricting post-implantation growth. In contrast, 2 mg/kg dose did not result in similar outcomes, highlighting indomethacin's dose-dependent effects. Successful pregnancy relies on the precise coordination of prostaglandin signaling, particularly in post-implantation development through the stromal compartment

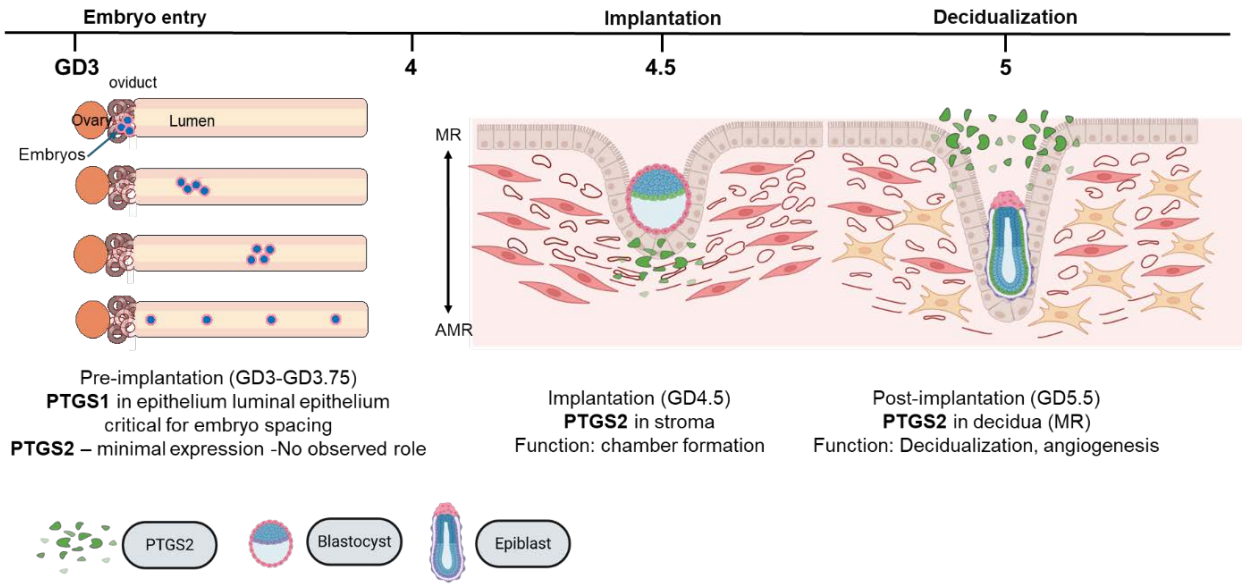

Figure 5.1. Molecular regulation of PTGS1 and PTGS2 at the maternal-fetal interface. During the pre-implantation phase, around day 3, PTGS1 shows high expression in the luminal epithelium, where it plays a critical role in embryo spacing and timely implantation. At this stage, PTGS2 is minimally expressed in the uterus. However, by the post-implantation period, days 4 to 5, PTGS2 becomes highly expressed in the stroma, where it is essential for the formation of the implantation chamber, decidualization, and vascular remodeling. In our genetic model, *Pgr*$^{cre/+}$*; Ptgs2*$^{f/f}$, the deletion of PTGS2 results in a 50% loss of pups; although these embryos implant, they fail to develop properly during the post-implantation phase. In contrast, the removal of both PTGS1 and PTGS2 leads to complete infertility, as the embryos are unable to attach. GD: gestational day. MR: mesometrial region, AMR: anti-mesometrial region.

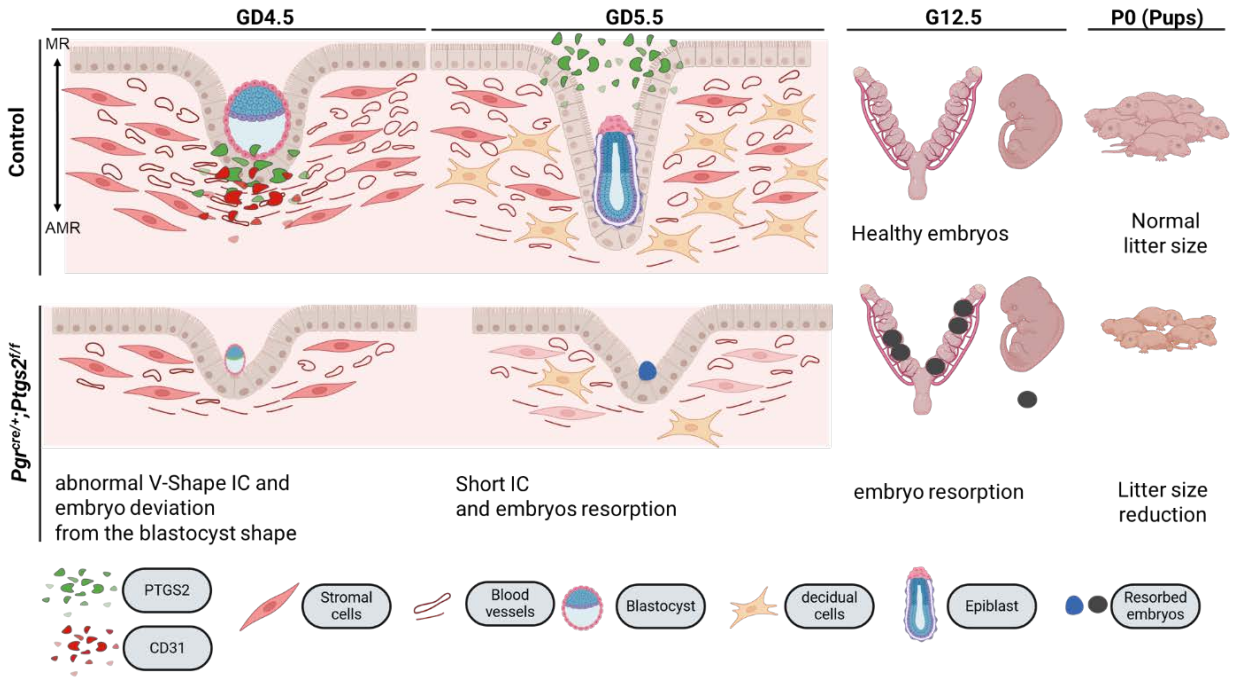

Figure 5.2. Stromal PTGS2 regulates post-implantation development. In control mice, stromal PTGS2 plays a crucial role in the proper formation of the embryo implantation chamber at GD4.5 and in the adequate elongation of the chamber by GD5.5. This process is essential for healthy embryonic development during both the decidualization and mid-gestation stages, ultimately contributing to standard litter sizes. In *Pgr*$^{cre/+}$*; Ptgs2*$^{f/f}$ mice, where stromal PTGS2 is absent, an abnormal V-shaped implantation chamber forms, leading to deviations in embryonic development from blastocyst-shaped embryos. The lack of PTGS2 further disrupts the elongation of the implantation chamber at GD5.5, resulting in embryo resorption during this stage, which subsequently leads to mid-gestation embryonic loss and a reduction in litter size. GD: gestational day. MR: mesometrial region, AMR: anti-mesometrial region.

5.2: Integration with literature and mechanistic insight

Our combined approach reveals distinct yet complementary roles for PTGS1 and PTGS2 in early pregnancy. While both enzymes contribute to prostaglandin synthesis, they show unique spatial and temporal requirements during implantation. Existing evidence indicates that prostaglandin signaling—primarily through PTGS2—fulfills multiple essential and different functions in female reproduction, especially during embryo implantation (Achache et al., 2010; Lim et al., 1997).

5.2.1: PTGS role and compensation

Our study reveals critical insights into PTGS1 function and potential compensatory mechanisms between PTGS enzymes. We found that pharmacological inhibition of PTGS1 did not affect embryo implantation outcomes in CD1 mice. This lack of effect might be attributed to compensation by PTGS2 (Reese et al., 1999) or to the non-essential nature of PTGS1 for successful implantation (Langenbach et al., 1995). Notably, concurrent inhibition of both PTGS1 and PTGS2 led to significant adverse effects, likely due to the timing of the inhibition, which coincides with the critical roles of both PTGS1 and PTGS2-derived prostaglandin (Aikawa et al., 2024; Chakraborty et al., 1996; Massri and Arora, 2025). Our indomethacin treatment, administered earlier on the day of embryo entry and attachment, clearly influenced the embryonic movement, an effect we did not observe in tissue-specific deletion models of PTGS2 (Massri and Arora, 2025). This suggests that PTGS1-derived prostaglandin specifically contribute to disruptions in embryo spacing. Additionally, when both enzymes were inhibited simultaneously, compensation was impossible, as there was no alternative source of prostaglandin to compensate for the loss of both enzymes.

This finding is consistent with the enrichment of PTGS1 in the uterine epithelium and the presence of calcium-dependent phospholipase A2 (cPLA2) prior to embryo implantation (Aikawa et al., 2024; Song et al., 2002), further reinforcing its significance in early spatial positioning events. Additionally, PTGS1 synthesizes multiple prostaglandin (PGE2, PGD2, PGI2, and

thromboxane A2 (TxA2), some of which exert their functions through their receptors located in the uterine smooth muscle during the peri-implantation period (Yang et al., 1997), further explaining its spacing effects. These findings were corroborated by Aikawa et al.'s PTGS1/PTGS2- double knockout models showing similar spacing defects.

Our integrated genetic and pharmacological approaches have revealed intricate compensatory relationships among prostaglandin pathways. The strain-specific differences in compensation—particularly notable in our CD1 background—highlight the significance of genetic context in prostaglandin signaling. Although PTGS1 can partially compensate for the loss of stromal PTGS2 in certain contexts, it fails to restore specific functions related to chamber formation and invasion. This selective compensation suggests that distinct molecular mechanisms are required for various aspects of implantation. Our data indicates a role for epithelial PTGS1 rather than PTGS2, which explains the normal fertility observed with our *Ltf*$^{cre/+}$*; Ptgs2*$^{f/f}$ and *Pax2*$^{cre/+}$*; Ptgs2*$^{f/f}$ models.

Understanding these compensatory mechanisms may enhance the creation of more effective therapeutic approaches considering redundant pathways. It is essential to recognize that while total prostaglandin inhibition can be harmful, PTGS1-specific inhibition via low-dose aspirin during pregnancy may be advantageous, particularly for women experiencing recurrent pregnancy loss in their first trimester (Bujold et al., 2014; Kozer et al., 2003).

5.2.2: PTGS2 temporal and special requirements

Our study revealed delayed implantation with concurrent PTGS1 and PTGS2 inhibition, along with the stromal ablation of PTGS2 in our genetic model. Furthermore, PTGS2's distinct role in angiogenesis was evident in our indomethacin-treated and *Pgr*$^{cre/+}$*; Ptgs2*$^{f/f}$ models showed faint blue dye reactions and abnormal vascular remodeling around implantation chambers. Interestingly, endothelial-specific PTGS2 deletion did not affect embryo implantation, indicating the vascular phenotype stems from stromal rather than endothelial PTGS2 loss. Inhibiting PTGS2 with 600 nmol Dup-697 had milder effects, likely because of PTGS1 compensation in CD1 mice.

In our stromal deletion model (*Pg*$^{rcre/+}$*; Ptgs2*$^{f/f}$), we also found a delay in implantation, accompanied by a faint blue dye reaction. This could be due to the shallow invasion of embryos into the uterine epithelium, as indicated by the abnormal morphology and elongation of the embryo implantation chamber during the post-implantation phase. We propose that stromal PTGS2 is crucial for embryo invasion, as defects appear only when PTGS2 is absent from both the anti-mesometrial and mesometrial poles of the stroma during the post-implantation stages. While PTGS1 is expressed in the secondary decidual zone at GD5.5 and supports decidual expansion, it did not compensate for PTGS2's functions in embryo invasion, thereby impacting the morphology of the embryo implantation chamber. These findings align with Aikawa et al.'s observations about PTGS2's post-implantation role. Notably, DP1 agonist and PGE2 supplementation rescued defective implantation, consistent with stromal PGD2 and PGE2 receptor expression post-implantation. This highlights PTGS2's distinct role in tissue morphogenesis beyond PTGS1's functions. Thus, our stromal deletion model provides an excellent system for studying decidualization mechanisms in control vs PTGS2-ablation conditions.

5.3: Advanced mechanistic insights

5.3.1: Coordination of implantation chamber architecture and vascular development

Our research indicates a multifaceted relationship between the creation of implantation chambers and vascular remodeling influenced by stromal PTGS2. In control uteri, the formation of chambers displays a distinct V-shaped structure alongside well-organized vascular development (Massri and Arora, 2025; Massri et al., 2023). In contrast, deleting stromal PTGS2 significantly disrupts this coordination. Notably, only 6 out of 24 samples exhibit a normal V-shape, compared to 13 out of 14 in control uteri, underscoring the essential function of PTGS2 in shaping tissue architecture. Additionally, there is a decrease in vessel density, specifically at the implantation sites, whereas the vascular structure in inter-implantation areas remains unaffected, suggesting a targeted regulation of vascular growth patterning at embryo implantation sites

(Massri and Arora, 2025; Massri et al., 2023). Moreover, the diminished accumulation of CD31-positive cells around the implantation chambers, noted in both our indomethacin model and the PTGS2-stromal deletion model, underscores the role of PTGS2 in orchestrating the vascular niche. The defects in chamber formation and vascular organization evident in our indomethacin model likely stem from the second treatment, which may coincide with PTGS2 expression in the uteri closer to embryo implantation (Chakraborty et al., 1996; Massri and Arora, 2025). Notably, the observed vascular defects in our indomethacin and *Pgr*$^{cre/+}$*; Ptgs2*$^{f/f}$ are associated with abnormal chamber elongation, suggesting that these processes are mechanistically interlinked rather than independent phenomena.

The spatial organization of this coordination is particularly significant. The expression of PTGS2 at both the anti-mesometrial and mesometrial poles is essential for proper chamber development (Massri and Arora, 2025), highlighting the importance of bidirectional signaling in guiding tissue architecture. The presence of PGD2, PGE2, and PGI2 receptors in these regions, along with the ability to correct defects using their respective agonists (Lim et al., 1999a; Lim et al., 1997; Sakamoto et al., 2024; Sugimoto et al., 2015; Yang et al., 1997), indicates that specific prostaglandin pathways are integral to this architectural organization. This precise spatial signaling involving prostaglandin may also clarify why global PTGS2 inhibition produces more severe phenotypes than tissue-specific deletion (Lim et al., 1997; Massri and Arora, 2025).

5.3.2: Temporal regulation of prostaglandin signaling

Our pharmacological studies revealed critical timing windows for prostaglandin signaling that were not evident from genetic models alone. Early PTGS1 and PTGS2 inhibition disrupted embryo spacing and movement, while later inhibition primarily affected post-implantation development. This separation in timing is reflected in the distinct phenotypes we observed: early treatment resulted in spacing defects. In contrast, later treatment caused defects in chamber formation, aligning with the genetic ablation of PTGS2 during post-implantation stages. These timing effects align with the sequential expression patterns of PTGS1 in epithelium (Aikawa et al.,

2024; Chakraborty et al., 1996) followed by PTGS2 in stroma (Massri and Arora, 2025), suggesting evolutionarily conserved temporal regulation of implantation events.

Our analysis reveals critical timing relationships in tissue development coordinated by prostaglandin signaling. The transition from initial attachment to chamber formation requires precise temporal control of PTGS enzymes, evidenced by the delay in implantation we observed with both pharmacological and genetic PTGS2 disruption. This timing mechanism appears distinct from the spacing effects mediated by epithelial PTGS1, suggesting the evolution of separate temporal control mechanisms for different aspects of the implantation process.

The progressive nature of chamber development defects in PTGS2-deficient uteri, from initial delayed implantation to abnormal elongation and poor invasion, suggests PTGS2 coordinates multiple developmental events in sequence (Lim et al., 1997). While initial V-shaped chambers can form, their subsequent development fails without proper PTGS2 signaling (Massri and Arora, 2025). This indicates distinct temporal requirements for early versus late chamber development. The correlation between timing of vascular remodeling and chamber elongation further supports PTGS2's role in developmental synchronization.

5.3.3: Molecular pathway and tissue integration

Our analysis reveals complex molecular hierarchies downstream of prostaglandin signaling that might coordinate the development of the implantation chamber. The coordinated defects observed in our *Pgr*$^{cre/+}$*; Ptgs2*$^{f/f}$ model suggest that PTGS2 regulates or works in coordination with multiple developmental pathways. Building on our previous understanding of PTGS2's role in implantation (Lim et al., 1997), our findings highlight specific interactions between pathways that govern tissue architecture and vascular development. Our analysis reveals some key developmental pathways downregulated in our *Pgr*$^{cre/+}$*; Ptgs2*$^{f/f}$ model.

<u>Bone morphogenetic protein 2 (BMP2)</u>

Our quantitative analysis indicated a reduction in *Bmp2* expression within the PTGS2-deficient stroma model, likely arising from the failed decidualization response observed in this

model. This suggests a notable correlation between Bmp2 signaling and abnormal chamber formation. Lee et al. demonstrated that BMP2 acts as an upstream regulator of PTGS2 in the uterus, with BMP2 deletion leading to complete infertility and failure of decidualization (Lee et al., 2007). The interrelationship between BMP2 and PTGS2 appears complex - while BMP2 can regulate PTGS2 expression, our data suggests PTGS2 may also influence BMP2 levels, indicating a potential feedback loop. This bidirectional regulation may explain why both BMP2 and PTGS2 deletion models show decidualization defects. Several factors are deregulated in BMP2-deficient uteri, including Wnt4, Fkbp4, Fkbp5, and PTGS2, which we did not assess in our model. This network of factors suggests that BMP2 coordinates decidualization through and independently of PTGS2, highlighting the complexity of regulatory networks controlling pregnancy success. The spatial correlation between BMP2 expression domains and regions of active decidualization in control uteri, contrasted with disrupted patterning in PTGS2-deficient tissue, further supports this regulatory relationship.

Wnt4

In addition to the reduced expression of *Bmp2*, our analysis showed a significant decrease in *Wnt4* expression in our stromal ablation model of PTGS2. This finding aligns with previous research by Franco et al., which demonstrated the importance of Wnt4 in implantation. Mice that lacked Wnt4 in the uterus were found to be subfertile due to defects in embryo implantation and issues with endometrial stromal cell survival, differentiation, and responsiveness to progesterone signaling (Franco et al., 2011). The temporal correlation between Wnt4 reduction and defects in decidualization response suggests that Wnt4 may mediate prostaglandin effects on tissue architecture. Notably, the decrease in Wnt4 expression coincides with the time implantation chambers should elongate, suggesting Wnt4's role in directing tissue morphogenesis. The connection between Wnt4 and progesterone responsiveness is particularly relevant, as proper decidualization requires progesterone signaling, suggesting PTGS2 may influence decidualization both directly and through modulation of progesterone responses via Wnt4. This

complex interaction between prostaglandin and Wnt signaling may explain chamber formation defects in our model.

Vascular remodeling

In addition to the correlation with Bmp2 and wnt4, our findings also suggest a disrupted vessel density, specifically at implantation sites, which extends Matsumoto et al.'s work on defective uterine angiogenesis in PTGS2-deficient mice due to aberration of the VEGF signaling pathway resulting in localized vascular defects (Matsumoto et al., 2002). This links our earlier observations with faint blue dye reactions observed in both genetic and pharmacological models, which are accompanied by the disrupted distribution of CD31-positive cells around the embryo implantation chamber. Yet these findings are related to loss of stromal PTGS2 but not endothelial PTGS2.

Our findings also reveal significant disruption of vascular development in PTGS2-deficient uteri. We observed reduced vessel density, specifically at implantation sites, which extends Matsumoto et al.'s work showing defective uterine angiogenesis in PTGS2-deficient mice due to aberrant VEGF signaling (Matsumoto et al., 2002). Interestingly, although the overall vessel diameter did not change, the density of vessels at the implantation sites saw a sharp decline compared to the inter-implantation areas, suggesting a precise spatial control of angiogenesis. This localized phenomenon aligns with our findings of subtle blue dye reactions in both genetic and pharmacological models. Furthermore, the disrupted distribution of CD31-positive cells around implantation chambers suggests that PTGS2 coordinates vessel formation and patterning. Importantly, these vascular defects stem from stromal rather than endothelial PTGS2 loss, as endothelial-specific deletion had no effect. This indicates that stromal PTGS2 regulates angiogenesis through paracrine signaling, possibly via local VEGF production, rather than through direct effects on endothelial cells.

Leukemia inhibitory factor (LIF)

Furthermore, we report reduced *Lif* expression with the delay in embryo implantation observed in our models, which build on Stewart et al. work showing the crucial role of LIF in blastocyst implantation (Stewart et al., 1992). This shows the integration of the PTGS2 signaling pathway with a broader signaling network that contributes to implantation and decidualization success.

Hierarchical organization of molecular pathways

Our data suggests a hierarchical organization of molecular pathways that explains several key observations across our models. First, the initiation of signaling by stromal PTGS2 explains why epithelial deletion had minimal effects on pregnancy outcomes. The local nature of prostaglandin production explains the spatial precision of implantation chamber defects, as evidenced by chamber-specific vascular and architectural abnormalities. The timing of pathway activation aligns precisely with our observed sequence of developmental defects: *Lif* downregulation precedes and likely causes delayed implantation. At the same time, the subsequent reduction in Wnt4 and Bmp2 expression correlates with defective decidualization and chamber formation. This temporal sequence demonstrates how early PTGS2-dependent events influence later developmental processes. The interdependence of these pathways helps explain why complete PTGS2 deficiency produces more severe phenotypes than disruption localized to specific tissues - the loss of PTGS2 simultaneously affects multiple essential signaling networks that cannot compensate for each other. This complex regulatory hierarchy provides a molecular framework for understanding how prostaglandin signaling coordinates the multiple tissue-level changes required for successful implantation.

The complex molecular pathways that coordinate the development of the implantation chamber and vascular remodeling through prostaglandin signaling raise important questions about how these mechanisms evolved. While our detailed analysis in mice uncovers specific roles for stromal PTGS2 in post-implantation development, the conservation of prostaglandin pathways

across species suggests that these mechanisms may represent fundamental requirements for a successful pregnancy, albeit with species-specific adaptations in their tissue-specific development.

5.4: Evolutionary perspective across species

Prostaglandin signaling pathways play fundamental roles in reproduction across mammalian species despite considerable variation in their implantation strategies. Although our studies focused on mice, extensive research has demonstrated the presence and importance of prostaglandin pathways in the reproductive tissues of various mammals, including rats, hamsters, and humans (Chakraborty et al., 1996; Cong et al., 2006; Evans and Kennedy, 1978; Kennedy et al., 2007; Wang et al., 2004b).

Studies in human endometrium reveal distinct PTGS expression patterns during implantation. PTGS1 is expressed in glandular and luminal epithelium, while PTGS2 localizes to luminal epithelium and perivascular cells (Marions and Danielsson, 1999). This contrasts with our findings in mice where PTGS1 functions in early implantation through epithelial expression (Aikawa et al., 2024; Chakraborty et al., 1996), and stromal PTGS2 is critical for post-implantation development (Chakraborty et al., 1996; Massri and Arora, 2025). These species-specific differences in PTGS tissue localization likely reflect evolutionary adaptations to different implantation strategies.

Even with species-specific variations in tissue localization, the preservation of prostaglandin pathways suggests that these signaling networks are vital mechanisms in mammalian reproduction. This preservation is particularly evident in the heightened expression of PTGS2 following embryo attachment, observed in a range of species from mice to humans. (Chakraborty et al., 1996; Kim et al., 1999; Stavreus-Evers et al., 2005). Understanding these evolutionary adaptations while recognizing the conserved pathways is essential for developing therapeutic strategies.

5.5: Clinical implications

The clinical relevance of prostaglandin signaling in human reproduction is particularly supported by studies in women experiencing recurrent implantation failure, who show alterations in endometrial prostaglandin productions (Achache et al., 2010; Salazar et al., 2010).

5.5.1: Therapeutic considerations for NSAIDs

Understanding these species-specific differences in prostaglandin regulation while recognizing the fundamental conservation of these pathways is crucial for translating findings from animal models to human medicine. Our findings indicate that inhibiting PTGS1 and PTGS2 during early pregnancy can severely disrupt implantation and the development of the embryo implantation chamber. Therefore, the use of non-selective NSAIDs should be approached with caution, especially in the early stages of pregnancy. It is important to highlight that in specific situations, low-dose aspirin may be advantageous for preventing early pregnancy loss in women and for alleviating conditions associated with preeclampsia (Bujold et al., 2014; Friedman, 1988). This benefit is achieved by restoring the balance of prostaglandin, specifically by reducing thromboxane levels, which subsequently enhances vascular function (Bujold et al., 2014; Friedman, 1988). Additionally, in BHP/5 mice that exhibit developed preeclampsia, there are associated peri-implantation defects linked to an upregulation of PTGS2 expression at the maternal-fetal interface. This situation can lead to a reduced influx of uterine natural killer cells, which are essential for decidualization (Massri et al., 2023). The administration of a single dose of celecoxib (a specific inhibitor of PTGS2) during early pregnancy showed improvements in both maternal and fetal outcomes (Sones et al., 2016), suggesting that therapeutic inhibition of PTGS2 could be a viable strategy in managing cases of preeclampsia (Sones et al., 2016).

5.5.2: Targeted therapeutic approaches

Moreover, the specific needs of tissues highlighted in PTGS2-derived prostaglandin signaling emphasize the possibility of developing more targeted therapeutic strategies aimed at particular compartments within the uterus. Furthermore, the finding that some prostaglandin

receptor agonists can reduce implantation defects in mice points to promising therapeutic options. (Lim et al., 1999a; Sakamoto et al., 2024).

5.5.3: Personalized medicine applications

Furthermore, personalized medicine approaches involving prostaglandin modulators may be especially important for women with altered prostaglandin levels that are associated with an increased risk of miscarriage (Salazar et al., 2010). Moreover, the finding regarding possible compensatory mechanisms between PTGS1 and PTGS2 may help clarify why some individuals exhibit greater sensitivity to NSAID effects than others (Li et al., 2018b; Reese et al., 1999; Salazar et al., 2010).

5.6: Limitations

While our studies have provided valuable and unique insights into the role and signaling of prostaglandin during the peri-implantation stages, it is important to acknowledge several technical limitations. For example, the Pgr-Cre system facilitates the deletion of PTGS2 across various reproductive tissues, which complicates the isolation of specific defects in the uterus, particularly within the uterine epithelium and stromal effects. Additionally, potential compensatory mechanisms during development may obscure some of the observed outcomes. Nonetheless, the pharmacological approach has alleviated some of these limitations by enabling temporal control over PTGS1 and PTGS2 functions; however, drug delivery to specific tissues continues to pose challenges.

Another limitation is the inherent difficulty of observing vascular development in real-time during the peri-implantation phase. While our experiments using blue dye, CD31 staining, and vascular density analysis have provided valuable insights into vascular changes in the post-implantation stages, they do not completely reflect the dynamic process of vessel remodeling. The advancement of improved live imaging techniques will certainly enhance our comprehension of these essential processes.

Additionally, although we employed significant methods to investigate the functions of PTGS enzymes during the peri-implantation stages, we did not integrate these models with techniques capable of measuring the impacted prostaglandin, which resulted in adverse pregnancy outcomes. Identifying the specific prostaglandin affected could offer valuable insights, particularly in relation to the translational

The translation of findings from mouse models to human contexts presents several challenges. While the accelerated progression of mouse pregnancy and the relatively small size of their implantation sites facilitate certain analyses, these models do not fully replicate the complexities of human implantation. This disparity highlights the need for caution when extrapolating data from murine studies to human applications, as significant physiological differences exist between species. The nuances of human reproductive biology may not be adequately captured in mouse studies, underscoring the importance of using complementary research methods to achieve a comprehensive understanding of implantation processes in humans. To bridge these gaps, complementary research methods such as utilizing human tissues, organoids, and advanced 3D culture systems can offer valuable insights into human reproductive biology.

5.7: Future directions

Future studies will need to address this fundamental question of whether uterine stromal PTGS2 function during embryo implantation reflects the accurate compartment-specific requirements of local prostaglandin availability. While previous studies used different techniques to illustrate prostaglandin and PTGS enzymes localization in the uterus during implantation in rats (Cong et al., 2006; Kennedy and Zamecnik, 1978), mice (Chakraborty et al., 1996), and hamsters (Wang et al., 2004b), still modern techniques can allow precise spatial mapping of these eicosanoids. While Aikawa et al. 2024 (Aikawa et al., 2024) revealed the expression patterns of the prostaglandin pathway, the spatial dynamic of their localization during the peri-implantation period remains unclear. For instance, utilizing mass spectrometry imaging techniques coupled

with cell-type specific genetic models can resolve this question. Specifically, the development of more precise genetic tools, particularly a stromal-specific deletion model of PTGS2 using stromal-specific Cre lines (Pdgfrβ-Cre), would allow a better understanding of compartment-specific requirements. This genetic approach, combined with quantitative and qualitative assessment of compartment-specific prostaglandin, could provide valuable insights into local prostaglandin function.

Understanding the spatial dynamics of prostaglandin localization in the uterine compartments could be essential for developing targeted therapeutic strategies for modulating prostaglandin signaling and functioning in specific uterine compartments while minimizing their systemic effects. Prostaglandin supplementation in a compartment-specific manner could determine whether maintaining a threshold concentration in specific uterine compartments is sufficient for embryo implantation.

Our findings highlight the critical role of stromal PTGS2 in prostaglandin production during embryo implantation. While previous studies have established that PGE2 and PGI2 serve distinct functions through their respective receptors (EP2/EP4 and PPARδ) (Lim et al., 1999a; Sakamoto et al., 2024). Further investigation is needed to understand how prostaglandin coordinates temporally and spatially to establish the essential microenvironment for successful implantation. Understanding these mechanisms could reveal new therapeutic targets for treating implantation failure while minimizing systemic effects.

Finally, one intriguing question that remains to be answered is why NSAIDs, specifically pre-implantation indomethacin treatment, replicate the phenotypes observed in *Pgr*$^{cre/+}$*; Ptgs2*$^{f/f}$ mice, resulting in a 50% loss of pups rather than causing complete infertility observed in *Ptgs1*$^{-/-}$*; Pgr*$^{cre/+}$*; Ptgs2*$^{f/f}$ mice, despite minimal PTGS2 expression when indomethacin is administered during pre-implantation stages at GD3 (Table 5.1).

Models	Key Outcomes
Pgr$^{cre/+}$; Ptgs2$^{f/f}$ (50% pup loss) (Massri and Arora, 2025)	Normal pre-implantation – 50% fail post-implantation
Ptgs1$^{-/-}$; Pgr$^{cre/+}$; Ptgs2$^{f/f}$ (Infertile) (Aikawa et al., 2024)	Failed pre-implantation – failed embryo attachment
Pre-implantation indomethacin (PTGS1 and PTGS2 inhibitor) (50% pup loss). Massri et al., in preparation	Delays implantation and causes embryo crowding

Table 5.1: Summary of genetic and pharmacological models phenotypes. In the *Pgr$^{cre/+}$; Ptgs2$^{f/f}$* model, where PTGS2 is ablated from the stroma, pre-implantation processes developed normally; however, there was a failure in post-implantation development, leading to a 50% reduction in litter size. In the *Ptgs1$^{-/-}$; Pgr$^{cre/+}$; Ptgs2$^{f/f}$* model, complete infertility was observed due to unsuccessful embryonic attachment. Additionally, in the pre-implantation indomethacin treatment model, delayed implantation, embryo crowding, and restricted post-implantation embryonic development resulted in a 50% reduction in litter size as well.

Future investigation into extra-uterine sources of PTGS2 is warranted, especially regarding embryonic PTGS2, endothelial PTGS2, and the potential contributions from immune cells. It is also important to note that we utilized Pax2cre (Ohyama and Groves, 2004), which targets uterine endothelial cells (Granger et al., 2024); however, this did not produce a significant effect, as indicated by our data (Massri and Arora, 2025). These non-uterine sources may offer compensatory mechanisms that help explain the differences observed between the genetic and pharmacological models. Additionally, a systematic comparison between NSAIDs and genetic models would be beneficial to clarify critical distinctions in PTGS inhibition levels, duration of effects, and the precise timing of pregnancy failure. This approach would assist in differentiating the outcomes of pharmacological versus genetic inhibition. Future research should prioritize key experimental strategies, including the development of additional cell-type specific deletions, comprehensive measurements of prostaglandin across uterine compartments, and single-cell sequencing to delineate expression patterns with high resolution. Mechanistic studies should

concentrate on the local versus systemic effects of prostaglandin signaling, investigate potential compensatory pathways in genetic models, and explore the non-PTGS effects of NSAIDs that may influence implantation outcomes.

BIBLIOGRAPHY

Achache, H. and Revel, A. (2006). Endometrial receptivity markers, the journey to successful embryo implantation. *Hum Reprod Update* **12**, 731-746.

Achache, H., Tsafrir, A., Prus, D., Reich, R. and Revel, A. (2010). Defective endometrial prostaglandin synthesis identified in patients with repeated implantation failure undergoing in vitro fertilization. *Fertil Steril* **94**, 1271-1278.

Aikawa, S. and Hirota, Y. (2024). Roles of lipid mediators in early pregnancy events. *Reprod Med Biol* **23**, e12597.

Aikawa, S., Matsuo, M., Akaeda, S., Sugimoto, Y., Arita, M., Isobe, Y., Sugiura, Y., Taira, S., Maeda, R., Shimizu-Hirota, R., et al. (2024). Spatiotemporally distinct roles of cyclooxygenase-1 and cyclooxygenase-2 at fetomaternal interface in mice. *JCI Insight* **9**.

Aiken, J. W. (1972). Aspirin and indomethacin prolong parturition in rats: evidence that prostaglandins contribute to expulsion of fetus. *Nature* **240**, 21-25.

Arora, R., Fries, A., Oelerich, K., Marchuk, K., Sabeur, K., Giudice, L. C. and Laird, D. J. (2016). Insights from imaging the implanting embryo and the uterine environment in three dimensions. *Development* **143**, 4749-4754.

Beenken, A. and Mohammadi, M. (2009). The FGF family: biology, pathophysiology and therapy. *Nat Rev Drug Discov* **8**, 235-253.

Bertolin, K. and D. Murphy, B. (2014). Reproductive Tract Changes During the Mouse Estrous Cycle In *The Guide to Investigation of Mouse Pregnancy* (ed. B. A. Croy, F. J. DeMayo, A. T. Yamada & S. L. Admason), pp. 832. Academic Press, 2013.

Bhurke, A., Bagchi, M. K. and Bagchi, I. C. (2018). Uterus: Growth Factors and Cytokines. In *Encyclopedia of Reproduction (Second edition)*, pp. Pages 333-338: Academic Press.

Biason-Lauber, A. and Chaboissier, M. C. (2015). Ovarian development and disease: The known and the unexpected. *Semin Cell Dev Biol* **45**, 59-67.

Bindu, S., Mazumder, S. and Bandyopadhyay, U. (2020). Non-steroidal anti-inflammatory drugs (NSAIDs) and organ damage: A current perspective. *Biochem Pharmacol* **180**, 114147.

Black, E., Khor, K. E., Kennedy, D., Chutatape, A., Sharma, S., Vancaillie, T. and Demirkol, A. (2019). Medication Use and Pain Management in Pregnancy: A Critical Review. *Pain Pract* **19**, 875-899.

Bonventre, J. V., Huang, Z., Taheri, M. R., O'Leary, E., Li, E., Moskowitz, M. A. and Sapirstein, A. (1997). Reduced fertility and postischaemic brain injury in mice deficient in cytosolic phospholipase A2. *Nature* **390**, 622-625.

Boshier, D. P. (1970). The pontamine blue reaction in pregnant sheep uteri. *J Reprod Fertil* **22**, 595-596.

Bujold, E., Roberge, S. and Nicolaides, K. H. (2014). Low-dose aspirin for prevention of adverse outcomes related to abnormal placentation. *Prenat Diagn* **34**, 642-648.

Bulletins—Gynecology, A. C. o. O. a. G. C. o. P. (2018). ACOG Practice Bulletin No. 200: Early Pregnancy Loss. *Obstet Gynecol* **132**, e197-e207.

Cabrera, R. A., Dozier, B. L. and Duffy, D. M. (2006). Prostaglandin-endoperoxide synthase (PTGS1 and PTGS2) expression and prostaglandin production by normal monkey ovarian surface epithelium. *Fertil Steril* **86**, 1088-1096.

Carp, H. J., Fein, A. and Nebel, L. (1988). Effect of diclofenac on implantation and embryonic development in the rat. *Eur J Obstet Gynecol Reprod Biol* **28**, 273-277.

Casado, M., Callejas, N. A., Rodrigo, J., Zhao, X., Dey, S. K., Boscá, L. and Martín-Sanz, P. (2001). Contribution of cyclooxygenase 2 to liver regeneration after partial hepatectomy. *FASEB J* **15**, 2016-2018.

Cha, J., Sun, X. and Dey, S. K. (2012). Mechanisms of implantation: strategies for successful pregnancy. *Nat Med* **18**, 1754-1767.

Chakraborty, I., Das, S. K. and Dey, S. K. (1995). Differential expression of vascular endothelial growth factor and its receptor mRNAs in the mouse uterus around the time of implantation. *J Endocrinol* **147**, 339-352.

Chakraborty, I., Das, S. K., Wang, J. and Dey, S. K. (1996). Developmental expression of the cyclo-oxygenase-1 and cyclo-oxygenase-2 genes in the peri-implantation mouse uterus and their differential regulation by the blastocyst and ovarian steroids. *J Mol Endocrinol* **16**, 107-122.

Chen, D. B., Hilsenrath, R., Yang, Z. M., Le, S. P., Kim, S. R., Chuong, C. J., Poindexter, A. N. and Harper, M. J. (1995). Leukaemia inhibitory factor in human endometrium during the menstrual cycle: cellular origin and action on production of glandular epithelial cell prostaglandin in vitro. *Hum Reprod* **10**, 911-918.

Chen, J. R., Cheng, J. G., Shatzer, T., Sewell, L., Hernandez, L. and Stewart, C. L. (2000). Leukemia inhibitory factor can substitute for nidatory estrogen and is essential to inducing a receptive uterus for implantation but is not essential for subsequent embryogenesis. *Endocrinology* **141**, 4365-4372.

Chen, Q., Zhang, Y., Elad, D., Jaffa, A. J., Cao, Y., Ye, X. and Duan, E. (2013). Navigating the site for embryo implantation: biomechanical and molecular regulation of intrauterine embryo distribution. *Mol Aspects Med* **34**, 1024-1042.

Chen, Q., Zhang, Y., Peng, H., Lei, L., Kuang, H., Zhang, L., Ning, L., Cao, Y. and Duan, E. (2011). Transient {beta}2-adrenoceptor activation confers pregnancy loss by disrupting embryo spacing at implantation. *J Biol Chem* **286**, 4349-4356.

Cheng, J. G. and Stewart, C. L. (2003). Loss of cyclooxygenase-2 retards decidual growth but does not inhibit embryo implantation or development to term. *Biol Reprod* **68**, 401-404.

Claesson-Welsh, L., Dejana, E. and McDonald, D. M. (2021). Permeability of the Endothelial Barrier: Identifying and Reconciling Controversies. *Trends Mol Med* **27**, 314-331.

Clark, K. and Myatt, L. (2008). Prostaglandins and the Reproductive Cycle. In *The Global Library of Women's Medicine (GLOWM)* (ed. P. V. Dadelszen & G. C. Di Renzo): (ISSN: 1756-2228).

Cong, J., Diao, H. L., Zhao, Y. C., Ni, H., Yan, Y. Q. and Yang, Z. M. (2006). Differential expression and regulation of cylooxygenases, prostaglandin E synthases and prostacyclin synthase in rat uterus during the peri-implantation period. *Reproduction* **131**, 139-151.

Cousins, F. L., Murray, A., Esnal, A., Gibson, D. A., Critchley, H. O. and Saunders, P. T. (2014). Evidence from a mouse model that epithelial cell migration and mesenchymal-epithelial transition contribute to rapid restoration of uterine tissue integrity during menstruation. *PLoS One* **9**, e86378.

Cox, C. M., Thoma, M. E., Tchangalova, N., Mburu, G., Bornstein, M. J., Johnson, C. L. and Kiarie, J. (2022). Infertility prevalence and the methods of estimation from 1990 to 2021: a systematic review and meta-analysis. *Hum Reprod Open* **2022**, hoac051.

Daikoku, T., Ogawa, Y., Terakawa, J., Ogawa, A., DeFalco, T. and Dey, S. K. (2014). Lactoferrin-iCre: a new mouse line to study uterine epithelial gene function. *Endocrinology* **155**, 2718-2724.

Daikoku, T., Wang, D., Tranguch, S., Morrow, J. D., Orsulic, S., DuBois, R. N. and Dey, S. K. (2005). Cyclooxygenase-1 is a potential target for prevention and treatment of ovarian epithelial cancer. *Cancer Res* **65**, 3735-3744.

Daniel, S., Koren, G., Lunenfeld, E., Bilenko, N., Ratzon, R. and Levy, A. (2014). Fetal exposure to nonsteroidal anti-inflammatory drugs and spontaneous abortions. *CMAJ* **186**, E177-182.

Das, A., Mantena, S. R., Kannan, A., Evans, D. B., Bagchi, M. K. and Bagchi, I. C. (2009). De novo synthesis of estrogen in pregnant uterus is critical for stromal decidualization and angiogenesis. *Proc Natl Acad Sci U S A* **106**, 12542-12547.

Das, S. K., Flanders, K. C., Andrews, G. K. and Dey, S. K. (1992). Expression of transforming growth factor-beta isoforms (beta 2 and beta 3) in the mouse uterus: analysis of the periimplantation period and effects of ovarian steroids. *Endocrinology* **130**, 3459-3466.

Das, S. K., Wang, J., Dey, S. K. and Mead, R. A. (1999). Spatiotemporal expression of cyclooxygenase 1 and cyclooxygenase 2 during delayed implantation and the periimplantation period in the Western spotted skunk. *Biol Reprod* **60**, 893-899.

Das, S. K., Wang, X. N., Paria, B. C., Damm, D., Abraham, J. A., Klagsbrun, M., Andrews, G. K. and Dey, S. K. (1994). Heparin-binding EGF-like growth factor gene is induced in the mouse uterus temporally by the blastocyst solely at the site of its apposition: a possible ligand for interaction with blastocyst EGF-receptor in implantation. *Development* **120**, 1071-1083.

Davis, B. J., Lennard, D. E., Lee, C. A., Tiano, H. F., Morham, S. G., Wetsel, W. C. and Langenbach, R. (1999). Anovulation in cyclooxygenase-2-deficient mice is restored by prostaglandin E2 and interleukin-1beta. *Endocrinology* **140**, 2685-2695.

Deanesly, R. (1967). The role of the fertilized egg: reactions in the guinea-pig uterus at ovo-implantation and after thread traumatization. *J Reprod Fertil* **14**, 243-248.

Dennis, E. A. and Norris, P. C. (2015). Eicosanoid storm in infection and inflammation. *Nat Rev Immunol* **15**, 511-523.

Diao, H., Li, R., El Zowalaty, A. E., Xiao, S., Zhao, F., Dudley, E. A. and Ye, X. (2015). Deletion of Lysophosphatidic Acid Receptor 3 (Lpar3) Disrupts Fine Local Balance of Progesterone and Estrogen Signaling in Mouse Uterus During Implantation. *Biol Reprod* **93**, 123.

Diao, H. L., Zhu, H., Ma, H., Tan, H. N., Cong, J., Su, R. W. and Yang, Z. M. (2007). Rat ovulation, implantation and decidualization are severely compromised by COX-2 inhibitors. *Front Biosci* **12**, 3333-3342.

Dimitriadis, E., Stoikos, C., Stafford-Bell, M., Clark, I., Paiva, P., Kovacs, G. and Salamonsen, L. A. (2006). Interleukin-11, IL-11 receptoralpha and leukemia inhibitory factor are dysregulated in endometrium of infertile women with endometriosis during the implantation window. *J Reprod Immunol* **69**, 53-64.

Dimitriadis, E., White, C. A., Jones, R. L. and Salamonsen, L. A. (2005). Cytokines, chemokines and growth factors in endometrium related to implantation. *Hum Reprod Update* **11**, 613-630.

Dinchuk, J. E., Car, B. D., Focht, R. J., Johnston, J. J., Jaffee, B. D., Covington, M. B., Contel, N. R., Eng, V. M., Collins, R. J. and Czerniak, P. M. (1995). Renal abnormalities and an altered inflammatory response in mice lacking cyclooxygenase II. *Nature* **378**, 406-409.

Douglas, N. C., Tang, H., Gomez, R., Pytowski, B., Hicklin, D. J., Sauer, C. M., Kitajewski, J., Sauer, M. V. and Zimmermann, R. C. (2009). Vascular endothelial growth factor receptor 2 (VEGFR-2) functions to promote uterine decidual angiogenesis during early pregnancy in the mouse. *Endocrinology* **150**, 3845-3854.

Dubois, R. N., Abramson, S. B., Crofford, L., Gupta, R. A., Simon, L. S., Van De Putte, L. B. and Lipsky, P. E. (1998). Cyclooxygenase in biology and disease. *FASEB J* **12**, 1063-1073.

Duffy, D. M., Ko, C., Jo, M., Brannstrom, M. and Curry, T. E. (2019). Ovulation: Parallels With Inflammatory Processes. *Endocr Rev* **40**, 369-416.

Duffy, D. M. and Stouffer, R. L. (2002). Follicular administration of a cyclooxygenase inhibitor can prevent oocyte release without alteration of normal luteal function in rhesus monkeys. *Hum Reprod* **17**, 2825-2831.

Edwards, A. K., Janzen-Pang, J., R. Peng, A., Tayade, C., Carniato, A., T. Yamada, A., Lima, P. D. A. and Tse, D. (2013). Microscopic Anatomy of the Pregnant Mouse Uterus Throughout Gestation. In *The Guide to Investigation of Mouse Pregnancy* (ed. B. A. Croy, F. J. DeMayo, A. T. Yamada & S. L. Admason), pp. 832: Academic Press, 2013.

Edwards, D. R., Aldridge, T., Baird, D. D., Funk, M. J., Savitz, D. A. and Hartmann, K. E. (2012). Periconceptional over-the-counter nonsteroidal anti-inflammatory drug exposure and risk for spontaneous abortion. *Obstet Gynecol* **120**, 113-122.

Esnault, C., Stewart, A., Gualdrini, F., East, P., Horswell, S., Matthews, N. and Treisman, R. (2014). Rho-actin signaling to the MRTF coactivators dominates the immediate transcriptional response to serum in fibroblasts. *Genes Dev* **28**, 943-958.

Evans, C. A. and Kennedy, T. G. (1978). The importance of prostaglandin synthesis for the initiation of blastocyst implantation in the hamster. *J Reprod Fertil* **54**, 255-261.

Ferenczy, A. (1994). Anatomy and Histology of the Uterine Corpus. In *Blaustein's Pathology of the Female Genital Tract* (ed. R. J. Kurman), pp. 327-366. New York, NY: Springer New York.

Filant, J., DeMayo, F. J., Pru, J. K., Lydon, J. P. and Spencer, T. E. (2014). Fibroblast growth factor receptor two (FGFR2) regulates uterine epithelial integrity and fertility in mice. *Biol Reprod* **90**, 7.

Flaws, J. A. and Spencer, T. E. (2018). Encyclopedia of Reproduction (Second Edition) (ed M. K. Skinner), pp. 1-2. Academic Press.

Flores, D., Madhavan, M., Wright, S. and Arora, R. (2020). Mechanical and signaling mechanisms that guide pre-implantation embryo movement. *Development* **147**.

Franco, H. L., Dai, D., Lee, K. Y., Rubel, C. A., Roop, D., Boerboom, D., Jeong, J. W., Lydon, J. P., Bagchi, I. C., Bagchi, M. K., et al. (2011). WNT4 is a key regulator of normal postnatal uterine development and progesterone signaling during embryo implantation and decidualization in the mouse. *FASEB J* **25**, 1176-1187.

Franco, H. L., Lee, K. Y., Broaddus, R. R., White, L. D., Lanske, B., Lydon, J. P., Jeong, J. W. and DeMayo, F. J. (2010). Ablation of Indian hedgehog in the murine uterus results in decreased cell cycle progression, aberrant epidermal growth factor signaling, and increased estrogen signaling. *Biol Reprod* **82**, 783-790.

Friedman, S. A. (1988). Preeclampsia: a review of the role of prostaglandins. *Obstet Gynecol* **71**, 122-137.

Frum, T. and Ralston, A. (2019). Visualizing HIPPO Signaling Components in Mouse Early Embryonic Development. *Methods Mol Biol* **1893**, 335-352.

Funk, C. D. (2001). Prostaglandins and leukotrienes: advances in eicosanoid biology. *Science* **294**, 1871-1875.

Félétou, M., Huang, Y. and Vanhoutte, P. M. (2011). Endothelium-mediated control of vascular tone: COX-1 and COX-2 products. *Br J Pharmacol* **164**, 894-912.

Gaytán, F., Tarradas, E., Morales, C., Bellido, C. and Sánchez-Criado, J. E. (2002). Morphological evidence for uncontrolled proteolytic activity during the ovulatory process in indomethacin-treated rats. *Reproduction* **123**, 639-649.

Governini, L., Luongo, F. P., Haxhiu, A., Piomboni, P. and Luddi, A. (2021). Main actors behind the endometrial receptivity and successful implantation. *Tissue Cell* **73**, 101656.

Govindasamy, N., Long, H., Jeong, H. W., Raman, R., Özcifci, B., Probst, S., Arnold, S. J., Riehemann, K., Ranga, A., Adams, R. H., et al. (2021). 3D biomimetic platform reveals the first interactions of the embryo and the maternal blood vessels. *Dev Cell* **56**, 3276-3287.e3278.

Granger, K., Fitch, S., Shen, M., Lloyd, J., Bhurke, A., Hancock, J., Ye, X. and Arora, R. (2024). Murine uterine gland branching is necessary for gland function in implantation. *Mol Hum Reprod* **30**.

Gross, G. A., Imamura, T., Luedke, C., Vogt, S. K., Olson, L. M., Nelson, D. M., Sadovsky, Y. and Muglia, L. J. (1998). Opposing actions of prostaglandins and oxytocin determine the onset of murine labor. *Proc Natl Acad Sci U S A* **95**, 11875-11879.

Gupta, R. A., Tan, J., Krause, W. F., Geraci, M. W., Willson, T. M., Dey, S. K. and DuBois, R. N. (2000). Prostacyclin-mediated activation of peroxisome proliferator-activated receptor delta in colorectal cancer. *Proc Natl Acad Sci U S A* **97**, 13275-13280.

Halder, J. B., Zhao, X., Soker, S., Paria, B. C., Klagsbrun, M., Das, S. K. and Dey, S. K. (2000). Differential expression of VEGF isoforms and VEGF(164)-specific receptor neuropilin-1 in the mouse uterus suggests a role for VEGF(164) in vascular permeability and angiogenesis during implantation. *Genesis* **26**, 213-224.

Hama, K., Aoki, J., Bandoh, K., Inoue, A., Endo, T., Amano, T., Suzuki, H. and Arai, H. (2006). Lysophosphatidic receptor, LPA3, is positively and negatively regulated by progesterone and estrogen in the mouse uterus. *Life Sci* **79**, 1736-1740.

Harper, K. A. and Tyson-Capper, A. J. (2008). Complexity of COX-2 gene regulation. *Biochem Soc Trans* **36**, 543-545.

Hata, A. N. and Breyer, R. M. (2004). Pharmacology and signaling of prostaglandin receptors: multiple roles in inflammation and immune modulation. *Pharmacol Ther* **103**, 147-166.

Herington, J. L., O'Brien, C., Robuck, M. F., Lei, W., Brown, N., Slaughter, J. C., Paria, B. C., Mahadevan-Jansen, A. and Reese, J. (2018). Prostaglandin-Endoperoxide Synthase 1 Mediates the Timing of Parturition in Mice Despite Unhindered Uterine Contractility. *Endocrinology* **159**, 490-505.

Herington, J. L., Underwood, T., McConaha, M. and Bany, B. M. (2009). Paracrine signals from the mouse conceptus are not required for the normal progression of decidualization. *Endocrinology* **150**, 4404-4413.

Hickey, M. and Fraser, I. (2003). Human uterine vascular structures in normal and diseased states. *Microsc Res Tech* **60**, 377-389.

Hirata, T. and Narumiya, S. (2011). Prostanoid receptors. *Chem Rev* **111**, 6209-6230.

Hizaki, H., Segi, E., Sugimoto, Y., Hirose, M., Saji, T., Ushikubi, F., Matsuoka, T., Noda, Y., Tanaka, T., Yoshida, N., et al. (1999). Abortive expansion of the cumulus and impaired

fertility in mice lacking the prostaglandin E receptor subtype EP(2). *Proc Natl Acad Sci U S A* **96**, 10501-10506.

Hyder, S. M. and Stancel, G. M. (1999). Regulation of angiogenic growth factors in the female reproductive tract by estrogens and progestins. *Mol Endocrinol* **13**, 806-811.

Ishikawa, T. O. and Herschman, H. R. (2006). Conditional knockout mouse for tissue-specific disruption of the cyclooxygenase-2 (Cox-2) gene. *Genesis* **44**, 143-149.

Jackson-Northey, K. and Evans, M. F. (2002). Taking NSAIDs during pregnancy. Is it safe? *Can Fam Physician* **48**, 483-485.

Jaén, R. I., Prieto, P., Casado, M., Martín-Sanz, P. and Boscá, L. (2018). Post-translational modifications of prostaglandin-endoperoxide synthase 2 in colorectal cancer: An update. *World J Gastroenterol* **24**, 5454-5461.

Jo, M., Brännström, M., Akins, J. W. and Curry, T. E. (2025). New insights into the ovulatory process in the human ovary. *Hum Reprod Update* **31**, 21-47.

Kane, N., Jones, M., Brosens, J. J., Saunders, P. T., Kelly, R. W. and Critchley, H. O. (2008). Transforming growth factor-beta1 attenuates expression of both the progesterone receptor and Dickkopf in differentiated human endometrial stromal cells. *Mol Endocrinol* **22**, 716-728.

Kang, Y. J., Mbonye, U. R., DeLong, C. J., Wada, M. and Smith, W. L. (2007). Regulation of intracellular cyclooxygenase levels by gene transcription and protein degradation. *Prog Lipid Res* **46**, 108-125.

Karpovich, N., Klemmt, P., Hwang, J. H., McVeigh, J. E., Heath, J. K., Barlow, D. H. and Mardon, H. J. (2005). The production of interleukin-11 and decidualization are compromised in endometrial stromal cells derived from patients with infertility. *J Clin Endocrinol Metab* **90**, 1607-1612.

Kennedy, T. G. (1977). Evidence for a role for prosaglandins in the initiation of blastocyst implantation in the rat. *Biol Reprod* **16**, 286-291.

---- (1979). Prostaglandins and increased endometrial vascular permeabiltiy resulting from the application of artificial stimulus to the uterus of the rat sensitized for the decidual cell reaction. *Biol Reprod* **20**, 560-566.

---- (1985). Evidence for the involvement of prostaglandins throughout the decidual cell reaction in the rat. *Biol Reprod* **33**, 140-146.

Kennedy, T. G., Gillio-Meina, C. and Phang, S. H. (2007). Prostaglandins and the initiation of blastocyst implantation and decidualization. *Reproduction* **134**, 635-643.

Kennedy, T. G. and Zamecnik, J. (1978). The concentration of 6-keto-prostaglandin F1alpha is markedly elevated at the site of blastocyst implantation in the rat. *Prostaglandins* **16**, 599-605.

Keys, J. L., King, G. J. and Kennedy, T. G. (1986). Increased uterine vascular permeability at the time of embryonic attachment in the pig. *Biol Reprod* **34**, 405-411.

Kihara, Y., Maceyka, M., Spiegel, S. and Chun, J. (2014). Lysophospholipid receptor nomenclature review: IUPHAR Review 8. *Br J Pharmacol* **171**, 3575-3594.

Kim, H., Kim, M., Im, S. K. and Fang, S. (2018a). Mouse Cre-LoxP system: general principles to determine tissue-specific roles of target genes. *Lab Anim Res* **34**, 147-159.

Kim, H. R., Kim, Y. S., Yoon, J. A., Yang, S. C., Park, M., Seol, D. W., Lyu, S. W., Jun, J. H., Lim, H. J., Lee, D. R., et al. (2018b). Estrogen induces EGR1 to fine-tune its actions on uterine epithelium by controlling PR signaling for successful embryo implantation. *FASEB J* **32**, 1184-1195.

Kim, J. J., Wang, J., Bambra, C., Das, S. K., Dey, S. K. and Fazleabas, A. T. (1999). Expression of cyclooxygenase-1 and -2 in the baboon endometrium during the menstrual cycle and pregnancy. *Endocrinology* **140**, 2672-2678.

Kim, M., Park, H. J., Seol, J. W., Jang, J. Y., Cho, Y. S., Kim, K. R., Choi, Y., Lydon, J. P., Demayo, F. J., Shibuya, M., et al. (2013). VEGF-A regulated by progesterone governs uterine angiogenesis and vascular remodelling during pregnancy. *EMBO Mol Med* **5**, 1415-1430.

Kong, C. S., Ordoñez, A. A., Turner, S., Tremaine, T., Muter, J., Lucas, E. S., Salisbury, E., Vassena, R., Tiscornia, G., Fouladi-Nashta, A. A., et al. (2021). Embryo biosensing by uterine natural killer cells determines endometrial fate decisions at implantation. *FASEB J* **35**, e21336.

Kozer, E., Costei, A. M., Boskovic, R., Nulman, I., Nikfar, S. and Koren, G. (2003). Effects of aspirin consumption during pregnancy on pregnancy outcomes: meta-analysis. *Birth Defects Res B Dev Reprod Toxicol* **68**, 70-84.

Langenbach, R., Morham, S. G., Tiano, H. F., Loftin, C. D., Ghanayem, B. I., Chulada, P. C., Mahler, J. F., Lee, C. A., Goulding, E. H., Kluckman, K. D., et al. (1995). Prostaglandin synthase 1 gene disruption in mice reduces arachidonic acid-induced inflammation and indomethacin-induced gastric ulceration. *Cell* **83**, 483-492.

Large, M. J., Wetendorf, M., Lanz, R. B., Hartig, S. M., Creighton, C. J., Mancini, M. A., Kovanci, E., Lee, K. F., Threadgill, D. W., Lydon, J. P., et al. (2014). The epidermal growth factor receptor critically regulates endometrial function during early pregnancy. *PLoS Genet* **10**, e1004451.

Lau, I. F., Saksena, S. K. and Chang, M. C. (1973). Pregnancy blockade by indomethacin, an inhibitor of prostaglandin synthesis: its reversal by prostaglandins and progesterone in mice. *Prostaglandins* **4**, 795-803.

Lee, K. Y., Jeong, J. W., Wang, J., Ma, L., Martin, J. F., Tsai, S. Y., Lydon, J. P. and DeMayo, F. J. (2007). Bmp2 is critical for the murine uterine decidual response. *Mol Cell Biol* **27**, 5468-5478.

Leslie, C. C. (2015). Cytosolic phospholipase A_2: physiological function and role in disease. *J Lipid Res* **56**, 1386-1402.

Li, D. K., Ferber, J. R., Odouli, R. and Quesenberry, C. (2018a). Use of nonsteroidal antiinflammatory drugs during pregnancy and the risk of miscarriage. *Am J Obstet Gynecol* **219**, 275.e271-275.e278.

Li, D. K., Liu, L. and Odouli, R. (2003). Exposure to non-steroidal anti-inflammatory drugs during pregnancy and risk of miscarriage: population based cohort study. *BMJ* **327**, 368.

Li, Q. (2014). Transforming growth factor β signaling in uterine development and function. *J Anim Sci Biotechnol* **5**, 52.

Li, Q., Kannan, A., DeMayo, F. J., Lydon, J. P., Cooke, P. S., Yamagishi, H., Srivastava, D., Bagchi, M. K. and Bagchi, I. C. (2011). The antiproliferative action of progesterone in uterine epithelium is mediated by Hand2. *Science* **331**, 912-916.

Li, W. J., Lu, J. W., Zhang, C. Y., Wang, W. S., Ying, H., Myatt, L. and Sun, K. (2021). PGE2 vs PGF2α in human parturition. *Placenta* **104**, 208-219.

Li, X., Ballantyne, L. L., Crawford, M. C., FitzGerald, G. A. and Funk, C. D. (2018b). Isoform-Specific Compensation of Cyclooxygenase (Ptgs) Genes during Implantation and Late-Stage Pregnancy. *Sci Rep* **8**, 12097.

Lim, H., Gupta, R. A., Ma, W. G., Paria, B. C., Moller, D. E., Morrow, J. D., DuBois, R. N., Trzaskos, J. M. and Dey, S. K. (1999a). Cyclo-oxygenase-2-derived prostacyclin mediates embryo implantation in the mouse via PPARdelta. *Genes Dev* **13**, 1561-1574.

Lim, H., Ma, L., Ma, W. G., Maas, R. L. and Dey, S. K. (1999b). Hoxa-10 regulates uterine stromal cell responsiveness to progesterone during implantation and decidualization in the mouse. *Mol Endocrinol* **13**, 1005-1017.

Lim, H., Paria, B. C., Das, S. K., Dinchuk, J. E., Langenbach, R., Trzaskos, J. M. and Dey, S. K. (1997). Multiple female reproductive failures in cyclooxygenase 2-deficient mice. *Cell* **91**, 197-208.

Lim, H. J. and Dey, S. K. (2009). HB-EGF: a unique mediator of embryo-uterine interactions during implantation. *Exp Cell Res* **315**, 619-626.

Liu, J., Carrière, P. D., Doré, M. and Sirois, J. (1997). Prostaglandin G/H synthase-2 is expressed in bovine preovulatory follicles after the endogenous surge of luteinizing hormone. *Biol Reprod* **57**, 1524-1531.

Livak, K. J. and Schmittgen, T. D. (2001). Analysis of relative gene expression data using real-time quantitative PCR and the 2(-Delta Delta C(T)) Method. *Methods* **25**, 402-408.

Loftin, C. D., Trivedi, D. B. and Langenbach, R. (2002). Cyclooxygenase-1-selective inhibition prolongs gestation in mice without adverse effects on the ductus arteriosus. *J Clin Invest* **110**, 549-557.

Lubahn, D. B., Moyer, J. S., Golding, T. S., Couse, J. F., Korach, K. S. and Smithies, O. (1993). Alteration of reproductive function but not prenatal sexual development after insertional disruption of the mouse estrogen receptor gene. *Proc Natl Acad Sci U S A* **90**, 11162-11166.

Lundström, V., Gréen, K. and Svanborg, K. (1979). Endogenous prostaglandins in dysmenorrhea and the effect of prostaglandin synthetase inhibitors (PGSI) on uterine contractility. *Acta Obstet Gynecol Scand Suppl* **87**, 51-56.

Lustgarten Guahmich, N., Farber, G., Shafiei, S., McNally, D., Redmond, D., Kallinos, E., Stuhlmann, H., Dufort, D., James, D. and Blobel, C. P. (2020). Endothelial deletion of ADAM10, a key regulator of Notch signaling, causes impaired decidualization and reduced fertility in female mice. *Angiogenesis* **23**, 443-458.

Lydon, J. P., DeMayo, F. J., Funk, C. R., Mani, S. K., Hughes, A. R., Montgomery, C. A., Shyamala, G., Conneely, O. M. and O'Malley, B. W. (1995). Mice lacking progesterone receptor exhibit pleiotropic reproductive abnormalities. *Genes Dev* **9**, 2266-2278.

Ma, W., Tan, J., Matsumoto, H., Robert, B., Abrahamson, D. R., Das, S. K. and Dey, S. K. (2001). Adult tissue angiogenesis: evidence for negative regulation by estrogen in the uterus. *Mol Endocrinol* **15**, 1983-1992.

Ma, W. G., Song, H., Das, S. K., Paria, B. C. and Dey, S. K. (2003). Estrogen is a critical determinant that specifies the duration of the window of uterine receptivity for implantation. *Proc Natl Acad Sci U S A* **100**, 2963-2968.

Machado, D. A., Ontiveros, A. E. and Behringer, R. R. (2022). Mammalian uterine morphogenesis and variations. *Curr Top Dev Biol* **148**, 51-77.

Madhavan, M. and Arora, R. (2022). Tracing early postnatal lineage of progesterone receptor in the mouse uterus. Wiley Online Library: Molecular Reproduction and Development.

Madhavan, M. K., DeMayo, F. J., Lydon, J. P., Joshi, N. R., Fazleabas, A. T. and Arora, R. (2022). Aberrant uterine folding in mice disrupts implantation chamber formation and embryo-uterine axes alignment. *Development*.

Mantena, S. R., Kannan, A., Cheon, Y. P., Li, Q., Johnson, P. F., Bagchi, I. C. and Bagchi, M. K. (2006). C/EBPbeta is a critical mediator of steroid hormone-regulated cell proliferation and differentiation in the uterine epithelium and stroma. *Proc Natl Acad Sci U S A* **103**, 1870-1875.

Marchetto, N. M., Begum, S., Wu, T., O'Besso, V., Yarborough, C. C., Valero-Pacheco, N., Beaulieu, A. M., Kitajewski, J. K., Shawber, C. J. and Douglas, N. C. (2020). Endothelial Jagged1 Antagonizes Dll4/Notch Signaling in Decidual Angiogenesis during Early Mouse Pregnancy. *Int J Mol Sci* **21**.

Marions, L. and Danielsson, K. G. (1999). Expression of cyclo-oxygenase in human endometrium during the implantation period. *Mol Hum Reprod* **5**, 961-965.

Massri, N. and Arora, R. (2025). Uterine stromal but not epithelial PTGS2 is critical for murine pregnancy success. *Reproduction*.

Massri, N., Loia, R., Sones, J. L., Arora, R. and Douglas, N. C. (2023). Vascular changes in the cycling and early pregnant uterus. *JCI Insight* **8**.

Matsumoto, H., Ma , W., Smalley, W., Trzaskos, J., Breyer, R. M. and Dey, S. K. (2001). Diversification of cyclooxygenase-2-derived prostaglandins in ovulation and implantation. *Biol Reprod* **64**, 1557-1565.

Matsumoto, H., Ma, W. G., Daikoku, T., Zhao, X., Paria, B. C., Das, S. K., Trzaskos, J. M. and Dey, S. K. (2002). Cyclooxygenase-2 differentially directs uterine angiogenesis during implantation in mice. *J Biol Chem* **277**, 29260-29267.

Mayoral Andrade, G., Vásquez Martínez, G., Pérez-Campos Mayoral, L., Hernández-Huerta, M. T., Zenteno, E., Pérez-Campos Mayoral, E., Martínez Cruz, M., Martínez Cruz, R., Matias-Cervantes, C. A., Meraz Cruz, N., et al. (2020). Molecules and Prostaglandins Related to Embryo Tolerance. *Front Immunol* **11**, 555414.

Micu, M. C., Micu, R. and Ostensen, M. (2011). Luteinized unruptured follicle syndrome increased by inactive disease and selective cyclooxygenase 2 inhibitors in women with inflammatory arthropathies. *Arthritis Care Res (Hoboken)* **63**, 1334-1338.

Mikuni, M., Pall, M., Peterson, C. M., Peterson, C. A., Hellberg, P., Brännström, M., Richards, J. S. and Hedin, L. (1998). The selective prostaglandin endoperoxide synthase-2 inhibitor, NS-398, reduces prostaglandin production and ovulation in vivo and in vitro in the rat. *Biol Reprod* **59**, 1077-1083.

Miller, D. J. (2018). Review: The epic journey of sperm through the female reproductive tract. *Animal* **12**, s110-s120.

Monsivais, D., Matzuk, M. M. and Pangas, S. A. (2017). The TGF-β Family in the Reproductive Tract. *Cold Spring Harb Perspect Biol* **9**.

Mulac-Jericevic, B., Mullinax, R. A., DeMayo, F. J., Lydon, J. P. and Conneely, O. M. (2000). Subgroup of reproductive functions of progesterone mediated by progesterone receptor-B isoform. *Science* **289**, 1751-1754.

Mutoh, T., Rivera, R. and Chun, J. (2012). Insights into the pharmacological relevance of lysophospholipid receptors. *Br J Pharmacol* **165**, 829-844.

Myatt, L. and Lye, S. J. (2004). Expression, localization and function of prostaglandin receptors in myometrium. *Prostaglandins Leukot Essent Fatty Acids* **70**, 137-148.

Nakhai-Pour, H. R., Broy, P., Sheehy, O. and Bérard, A. (2011). Use of nonaspirin nonsteroidal anti-inflammatory drugs during pregnancy and the risk of spontaneous abortion. *CMAJ* **183**, 1713-1720.

Nielsen, G. L., Sørensen, H. T., Larsen, H. and Pedersen, L. (2001). Risk of adverse birth outcome and miscarriage in pregnant users of non-steroidal anti-inflammatory drugs: population based observational study and case-control study. *BMJ* **322**, 266-270.

Nowak, R. A. (2018). Estrous and Menstrual Cycles. In *Encyclopedia of Reproduction (Second Edition)* (ed M. K. Skinner), pp. 114-120. Academic Press.

Ohyama, T. and Groves, A. K. (2004). Generation of Pax2-Cre mice by modification of a Pax2 bacterial artificial chromosome. *Genesis* **38**, 195-199.

Olson, D. M. and Ammann, C. (2007). Role of the prostaglandins in labour and prostaglandin receptor inhibitors in the prevention of preterm labour. *Front Biosci* **12**, 1329-1343.

Ornitz, D. M. and Itoh, N. (2015). The Fibroblast Growth Factor signaling pathway. *Wiley Interdiscip Rev Dev Biol* **4**, 215-266.

Padmanabhan, V., Puttabyatappa, M. and Cardoso, R. C. (2018). Hypothalamus–Pituitary–Ovary Axis. Encyclopedia of Reproduction (Second Edition). In *Encyclopedia of Reproduction (Second Edition)* (ed M. K. Skinner), pp. 121-129. Academic Press.

Pakrasi, P. L. and Dey, S. K. (1982). Blastocyst is the source of prostaglandins in the implantation site in the rabbit. *Prostaglandins* **24**, 73-77.

Pakrasi, P. L. and Jain, A. K. (2008). Cyclooxygenase-2-derived endogenous prostacyclin reduces apoptosis and enhances embryo viability in mouse. *Prostaglandins Leukot Essent Fatty Acids* **79**, 27-33.

Pall, M., Fridén, B. E. and Brännström, M. (2001). Induction of delayed follicular rupture in the human by the selective COX-2 inhibitor rofecoxib: a randomized double-blind study. *Hum Reprod* **16**, 1323-1328.

Pang, S. C., Janzen- Pang, J., Tse, M. Y., Croy, B. A. and Lima, P. D. A. (2013a). The Cycling and Pregnant Mouse: Gross Anatomy. In *The Guide to Investigation of Mouse Pregnancy* (ed. B. A. Croy, F. J. DeMayo, A. T. Yamada & S. L. Admason), pp. 832: Academic Press, 2013.

Pang, S. C., Janzen-Pang, J., Tse, M. Y., Croy, B. A. and Lima, P. D. A. (2013b). The Cycling and Pregnant Mouse : Gross Anatomy. In *The Guide to Investigation of Mouse Pregnancy* (ed. B. A. Croy, A. T. Yamada, F. DeMayo & S. L. Adamson), pp. 832: Academic Press.

Papay, K. D. and Kennedy, T. G. (2000). Characterization of temporal and cell-specific changes in transcripts for prostaglandin E(2) receptors in pseudopregnant rat endometrium. *Biol Reprod* **62**, 1515-1525.

Paria, B. C., Ma, W., Tan, J., Raja, S., Das, S. K., Dey, S. K. and Hogan, B. L. (2001). Cellular and molecular responses of the uterus to embryo implantation can be elicited by locally applied growth factors. *Proc Natl Acad Sci U S A* **98**, 1047-1052.

Park, C. J., Lin, P. C., Zhou, S., Barakat, R., Bashir, S. T., Choi, J. M., Cacioppo, J. A., Oakley, O. R., Duffy, D. M., Lydon, J. P., et al. (2020a). Progesterone Receptor Serves the Ovary as a Trigger of Ovulation and a Terminator of Inflammation. *Cell Rep* **31**, 107496.

Park, Y. G., Choi, J. and Seol, J. W. (2020b). Angiopoietin-2 regulated by progesterone induces uterine vascular remodeling during pregnancy. *Mol Med Rep* **22**, 1235-1242.

Patel, B., Elguero, S., Thakore, S., Dahoud, W., Bedaiwy, M. and Mesiano, S. (2015). Role of nuclear progesterone receptor isoforms in uterine pathophysiology. *Hum Reprod Update* **21**, 155-173.

Pierce, K. L., Fujino, H., Srinivasan, D. and Regan, J. W. (1999). Activation of FP prostanoid receptor isoforms leads to Rho-mediated changes in cell morphology and in the cell cytoskeleton. *J Biol Chem* **274**, 35944-35949.

Psychoyos, A., Nikas, G. and Gravanis, A. (1995). The role of prostaglandins in blastocyst implantation. *Hum Reprod* **10 Suppl 2**, 30-42.

Qublan, H., Amarin, Z., Nawasreh, M., Diab, F., Malkawi, S., Al-Ahmad, N. and Balawneh, M. (2006). Luteinized unruptured follicle syndrome: incidence and recurrence rate in infertile women with unexplained infertility undergoing intrauterine insemination. *Hum Reprod* **21**, 2110-2113.

Rabbani, M. L. and Rogers, P. A. (2001). Role of vascular endothelial growth factor in endometrial vascular events before implantation in rats. *Reproduction* **122**, 85-90.

Reese, J., Brown, N., Paria, B. C., Morrow, J. and Dey, S. K. (1999). COX-2 compensation in the uterus of COX-1 deficient mice during the pre-implantation period. *Mol Cell Endocrinol* **150**, 23-31.

Reese, J., Paria, B. C., Brown, N., Zhao, X., Morrow, J. D. and Dey, S. K. (2000). Coordinated regulation of fetal and maternal prostaglandins directs successful birth and postnatal adaptation in the mouse. *Proc Natl Acad Sci U S A* **97**, 9759-9764.

Reese, J., Zhao, X., Ma, W. G., Brown, N., Maziasz, T. J. and Dey, S. K. (2001). Comparative analysis of pharmacologic and/or genetic disruption of cyclooxygenase-1 and cyclooxygenase-2 function in female reproduction in mice. *Endocrinology* **142**, 3198-3206.

Regan, J. W. (2003). EP2 and EP4 prostanoid receptor signaling. *Life Sci* **74**, 143-153.

Ricciotti, E. and FitzGerald, G. A. (2011). Prostaglandins and inflammation. *Arterioscler Thromb Vasc Biol* **31**, 986-1000.

Richards, J. S. and Pangas, S. A. (2010). The ovary: basic biology and clinical implications. *J Clin Invest* **120**, 963-972.

Richards, J. S., Russell, D. L., Ochsner, S. and Espey, L. L. (2002). Ovulation: new dimensions and new regulators of the inflammatory-like response. *Annu Rev Physiol* **64**, 69-92.

Robb, L., Li, R., Hartley, L., Nandurkar, H. H., Koentgen, F. and Begley, C. G. (1998). Infertility in female mice lacking the receptor for interleukin 11 is due to a defective uterine response to implantation. *Nat Med* **4**, 303-308.

Rogers, P. W., Murphy, C. R. and Gannon, B. J. (1982). Changes in the spatial organization of the uterine vasculature during implantation in the rat. *J Reprod Fertil* **65**, 211-214.

Rouzer, C. A. and Marnett, L. J. (2009). Cyclooxygenases: structural and functional insights. *J Lipid Res* **50 Suppl**, S29-34.

---- (2020). Structural and Chemical Biology of the Interaction of Cyclooxygenase with Substrates and Non-Steroidal Anti-Inflammatory Drugs. *Chem Rev* **120**, 7592-7641.

Ruan, Y. C., Zhou, W. and Chan, H. C. (2011). Regulation of smooth muscle contraction by the epithelium: role of prostaglandins. *Physiology (Bethesda)* **26**, 156-170.

Sakamoto, R., Fujiwara, T., Kawano, Y., Aikawa, S., Inazumi, T., Nakayama, O., Kawasaki-Shirata, Y., Hashimoto-Iwasaki, M., Sugimoto, T., Tsuchiya, S., et al. (2024). Uterine prostaglandin DP receptor-induced upon implantation contributes to decidualization together with EP4 receptor. *J Lipid Res* **65**, 100636.

Salazar, L. A., Inostroza, M., Jara, C., Vega, F., García, R., Ciuffardi, I. and Guzmán, N. (2010). Association of -765G>C polymorphism of the COX-2 gene with recurrent embryo implantation failure in Southern Chilean women. *Clin Chim Acta* **411**, 1822-1824.

Scherle, P. A., Ma, W., Lim, H., Dey, S. K. and Trzaskos, J. M. (2000). Regulation of cyclooxygenase-2 induction in the mouse uterus during decidualization. An event of early pregnancy. *J Biol Chem* **275**, 37086-37092.

Scott, C. A., van Huyen, D. and Bany, B. M. (2012). Angiopoietin-like gene expression in the mouse uterus during implantation and in response to steroids. *Cell Tissue Res* **348**, 199-211.

Segi, E., Sugimoto, Y., Yamasaki, A., Aze, Y., Oida, H., Nishimura, T., Murata, T., Matsuoka, T., Ushikubi, F., Hirose, M., et al. (1998). Patent ductus arteriosus and neonatal death in prostaglandin receptor EP4-deficient mice. *Biochem Biophys Res Commun* **246**, 7-12.

Shah, B. H. and Catt, K. J. (2005). Roles of LPA3 and COX-2 in implantation. *Trends Endocrinol Metab* **16**, 397-399.

Simmons, D. L., Botting, R. M. and Hla, T. (2004). Cyclooxygenase isozymes: the biology of prostaglandin synthesis and inhibition. *Pharmacol Rev* **56**, 387-437.

Simon, L., Spiewak, K. A., Ekman, G. C., Kim, J., Lydon, J. P., Bagchi, M. K., Bagchi, I. C., DeMayo, F. J. and Cooke, P. S. (2009). Stromal progesterone receptors mediate induction of Indian Hedgehog (IHH) in uterine epithelium and its downstream targets in uterine stroma. *Endocrinology* **150**, 3871-3876.

Skinner, K. A. and Challis, J. R. (1985). Changes in the synthesis and metabolism of prostaglandins by human fetal membranes and decidua at labor. *Am J Obstet Gynecol* **151**, 519-523.

Smith, W. L., DeWitt, D. L. and Garavito, R. M. (2000). Cyclooxygenases: structural, cellular, and molecular biology. *Annu Rev Biochem* **69**, 145-182.

Smith, W. L. and Song, I. (2002). The enzymology of prostaglandin endoperoxide H synthases-1 and -2. *Prostaglandins Other Lipid Mediat* **68-69**, 115-128.

Snabes, M. C. and Harper, M. J. (1984). Site of action of indomethacin on implantation in the rabbit. *J Reprod Fertil* **71**, 559-565.

Sones, J. L., Cha, J., Woods, A. K., Bartos, A., Heyward, C. Y., Lob, H. E., Isroff, C. E., Butler, S. D., Shapiro, S. E., Dey, S. K., et al. (2016). Decidual Cox2 inhibition improves fetal and maternal outcomes in a preeclampsia-like mouse model. *JCI Insight* **1**.

Song, H., Lim, H., Das, S. K., Paria, B. C. and Dey, S. K. (2000). Dysregulation of EGF family of growth factors and COX-2 in the uterus during the preattachment and attachment reactions of the blastocyst with the luminal epithelium correlates with implantation failure in LIF-deficient mice. *Mol Endocrinol* **14**, 1147-1161.

Song, H., Lim, H., Paria, B. C., Matsumoto, H., Swift, L. L., Morrow, J., Bonventre, J. V. and Dey, S. K. (2002). Cytosolic phospholipase A2alpha is crucial [correction of A2alpha deficiency is crucial] for 'on-time' embryo implantation that directs subsequent development. *Development* **129**, 2879-2889.

Song, Y. and Fazleabas, A. T. (2021). Endometrial Organoids: A Rising Star for Research on Endometrial Development and Associated Diseases. *Reprod Sci* **28**, 1626-1636.

Sookvanichsilp, N. and Pulbutr, P. (2002). Anti-implantation effects of indomethacin and celecoxib in rats. *Contraception* **65**, 373-378.

Soyal, S. M., Mukherjee, A., Lee, K. Y., Li, J., Li, H., DeMayo, F. J. and Lydon, J. P. (2005). Cre-mediated recombination in cell lineages that express the progesterone receptor. *Genesis* **41**, 58-66.

Stavreus-Evers, A., Koraen, L., Scott, J. E., Zhang, P. and Westlund, P. (2005). Distribution of cyclooxygenase-1, cyclooxygenase-2, and cytosolic phospholipase A2 in the luteal phase human endometrium and ovary. *Fertil Steril* **83**, 156-162.

Stewart, C. L. (1994). Leukaemia inhibitory factor and the regulation of pre-implantation development of the mammalian embryo. *Mol Reprod Dev* **39**, 233-238.

Stewart, C. L., Kaspar, P., Brunet, L. J., Bhatt, H., Gadi, I., Köntgen, F. and Abbondanzo, S. J. (1992). Blastocyst implantation depends on maternal expression of leukaemia inhibitory factor. *Nature* **359**, 76-79.

Su, R. W. and Fazleabas, A. T. (2015). Implantation and Establishment of Pregnancy in Human and Nonhuman Primates. *Adv Anat Embryol Cell Biol* **216**, 189-213.

Sugimoto, Y., Inazumi, T. and Tsuchiya, S. (2015). Roles of prostaglandin receptors in female reproduction. *J Biochem* **157**, 73-80.

Sugimoto, Y. and Narumiya, S. (2007). Prostaglandin E receptors. *J Biol Chem* **282**, 11613-11617.

Sugimoto, Y., Yamasaki, A., Segi, E., Tsuboi, K., Aze, Y., Nishimura, T., Oida, H., Yoshida, N., Tanaka, T., Katsuyama, M., et al. (1997). Failure of parturition in mice lacking the prostaglandin F receptor. *Science* **277**, 681-683.

Takemori, K., Okamura, H., Kanzaki, H., Koshida, M. and Konishi, I. (1984). Scanning electron microscopy study on corrosion cast of rat uterine vasculature during the first half of pregnancy. *J Anat* **138 (Pt 1)**, 163-173.

Tan, W., Chen, L., Guo, L., Ou, X., Xie, D. and Quan, S. (2014). Relationship between macrophages in mouse uteri and angiogenesis in endometrium during the peri-implantation period. *Theriogenology* **82**, 1021-1027.

Tanabe, T. and Tohnai, N. (2002). Cyclooxygenase isozymes and their gene structures and expression. *Prostaglandins Other Lipid Mediat* **68-69**, 95-114.

Thomas, J., Fairclough, A., Kavanagh, J. and Kelly, A. J. (2014). Vaginal prostaglandin (PGE2 and PGF2a) for induction of labour at term. *Cochrane Database Syst Rev* **2014**, CD003101.

Thorpe, P. G., Gilboa, S. M., Hernandez-Diaz, S., Lind, J., Cragan, J. D., Briggs, G., Kweder, S., Friedman, J. M., Mitchell, A. A., Honein, M. A., et al. (2013). Medications in the first trimester of pregnancy: most common exposures and critical gaps in understanding fetal risk. *Pharmacoepidemiol Drug Saf* **22**, 1013-1018.

Turesheva, A., Aimagambetova, G., Ukybassova, T., Marat, A., Kanabekova, P., Kaldygulova, L., Amanzholkyzy, A., Ryzhkova, S., Nogay, A., Khamidullina, Z., et al. (2023). Recurrent Pregnancy Loss Etiology, Risk Factors, Diagnosis, and Management. Fresh Look into a Full Box. *J Clin Med* **12**.

Vander Borght, M. and Wyns, C. (2018). Fertility and infertility: Definition and epidemiology. *Clin Biochem* **62**, 2-10.

Wang, H. and Dey, S. K. (2006). Roadmap to embryo implantation: clues from mouse models. *Nat Rev Genet* **7**, 185-199.

Wang, H., Ma, W. G., Tejada, L., Zhang, H., Morrow, J. D., Das, S. K. and Dey, S. K. (2004a). Rescue of female infertility from the loss of cyclooxygenase-2 by compensatory up-regulation of cyclooxygenase-1 is a function of genetic makeup. *J Biol Chem* **279**, 10649-10658.

Wang, H., Xie, H., Sun, X., Tranguch, S., Zhang, H., Jia, X., Wang, D., Das, S. K., Desvergne, B., Wahli, W., et al. (2007). Stage-specific integration of maternal and embryonic peroxisome proliferator-activated receptor delta signaling is critical to pregnancy success. *J Biol Chem* **282**, 37770-37782.

Wang, X., Li, X., Wang, T., Wu, S. P., Jeong, J. W., Kim, T. H., Young, S. L., Lessey, B. A., Lanz, R. B., Lydon, J. P., et al. (2018). SOX17 regulates uterine epithelial-stromal cross-talk acting via a distal enhancer upstream of Ihh. *Nat Commun* **9**, 4421.

Wang, X., Su, Y., Deb, K., Raposo, M., Morrow, J. D., Reese, J. and Paria, B. C. (2004b). Prostaglandin E2 is a product of induced prostaglandin-endoperoxide synthase 2 and microsomal-type prostaglandin E synthase at the implantation site of the hamster. *J Biol Chem* **279**, 30579-30587.

Wang, Y., Zhao, A. M. and Lin, Q. D. (2010). Role of cyclooxygenase-2 signaling pathway dysfunction in unexplained recurrent spontaneous abortion. *Chin Med J (Engl)* **123**, 1543-1547.

Wei, Q., Levens, E. D., Stefansson, L. and Nieman, L. K. (2010). Indian Hedgehog and its targets in human endometrium: menstrual cycle expression and response to CDB-2914. *J Clin Endocrinol Metab* **95**, 5330-5337.

Winuthayanon, W., Hewitt, S. C. and Korach, K. S. (2014). Uterine epithelial cell estrogen receptor alpha-dependent and -independent genomic profiles that underlie estrogen responses in mice. *Biol Reprod* **91**, 110.

Winuthayanon, W., Hewitt, S. C., Orvis, G. D., Behringer, R. R. and Korach, K. S. (2010). Uterine epithelial estrogen receptor α is dispensable for proliferation but essential for complete biological and biochemical responses. *Proc Natl Acad Sci U S A* **107**, 19272-19277.

Winuthayanon, W., Lierz, S. L., Delarosa, K. C., Sampels, S. R., Donoghue, L. J., Hewitt, S. C. and Korach, K. S. (2017). Juxtacrine Activity of Estrogen Receptor α in Uterine Stromal Cells is Necessary for Estrogen-Induced Epithelial Cell Proliferation. *Sci Rep* **7**, 8377.

Woodward, D. F., Jones, R. L. and Narumiya, S. (2011). International Union of Basic and Clinical Pharmacology. LXXXIII: classification of prostanoid receptors, updating 15 years of progress. *Pharmacol Rev* **63**, 471-538.

Yang, Z. M., Das, S. K., Wang, J., Sugimoto, Y., Ichikawa, A. and Dey, S. K. (1997). Potential sites of prostaglandin actions in the periimplantation mouse uterus: differential expression and regulation of prostaglandin receptor genes. *Biol Reprod* **56**, 368-379.

Ye, X., Hama, K., Contos, J. J., Anliker, B., Inoue, A., Skinner, M. K., Suzuki, H., Amano, T., Kennedy, G., Arai, H., et al. (2005). LPA3-mediated lysophosphatidic acid signalling in embryo implantation and spacing. *Nature* **435**, 104-108.

Ye, X., Herr, D. R., Diao, H., Rivera, R. and Chun, J. (2011). Unique uterine localization and regulation may differentiate LPA3 from other lysophospholipid receptors for its role in embryo implantation. *Fertil Steril* **95**, 2107-2113, 2113.e2101-2104.

Yu, J., Berga, S. L., Zou, W., Yook, D. G., Pan, J. C., Andrade, A. A., Zhao, L., Sidell, N., Bagchi, I. C., Bagchi, M. K., et al. (2017). IL-1β Inhibits Connexin 43 and Disrupts Decidualization of Human Endometrial Stromal Cells Through ERK1/2 and p38 MAP Kinase. *Endocrinology* **158**, 4270-4285.

Yung, Y. C., Stoddard, N. C. and Chun, J. (2014). LPA receptor signaling: pharmacology, physiology, and pathophysiology. *J Lipid Res* **55**, 1192-1214.

Zhang, J., Goods, B. A., Pattarawat, P., Wang, Y., Haining, T., Zhang, Q., Shalek, A. K., Duncan, F. E., Woodruff, T. K. and Xiao, S. (2023). An ex vivo ovulation system enables the discovery of novel ovulatory pathways and nonhormonal contraceptive candidates†. *Biol Reprod* **108**, 629-644.

Zhu, L. and Pollard, J. W. (2007). Estradiol-17beta regulates mouse uterine epithelial cell proliferation through insulin-like growth factor 1 signaling. *Proc Natl Acad Sci U S A* **104**, 15847-15851.